

**ARTIFICIAL MATERIAL 3D PRINTED TEACHING
TOOLS FOR CARDIAC SURGICAL SKILLS TRAINING**

ARTIFICIAL MATERIAL 3D PRINTED TEACHING TOOLS FOR
CARDIAC SURGICAL SKILLS TRAINING

By

HAMAD MUBARAK BUBSHAIT, B.SC., MEEI

A Thesis Submitted to The School of Graduate Studies in Partial Fulfilment
of The Requirements for The Degree Doctor of Philosophy

McMaster University © Copyright by Hamad Bubshait, March 2021

Doctor of Philosophy (2021)

(Mechanical Engineering)

McMaster University

Hamilton, Ontario

TITLE: Artificial Material 3D Printed Teaching
Tools for Cardiac Surgical Skills Training

AUTHOR: Hamad Mubarak Bubshait, MEEI, B.Sc.

SUPERVISOR: Dr. Gregory R. Wohl, Associate Professor

NUMBER OF PAGES: xix, 160

TO MY FAMILY

Lay Abstract

Typically, surgeons use post-mortem human tissues (cadavers) and animal tissues for surgical skills training. However, those methods can be both expensive and limited in availability. Therefore, other non-biological methods are introduced constantly to provide viable alternatives. Those methods include producing models using 3D printing, virtual reality (VR) simulation and even using household items to create training models. However, to date, there is a lack of highly accurate representation of real tissues (fidelity) of most models for cardiac surgical training. The purpose of this research was to develop and manufacture surgical skill training tools for cardiac surgeons focusing on the aortic valve cardiac tissues. The research was divided into several parts including developing computer models using patient-specific medical imaging, developing a general training model and training models manufacturing. Also, the research included manufacturing materials selection process as well as plans for testing the training models in training sessions.

Abstract

Cardiac surgeons rely on simulation training to improve their surgical skills. The focus of this research was on creating a 3D aortic valve model for cardiac surgical skills training. The research was divided into four different stages including CAD model development, tissue testing using surgical tools, aortic valve model manufacturing and model evaluation.

First, the development of a patient-specific aortic valve model was carried out. The process involved heavily processing CT scanned data of the aortic valve to extract the geometric information via segmentation. Patient-specific models are critical for pre-operative planning and training. However, those models are not ideal for large volume quantities due to the high production costs and the extensive manual labour required to process the models. Therefore, another approach was chosen to produce a generic model that was more suitable for large volume quantities. The generic aortic valve model was developed using data obtained from the literature. The contribution in this stage was developing the methodology to reverse engineer patient-specific cardiac tissues. Additionally, a generic CAD model of the aortic valve was developed.

Second, to select suitable materials for the model, samples from biological tissues and polymers were tested using a surgical tool. The contribution in this stage was documenting the forces and displacements obtained from puncturing and cutting the samples using suturing needles and scalpel blades.

Third, the aortic valve model was manufactured using two approaches including AM and casting. The contribution in this stage revolved around the development of several moulds for casting.

Finally, evaluation of the model was done via an initial assessment session with surgical residents. Although the model was not evaluated in extensive training sessions, a plan highlighting the important elements to do that was included in this research. Thus, the contribution in this stage was developing the model testing plan.

Acknowledgements

I would like to express my appreciation to my supervisor Dr. Greg Wohl for his guidance, help and support. His actions and words gave me great motivation and empowerment to overcome all the challenges that I faced in this project. Also, I would like to extend my appreciation to my Ph.D. committee members Dr. Cheryl Quenneville and Dr. Stephen Veldhuis. Their feedback helped me to focus and stay on track throughout this project.

I would like to express my appreciation to Dr. Allan Spence for all his continuous help and support during my Ph.D. journey. Also, I would like to thank all the cardiac surgeons and cardiac residents who helped me in this project especially Dr. Dominic Parry whose feedback and insights helped in shaping the foundations of this project.

I would like to thank Dr. Zahra Motamed for her help and support in this project. Also, I am thankful for all the help and support that I got from my colleagues, technicians, volunteers and staff at the mechanical engineering department. I would like to also thank Siobhan Knights for her help and support with the project.

This project was funded by the Saudi Arabian Cultural Bureau in Canada, and I would like to thank them for giving me this great opportunity.

Finally, I would like to thank my family for their help and support during this journey. They encouraged me to aspire to greatness.

Table of Contents

Lay Abstract.....	iv
Abstract.....	v
Acknowledgements.....	vii
Table of Contents.....	viii
List of Figures.....	xii
List of Tables.....	xvi
List of Abbreviations and Symbols.....	xvii
Declaration of Academic Achievement.....	xix
1. Introduction.....	1
1.1. Background.....	1
1.2. Research Proposal and Objectives.....	3
1.3. Research Contributions.....	5
1.4. Thesis Document Outline.....	6
2. Background.....	9
2.1. Literature Review.....	9
2.2. Aortic Valve Background.....	13
2.2.1. Aortic Valve Anatomy.....	13
2.2.2. Aortic Valve Pathologies.....	17

2.2.3. Aortic Surgical Repairs Strategies	23
2.3. Manufacturing Methods Background	26
2.3.1. Additive Manufacturing.....	26
2.3.2. Casting of Models	34
3. Development of Aortic Model and Manufacturing Process	38
3.1. Introduction	38
3.1.1. Part 1: Patient-Specific Aortic Valve Model	39
3.1.2. Part 2: General CAD Model	43
3.1.3. Part 3: Aortic Valve Model Manufacturing Processes.....	46
3.2. Materials and Methods	47
3.2.1. Part 1: Patient-Specific Aortic Valve Model	47
3.2.2. Part 2: General CAD Model	52
3.2.3. Part 3: Aortic Valve Model Manufacturing Processes.....	54
3.3. Results and Discussion	58
3.3.1. Part 1: Patient-Specific Aortic Valve Model	58
3.3.2. Part 2: General CAD Model	62
3.3.3. Part 3: Aortic Valve Model Manufacturing Processes.....	64
3.4. Conclusion.....	69
4. Mechanical Testing of Aortic Tissues and Manufacturing Materials.....	72

4.1.	Introduction	72
4.2.	Materials and Methods	77
4.2.1.	Materials Tested.....	78
4.2.2.	Testing Protocols	80
4.3.	Results and Discussion	86
4.3.1.	Needle and Blade Tests of t = 0.5 mm Group.....	88
4.3.2.	Needle and Blade Tests of t = 2 mm Group.....	94
4.3.3.	Needle and Blade Tests of t = 3 mm Group.....	97
4.3.4.	Needle Tests of Manufactured Models	100
4.4.	Discussion.....	103
4.5.	Conclusions	105
5.	Educational Model Evaluation.....	106
5.1.	Introduction	106
5.2.	Materials and Methods	110
5.2.1.	An Initial Assessment With Surgical Trainees	110
5.2.2.	Plans Developed for Trainee Skills Assessment.....	112
5.3.	Results and Discussion	119
5.4.	Conclusions	123
6.	Conclusion and Future Work.....	125

6.1. Recommendations	125
6.1.1. Aortic Valve CAD Design	125
6.1.2. Tissues Testing.....	126
6.1.3. Aortic Valve Manufacturing	127
6.1.4. Educational Model Testing	128
6.2. Future Work.....	129
References.....	131
Appendices.....	143
A. Additive Manufacturing Models	143
A.1. First Mould Design Iteration.....	143
A.2. Second Mould Design Iteration	150
A.3. Educational Model Design Steps	157
B. Educational Model Evaluation	158

List of Figures

Figure 2.1. Heart valves anatomy	14
Figure 2.2. Aorta anatomy	16
Figure 2.3. Bicuspid aortic valve type	19
Figure 2.4. Aortic valve diseases	20
Figure 2.5. Ascending aorta aneurysm	22
Figure 2.6. Aortic root aneurysm.....	22
Figure 2.7. Aortic valve insufficiency classification	24
Figure 2.8. Aortic valve sparing surgical repair strategies	25
Figure 2.9. 3D printed aortic valves.....	30
Figure 3.1. CT scan of aortic valve.....	42
Figure 3.2. Simplified aortic root diagram.....	44
Figure 3.3. Aortic valve geometry approximation.....	45
Figure 3.4. CT scan of the aortic valve	47
Figure 3.5. Initial aortic tissues segmentation in VMTK Lab software.....	50
Figure 3.6. Aortic valve reverse engineering techniques.....	51
Figure 3.7. AM model with fixture.....	55
Figure 3.8. Aortic valve model made from Silicone.....	56
Figure 3.9. Aortic valve model training box.....	57
Figure 3.10. Segmentation results.....	59
Figure 3.11. CAD reconstruction results	61
Figure 3.12. First aortic valve CAD design iteration.....	62

Figure 3.13. Second design iteration.....	63
Figure 3.14. Third design iteration.....	64
Figure 3.15. Aortic valve model casts; A. First iteration; B: Second iteration.....	68
Figure 4.1. Mitral valve repair test bed.....	76
Figure 4.2. Analysis of suture manipulation forces	76
Figure 4.3. Test samples of casting materials	80
Figure 4.4. Instron testing setup and testing materials.....	82
Figure 4.5. Surgical tools holder.....	83
Figure 4.6. Surgical tools used for the testing.	84
Figure 4.7. Needle test sample result	87
Figure 4.8. Blade test sample result	87
Figure 4.9. Comparison of forces for needle puncture and scalpel blade cutting tests for each of the materials tested at 0.5 mm..	89
Figure 4.10. Comparison of displacement at max force for needle puncture and scalpel blade cutting tests for each of the materials tested at 0.5 mm thickness.....	89
Figure 4.11. Representative needle tests of some 0.5 mm samples	93
Figure 4.12. Blade tests of some 0.5 mm samples	93
Figure 4.13. Comparison of forces for needle puncture and scalpel blade cutting tests for each of the materials tested at 2 mm..	95
Figure 4.14. Comparison of displacement at max force for needle puncture and scalpel blade cutting tests for each of the materials tested at 2 mm thickness.....	96

Figure 4.15 Comparison of forces for needle puncture and scalpel blade cutting tests for each of the materials tested at 3 mm.....	98
Figure 4.16. Comparison of displacement at max force for needle puncture and scalpel blade cutting tests for each of the materials tested at 3 mm thickness.....	99
Figure 4.17. Comparison of forces for needle puncture and scalpel blade cutting for TangoPlus and silicone A10 at 0.75 mm.	101
Figure 4.18. Comparison of forces for needle puncture and scalpel blade cutting tests for silicone A10 and polyurethane at 0.9 mm.....	102
Figure 4.19. Comparison of displacement at max force for needle puncture and scalpel blade cutting tests for TangoPlus and silicone A10 at 0.75 mm thickness.	102
Figure 4.20. Comparison of displacement at max force for needle puncture and scalpel blade cutting tests for silicone A10 and polyurethane at 0.9 mm thickness..	103
Figure 5.1. Miller’s pyramid for assessing clinical competence	107
Figure 5.2. Surgical training setup showing aortic valve and aortic graft stations.....	109
Figure 5.3. Aortic valve models used in the initial assessment session.....	111
Figure 5.4. Qualitative rating scale	115
Figure 5.5. OSATS global rating scale	115
Figure 5.6. Example of a checklist.....	119
Figure 5.7. Models evaluation by surgical residents.....	121
Figure A.1. Casting mould v1	146
Figure A.2. Casting mould v1 Sections	147
Figure A.3. Casting mould v2.....	150

Figure A.4. Coronary arteries locks	152
Figure A.5. Summary of mould v2 outer sections	153
Figure A.6. Summary of mould v2 inner sections	154
Figure A.7. Locking mechanism.....	155
Figure A.8. Ascending aorta aneurysm.....	157
Figure B.1. Modified OSATS global rating scale.....	158
Figure B.2. Modified OSATS including a checklist.....	159
Figure B.3. Rating scale sample for assessment of coronary anastomosis.....	160

List of Tables

Table 3-1. Summary of the pros and cons of AM and casting.....	67
Table 4-1. Recommended mechanical properties of aortic valve leaflet	74
Table 4-2. Tests materials	79
Table 4-3. Needle puncture tests for $t = 0.5$ mm	91
Table 4-4. Blade cutting tests for $t = 0.5$ mm	92
Table 4-5. Needle puncture tests $t = 2$ mm	95
Table 4-6. Scalpel blade cutting tests $t = 2$ mm.....	96
Table 4-7. Needle tests $t = 3$ mm	98
Table 4-8. Blade tests $t = 3$ mm	99
Table 4-9. Needle tests $t = 0.75$ mm	101
Table 4-10. Needle tests $t = 0.9$ mm	101

List of Abbreviations and Symbols

ABS	Acrylonitrile Butadiene Styrene
AI	Aortic Insufficiency
AM	Additive Manufacturing
CAD	Computer Aided Design
CAM	Computer Aided Manufacturing
CT	Computed Tomography
DICOM	Digital Imaging and Communication in Medicine
FAA	Functional Aortic Annulus
FDM	Fused Depositing Modeling
LA	Left Atrium
LC	Left Coronary
LCC	Left Coronary Commissure
MRI	Magnetic Resonance Imaging
NC	Non-Coronary
NCC	Noncoronary Commissure
NURBS	Non-Uniform Rational Basis Spline
OSATS	Objective Structured Assessment of Technical Skills
PAR	Paravalvular Aortic Regurgitation
PC-ABS	Polycarbonate - Acrylonitrile Butadiene Styrene
PETG	Polyethylene Terephthalate
PLA	Polylactic Acid

RC	Right Coronary
RCC	Right Coronary Commissure
Ru A20	Rubber-Like Polyurethane with A Shore Value of A20
Ru A30	Rubber-Like Urethane with A Shore Value of A30
RVOT	Right Ventricular Outflow Tract
SCA	Sub-Commissural Annuloplasty
Si A10	Silicone with A Shore Value of A10
Si A20	Silicone with A Shore Value of A20
STJ	Sinotubular Junction
STL	Stereolithography
TAVR	Transcatheter Aortic Valve Replacement
TEE	Transesophageal Echocardiography
TTE	Transthoracic Echocardiogram
UV	Ultraviolet
VAJ	Ventriculo-Aortic Junction

Declaration of Academic Achievement

In Chapter 3, the need to create an aortic valve model was highlighted. This chapter included a complete cycle to produce the aortic valve model from design to manufacturing. Thus, a reverse engineering methodology was investigated to model and manufacture aortic valve patient-specific and general training models in Parts one and two. This resulted in choosing to focus on creating a general CAD model for the training. The results of the patient-specific design analysis were published in international CAD conferences. In part three, I compared the aortic valve AM and casting manufacturing methods. This involved designing and manufacturing moulds for the casting process. Also, I designed educational tools for cardiac surgeons, including simplified aortic valve models, realistic aortic valve models and training box model.

In Chapter 4, I highlighted the need to conduct experimentation to select suitable materials for the aortic valve model via tissue testing using surgical tools, including a scalpel blade and a suturing needle. This was due to the limited literature on these applications. Therefore, I conducted mechanical testing of aortic tissues and manufacturing materials. The results of the experiments could be used to guide materials selections for soft tissues as well as force feedback for virtual simulations of surgical tools. The results are pending publications.

In Chapter 5, I conducted an initial assessment of the aortic valve model and proposed plans for the performance evaluation of the model during training sessions.

Chapter 1

1. Introduction

1.1. Background

Many modelling challenges are addressed using reverse engineering and rapid prototyping techniques. These challenges typically range anywhere from simple mechanical structures such as a hose bracket to complex biological structures such as cardiac tissues. These structures usually do not have prior well-defined geometric data and can be difficult to manufacture using conventional methods due to the complexity of the geometry (biological structures) or the lack of access to a machine shop (remote areas/ships/space).

The thesis's central theme was to create a 3D model of the aortic valve as an educational tool for cardiac surgeons specifically for aortic valve repair techniques. The motivation behind this focus was based on collaboration with a cardiac surgeon (Dr. Dominic Parry) to develop an experimental setup that can help surgeons improve their surgical skills by training on relatively inexpensive educational models. Currently, surgeons use animal hearts in wet labs for surgical skills training (Izawa et al., 2016; Schachner et al., 2007; Swindle et al., 1988; Tsang et al., 2016). This approach is viable but not ideal since animal heart anatomies and pathologies are not identical to those of humans. Also, wet labs can have relatively high trainees to training samples ratio, such as four to five trainees working on one sample. Moreover, tissue utilization protocols may be necessary to handle animal

tissues for training purposes. Another approach is to use cadavers, which are post-mortem human tissues. Using cadavers is considered the gold standard in surgery simulation training because those cadavers accurately represent human anatomies and pathologies (Badash et al., 2016). However, cadavers are post-mortem tissues that require tissue utilization protocols as well as careful processing and storage. Some of the challenges involving using cadavers include their high costs, special training environment (wet labs), and limited availability. Other options included virtual reality and robot-assisted simulators; however, they are extremely expensive (Badash et al., 2016).

Recent developments in additive manufacturing technologies have made them suitable for the rapid prototyping of surgical training simulators. Yoo et. al, showcased cardiac surgical training sessions using training models with compliant polymer materials manufactured using polyjet 3D printers (Yoo et al., 2017). The surgeons' feedback was very positive regarding the models. The researchers' approach was to use patient-specific CT or MRI scans to create the models. The resolutions of the CT and MRI images were not high enough to represent smaller heart tissues such as the valves and the chords. 3D printing highly compliant materials require special printers and materials. The costs of that equipment are expensive. Cardiac surgeons sometimes use inexpensive materials to create low to mid-fidelity training simulators (De Raet et al., 2013; Hossien, 2015; Hossien et al., 2016). Such models have included construction from affordable materials, such as straws, sponges, tins and plastic boxes. Although the costs are very low, the models are limited in terms of the geometry representations and the scope of the surgical skills that can be trained.

1.2. Research Proposal and Objectives

The purpose of this work was to use rapid prototyping techniques (e.g., 3D printing) to create physical models that can represent the geometries and mechanical response of the cardiac tissues with high fidelity. These models can then be used for surgical skills training. The cardiac tissue of interest was the aortic root. This cardiac tissue presented an interesting situation when it comes to surgical repair interventions. For instance, the gold standard and treatment of choice for aortic valve stenosis and insufficiency (two major categories of aortic valve diseases) were valve replacement (Augoustides et al., 2010). However, according to David and colleagues, the treatment of choice for aortic valve insufficiency is now valve-sparing surgical repair (David et al., 2015). The purpose of this project was to address these valve-sparing techniques. This project did not address pathologies that typically require the replacement of the aortic valve with an artificial valve or graft.

This thesis project focused on exploring the application of a reverse engineering workflow in the medical field by creating educational surgical skills training tools for cardiac surgeons using rapid prototyping techniques such as additive manufacturing. O'Brien et al. (2016) reviewed the application of additive manufacturing in medical education including 68 applications divided into three categories: 1) patient-specific models for pre-operative planning, 2) printing training devices for simulation-based medical education and 3) 3D printing moulds for casting soft model parts (O'Brien et al., 2016). Most of the applications were concentrated on the pre-operative planning models and the simulation models. In

contrast, not many applications were using the moulds casting method. I proposed to explore all these areas of application in the thesis project.

A seminar hosting a panel of expert cardiac surgeons was held in 2015 regarding aortic valve repairs (David et al., 2015). Some of the key points included that valve-sparing surgery is the treatment of choice for a patient with aortic valve insufficiency including bicuspid valve pathology. The panel also discussed some of the challenges related to the aortic valve-sparing procedures including aortic root remodelling and aortic valve reimplantation (David et al., 2015). The discussion covered the cases that are suitable for each procedure as well as some of the steps involved in each operation, such as measuring the graft used for the repairs. Also, Dr. El Khoury stated the aortic root remodelling was less teachable compared to the reimplantation procedure (David et al., 2015). Some of the challenges regarding the remodelling procedure included excessive bleeding due to long suture lines and the need to include additional repair steps such as annuloplasty, which is reinforcing the aortic valve by suturing a ring around it. Therefore, the surgeons can benefit from training on a synthetic aortic valve model to enhance their proficiency in these operations.

The thesis project objectives were the following:

1. Create a CAD model of the aortic valve.

2. Select suitable materials for manufacturing. This step included testing the mechanical properties of the aortic valve and surrounding regions to identify the best materials for direct 3D printing and moulds casting. The subsequent step was to compare both manufacturing approaches in terms of cost and model performances.
3. Produce an aortic valve educational model that is suitable for surgical training.
4. Evaluate the performance of the aortic valve educational model by conducting surgical training sessions.

1.3. Research Contributions

The research contributions from this work were the following:

1. Investigated a reverse engineering workflow to obtain the geometry of the aortic valve for patient-specific models.
2. Created a general 3D model of the aortic valve.
3. Conducted mechanical testing of aortic tissues and synthetic materials to select suitable materials for manufacturing an aortic valve training model.
4. Produced a functional aortic valve educational tool for surgical skills training that was evaluated by cardiac surgical residents.
5. Proposed plans for aortic valve model evaluation for training sessions.

1.4. Thesis Document Outline

The document was written based on the major tasks that were undertaken to fulfill the research objectives. The objectives were divided into four main stages: creating a CAD model, choosing a suitable material for the model, model manufacturing and model testing. The first stage involved investigating two methods to create the CAD model of the aortic valve. Those methods were patient-specific CAD models and general CAD models. The end objective was to create a physical aortic valve model that can be tested by cardiac surgeons. Therefore, it was essential to choose suitable materials and manufacturing methods. Finally, the model had to be tested by cardiac surgeons in a training session.

The following are descriptions of each chapter:

Chapter 1: Introduction

The introduction included a brief description of the main components of the research project. Those components were the research motivation, research objectives, contributions and the general structure of this document.

Chapter 2: Background

Information regarding the literature review was included in this chapter. The research was about creating an aortic valve model as an educational tool for cardiac surgical skills training. Therefore, background information about the aortic root anatomy, pathologies and surgical repairs were included as well.

Chapter 3: Development of Aortic Model and Manufacturing Process

The information included in this chapter was related to the complete cycle of creating an aortic valve training model from model design to manufacturing. The chapter was divided into three parts including patient-specific model (Part 1), general model (Part 2) and aortic valve model manufacturing (Part 3). In Part 1, a CAD model of a patient-specific aortic valve was obtained. In Part 2, a general aortic valve CAD model was developed. Finally, Part 3 included the manufacturing processes done to produce the aortic valve model.

Chapter 4: Mechanical Testing of Aortic Tissues and Manufacturing Materials

Data for the mechanical properties of the aortic valve are available in the scientific literature, but the focus is on properties under tensile loading. The information on the forces required to cut or puncture aortic tissue during surgical repairs is limited and is insufficient to guide material selection for creating surgical training models. The testing provided information on how the suturing needle and scalpel blades interacted with the materials and how the force of cutting varied among them. This was important because based on this data, materials with similar properties were chosen for manufacturing.

Chapter 5: Educational Model Evaluation

This chapter included the plans developed to evaluate the surgical training model through training sessions and surgeon feedback.

Chapter 6: Conclusion and Future Work

The final chapter of the document included a summary of the takeaways from the research as well as the future direction of the research.

Chapter 2

2. Background

2.1. Literature Review

Many aspects of surgical skills training can be challenging such as procuring suitable testing materials and the lack of suitable training models. In cardiac surgery, surgeons typically use animal hearts for simulation training (Lodge & Grantcharov, 2011). This is because on-patient hands-on training can be very risky. Animal hearts are not ideal because they do not have the same pathologies found in human hearts. Also, having different anatomies can make the training less realistic using those animal hearts. For those reasons, there is a need for adequate simulation training models. Also, adequate training models can contribute to increasing the technical proficiency of the surgeons. There is a negative correlation between mortality and morbidity after congenital heart surgery and the technical proficiency of the cardiac surgeon (Yoo et al., 2017). Moreover, the number of congenital heart surgeries performed by the cardiac surgeon and the institution are also components of this correlation (Yoo et al., 2017).

Operative confidence can be an important influencing factor regarding the need for simulation training. A survey conducted by Fonseca and colleagues regarding the operative confidence of 5th-year general surgery showed that about 72% of 653 surgeons had expected post-residency confidence (Fonseca et al., 2014).

Most surgeons (95%) were confident in doing basic laparoscopy, but only 57% reported having confidence performing an advanced laparoscopy. Also, the surgeons' operative confidence dropped to 18% for common bile duct exploration surgery. In cases more specific to cardiac surgery, it has been demonstrated that simulation training can improve surgical skills and surgeon confidence (Feins et al., 2017; Mokadam et al., 2017).

A meta-analysis study conducted by Ribeiro and colleagues concluded that improved learning outcomes for cardiac surgical trainees are associated with simulation training (Ribeiro et al., 2018). Another possible advantage of using simulation training is that it can be done independently without supervision (Enter et al., 2015). Their study concluded that the achievement of the competency in basic cardiothoracic task training is similar between supervised trainees and unsupervised trainees using low fidelity task simulators and task training orientation. It is possible that simulation training benefits can extend to different members of a medical team beyond the physicians. In a study about using 3D printed cardiac models after congenital heart surgery, Olivieri and colleagues demonstrated that simulation training benefits not only physicians but also nurses and ancillary healthcare givers (Olivieri et al., 2016).

Using physical 3D models for simulation training can be effective, and lead to improvements in technical skills. This is supported by a study by Yoo and colleagues (2017) who used 3D printing for congenital heart surgery training (Yoo et al., 2017).

The materials and methods used in this study included using CT scans to acquire the geometry of the heart, computer-aided designs of different congenital heart pathologies, and 3D printed models using a compliant polymer material. Key findings of the study included that using 3D printing for simulation training can improve technical skills and that different pathologies can be successfully produced using this approach. Also, the study pointed out that the touch and feel of the 3D printed models as well as the realistic representations of the heart valves were highly relevant to the fidelity of the models. The limitations of the study included high production costs and demanding labour-intensive processing of the models. Also, the study was limited to patient-specific pediatric cardiac tissues.

The educational tools proposed in this research project were centred around creating a 3D printed model of the aortic valve. This research focus was supported by Dr. Dominic Parry who was a cardiac surgeon at Hamilton General Hospital. Additionally, a study conducted by Baker and colleagues regarding the development of a cardiac surgery simulation curriculum determined that it can be helpful to create aortic valve simulation training (Baker et al., 2012).

Simulation in healthcare education has many barriers including an increased need for financial support, the need for a dedicated simulation technician, and the need for collaborations (Qayumi et al., 2014). This research was an attempt to add to the efforts in clearing some of those barriers in Canada. This can be realized by creating relatively simple

educational tools that can be operated without the need for dedicated technicians. However, educational models cannot be adequately developed without the involvement of cardiac surgeons and institutional support. Therefore, a collaboration between McMaster University and Hamilton General Hospital can add tremendous value to this endeavour.

The scientific literature supports the theory that simulation training can have positive impacts on the surgeons' technical skills (Ribeiro et al., 2018). However, much needs to be done to improve the quality of the simulations. Major challenges in developing simulation training include selecting materials that mimic the feel and behaviour of real tissue and creating cost-effective models that are suitable for scalability to accommodate training repetition easily. Also, creating educational models for cardiac tissues such as the aortic valve has yet to be fully researched.

The objective of this research was to create aortic valve educational tools of high fidelity. This meant that generally, the model had to be highly realistic in resembling real tissues. In this research, measuring the fidelity of the model was done by comparing the model geometries to those of human hearts and the mechanical behaviour of the interaction between the surgical tools and the materials of the model to those values of porcine tissues. Also, the evaluation of the model by cardiac surgeons was a critical factor. For instance, if a model were to be acknowledged by the cardiac surgeons to be of high fidelity, had accurate geometry and no significant statistical differences compared to porcine tissues under surgical tools manipulation, then the model would be considered of high fidelity. The

usefulness of high-fidelity (using the general definition) models in cardiac surgery simulation has been reported by Mokadam and colleagues (Mokadam et al., 2017). Most of the residents and faculty members surveyed in that study deemed high fidelity models to be extremely useful. Additionally, Sidhu and colleagues determined that there was a correlation between skills acquisition and the fidelity level of the model in laboratory-based vascular anastomosis training. The results were that training using high fidelity models could increase skills acquisition better than low fidelity models (Sidhu et al., 2007).

The following sections will briefly provide background information regarding the aortic valve. The goal is to introduce the aortic valve cardiac tissues and discuss some of its key pathologies and how they are typically treated.

2.2. Aortic Valve Background

2.2.1. Aortic Valve Anatomy

The cardiac tissue of interest in this project was the aortic valve, which is one of the four main valves inside the heart (Figure 2.1). Located on the left side of the heart (known as the “systemic” side of the heart), the aortic valve is a gateway for the oxygenated blood to be pumped to most of the body through the aorta. The opening and closing of the aortic valve are governed by differences in pressure between the left ventricle and the aorta. In the cardiac cycle of the left ventricle, blood flows from the left atrium to the left ventricle by passing through the mitral valve. After that, the left ventricle contracts leading to

increasing pressure (systole). When the pressure inside the left ventricle is more than the pressure inside the aorta, the aortic valve leaflets open to allow the blood to go through. The aortic valve closes passively when the pressure in the left ventricle drops below the pressure in the aorta. Finally, the left ventricle relaxes and expands (diastole) causing a decrease in the pressure and allowing blood to enter again from the left atrium. The significance of the aortic valve can be inferred from its functionality as it acts as a gateway that supplies the whole body with blood. Moreover, the aortic valve is connected to the coronary arteries via the leaflets.

The coronary arteries are responsible for supplying the heart with the necessary blood to function. Figure 2.1 shows the anatomy of the heart's valves with visual representations of key areas in each valve such as the leaflets and cords.

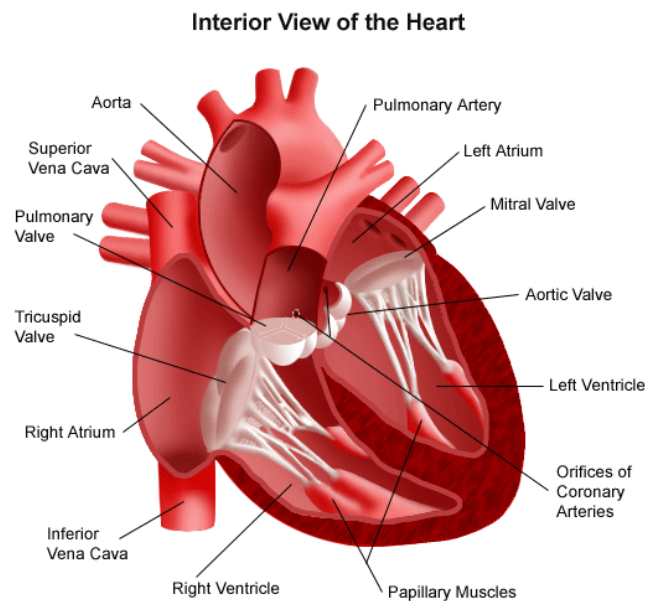
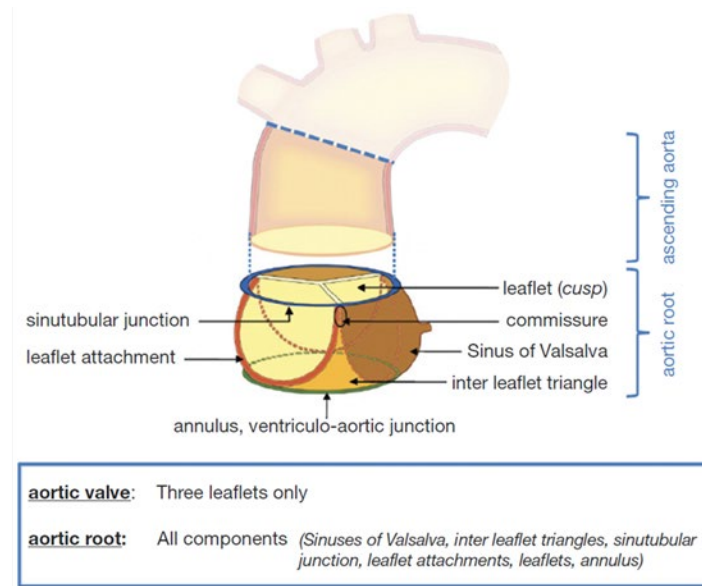


Figure 2.1. Heart valves anatomy (Ulrich, 2012).

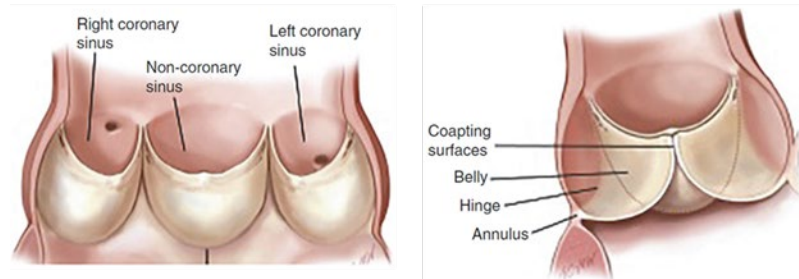
The original research direction started with a focus on the mitral valve cardiac tissue. The shift of focus to the aortic valve was done after meeting with Dr. Dominic Parry (Hamilton General Hospital Cardiac Surgery Dept.). The decision was made after comparing the mitral valve and the aortic valve in terms of the complexity of the geometry and pathology. A major difference between the aortic and mitral valves is the presence of very fine cords (the chordae tendineae) as an integral structure of the mitral valve apparatus. Moreover, compared to the aortic valves mitral valve leaflets have relatively complex surfaces.

The aortic valve is composed of three separate leaflets that press together (coaptation) to form the valve seal. The relative simplicity of the geometry and the possibility to mimic different variations of the valve made the aortic valve a suitable introductory case to cardiac tissue modelling. Thus, we decided to focus on the aortic valve in this research.

The aorta anatomy can be divided into three distinctive sections: aortic valve, aortic root and ascending aorta. Figure 2.2 shows the anatomy of these sections with more emphasis on the aortic valve. Beginning from the bottom of the aorta, the aortic valve (only the three leaflets) separates the aortic root and the left ventricle. The valve is surrounded by the ventriculo-aortic junction (VAJ), which separates the aorta and left ventricle walls. The aortic valve is attached to the aortic root by the annulus.



A



B

Figure 2.2. Aorta anatomy, A. Aortic root and ascending aorta (Charitos & Sievers, 2013), B. Internal anatomy of aortic valve leaflets (Schubert & Ghanta, 2016).

The portions of the aortic wall enclosed by the aortic valve leaflets and annulus are known as the sinuses of Valsalva. These sinuses have thinner wall thickness compared to the rest of the aorta and have unique curvature shapes. The valve leaflets are joined by commissures. The area between the commissure, leaflet attachment and VAJ is the inter leaflet triangle. Finally, the aortic root and ascending aorta are separated by the sinotubular junction (STJ). Although the components of the aorta are relatively simple when inspected individually, their collective functions are very complex.

The smallest changes in any component can affect the optimum performance of the whole structure (Charitos & Sievers, 2013). For example, the aortic valve has a natural anomaly that can occur in 1-2% of the population known as a congenital aortic valve or the bicuspid aortic valve (Schubert & Ghanta, 2016). In this case, two of the three aortic valve leaflets are joined together instead of the normal case of three separate leaflets.

2.2.2. Aortic Valve Pathologies

The main aortic valve diseases are a congenital bicuspid aortic valve, aortic valve insufficiency (regurgitation), and aortic valve stenosis. In this research, the only diseases that are covered are functional pathologies that primarily affect the geometric arrangement of the aortic valve; for example, aortic aneurysm and loss of coaptation (a sealing mechanism) of the aortic valve leaflets. These pathologies are signs of a possible aortic valve insufficiency condition that can be treated via a valve-sparing procedure. In contrast to functional pathology, degenerative pathologies such as aortic valve stenosis are

associated with a change in tissue mechanical properties due to calcification of the valves. These degenerative pathologies were not the focus of this research since they typically require aortic valve replacement.

The presence of a congenital bicuspid condition can lead to the development of other aortic valve diseases. The main pathology of interest in this research was the aortic aneurysm as it was an example of a functional pathology that can be treated via valve-sparing procedure.

2.2.2.1. Aortic Valve Bicuspid

The aortic valve bicuspid is a common anatomic variant of the aortic valve. In this anomaly, two aortic valve leaflets are joined together as one leaflet. Optimal blood flow from the left ventricle into the aorta requires three separate leaflets, and so the fusion of two leaflets in the bicuspid variant can affect the performance of the aortic valve. Found in 1-2% of the population, the bicuspid valve is responsible for the development of almost 50% of aortic valve stenosis and is a possible cause of aortic valve insufficiency (Schubert & Ghanta, 2016). The most common bicuspid configuration is the joining of the right and left coronary leaflets. Another less prevalent configuration is the joining of the right coronary and non-coronary leaflets (Schubert & Ghanta, 2016).

The bicuspid aortic valve can have only two symmetric leaflets rather than one free leaflet and two fused leaflets configuration. This type is called type 0 bicuspid aortic valve as seen in Figure 2.3 A. Other variations of the bicuspid aortic valve involve two leaflets joined by a raphe (biological seam marking the area between the cusps). These variations fall within type 1 bicuspid aortic valve cases (Figure 2.3 B and C) (Boodhwani & El Khoury, 2009).

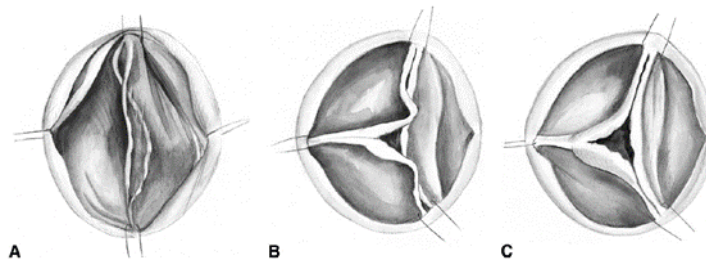


Figure 2.3. Bicuspid aortic valve types: A) Type 0, B) Type 1 prolapse, C) Type 1 restriction (Boodhwani and El Khoury 2009)

2.2.2.2. Aortic Valve Stenosis

Calcium and scar tissue build-up can cause the aortic valve leaflets to become inflamed and stiff. This degenerative change in the leaflets is what is known as stenosis. Aortic stenosis results in the obstruction of the blood flow to the aorta causing the heart to work harder to pump the blood. Aortic stenosis diseases can take decades to develop as severe cases fully and might not have apparent symptoms (Nishimura, 2002). Figure 2.4 B shows an example of aortic valve stenosis.

2.2.2.3. Aortic Valve Insufficiency (Regurgitation)

In a normal aortic valve, the left ventricle contraction (systole, Figure 2.4 A.) and relaxation (diastole, Figure 2.4 C.) pump the blood without any obstructions or backflow issues. However, in the aortic valve insufficiency, the aortic valve leaflets do not fully close during diastole causing some of the blood to backflow from the aortic root to the left ventricle. This backflow phenomenon can cause the heart to work harder to pump the same amount of blood. An example of this condition can be seen in Figure 2.4 D.

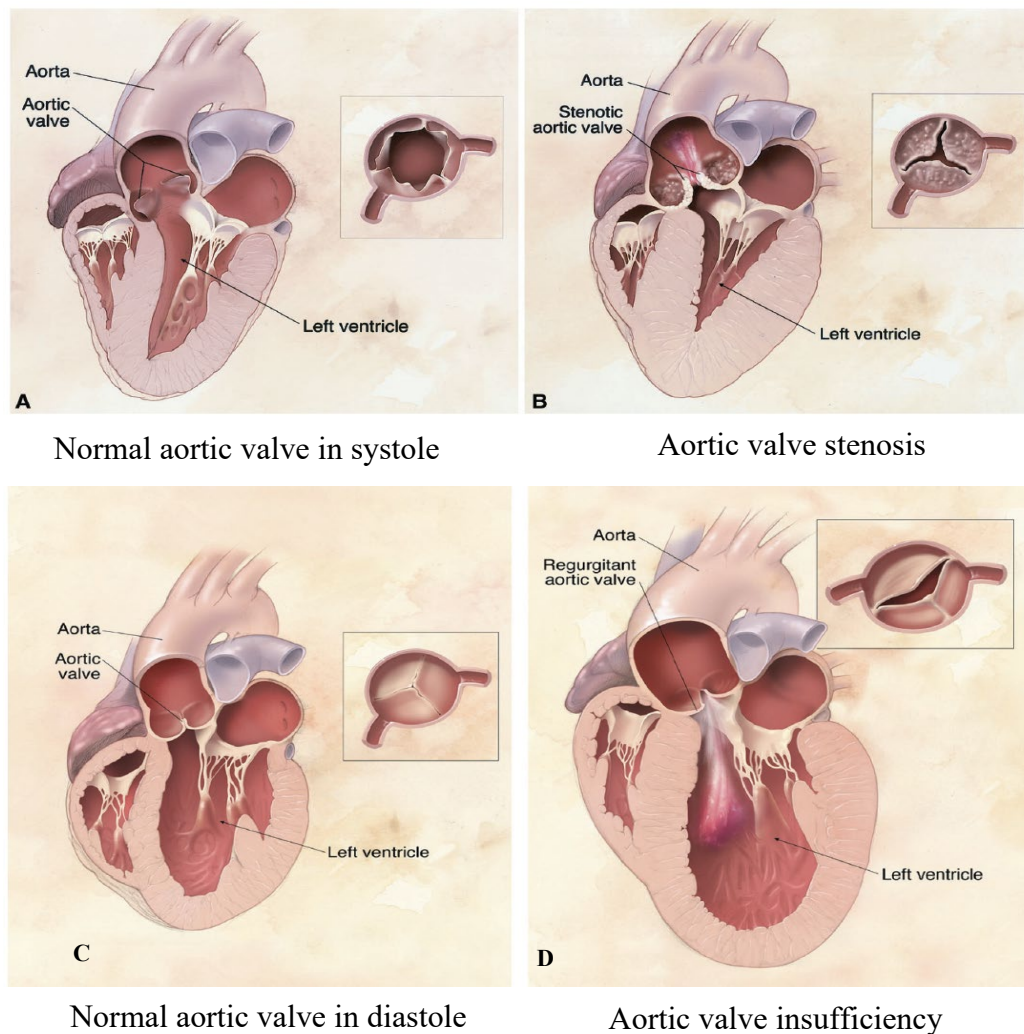


Figure 2.4. Aortic valve diseases (Nishimura 2002)

Compensating for additional pumping requirements can lead to left ventricle abnormal enlargement as seen in Figure 2.4 B (Nishimura, 2002).

2.2.2.4. Aortic Aneurysm

An aneurysm is defined as a local dilation of the aorta that is more than 50% of the predicted dimensions (Heart et al., 2015). The aneurysm can occur anywhere along the aorta sections including the root, ascending, arch and descending sections. The ascending aorta aneurysm could affect the aortic root, and it accounts for more than 50% of the thoracic aortic aneurysm (TAA) cases (Heart et al., 2015). Figures 2.5 and 2.6 show illustrations of the ascending aorta and aortic root aneurysms pathologies.

The traditional approach to treat aortic valve pathologies was to replace the valve with a prosthetic valve (Tian et al., 2013). However, this is no longer the case in treating aortic pathologies that were suitable for valve-sparing operations (Tian et al., 2013). Those valve-sparing operations would preserve the aortic valve to reduce the possibility of re-operation and to eliminate the need to take anticoagulation medication (life long medication while having a prosthetic aortic valve) (Tian et al., 2013). Figure 2.6 shows the surgical repairs.

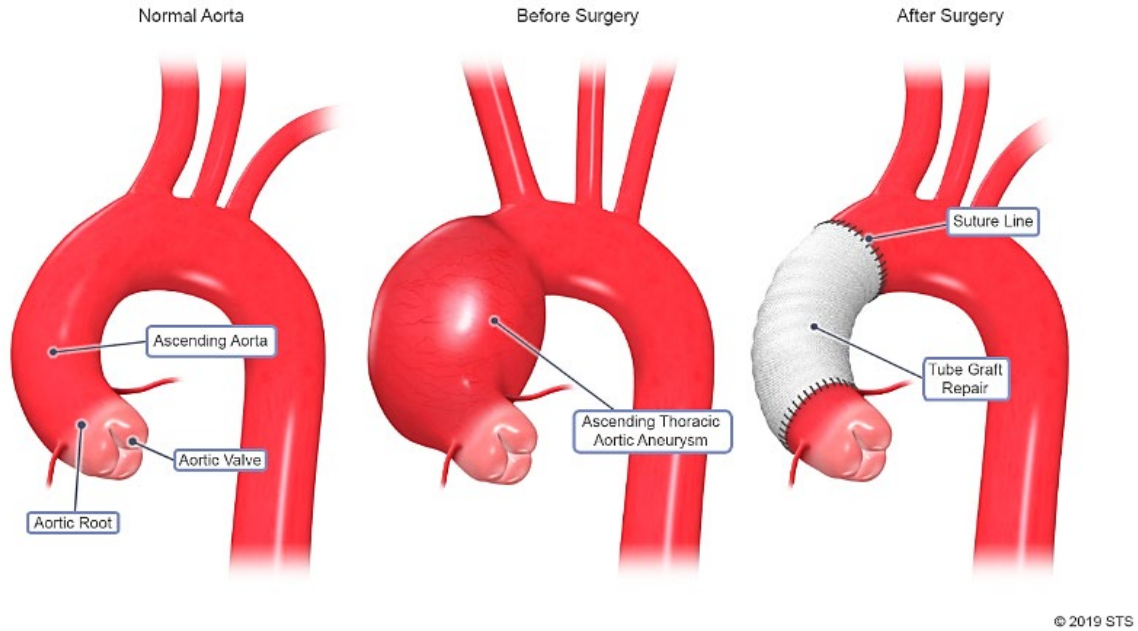


Figure 2.5. Ascending aorta aneurysm (Thoracic Aortic Aneurysm, 2019).

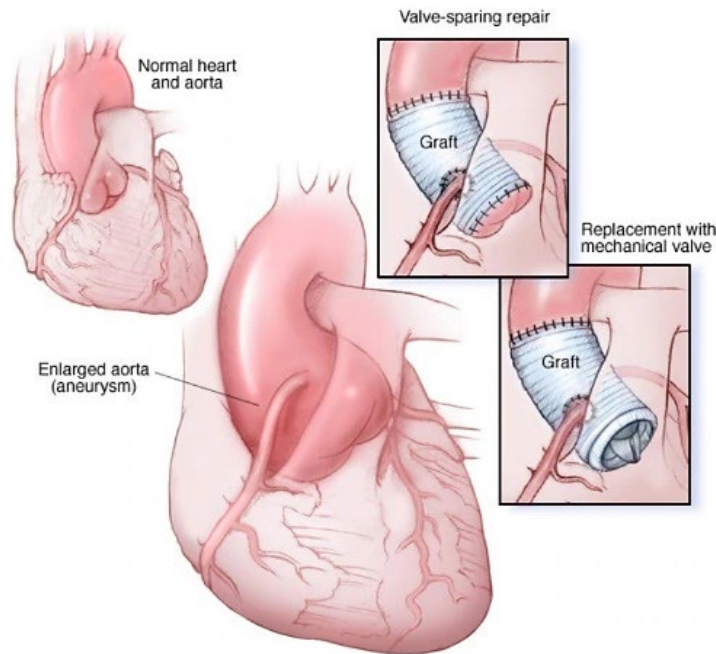


Figure 2.6. Aortic root aneurysm (Aortic Root Surgery, 2015).

2.2.3. Aortic Surgical Repairs Strategies

Surgical repairs are only considered for aortic valve insufficiency. For many years, the gold standard was valve replacement as the option to consider for aortic valve diseases (Augoustides et al., 2010). Even now, some of the aortic valve conditions such as stenosis cannot be adequately treated without valve replacement. Recently, aortic valve-sparing repairs became widely adopted with promising results (David et al., 2015). The advancement of aortic valve repairs is the result of a better understanding of the anatomy and the proper classification of the pathologies and how to repair them (Boodhwani & El Khoury, 2009). These procedures require important skills training for the surgeons so that they can develop proficiency in the repair and grafting procedures.

A key step toward realizing the overall objective of the thesis project was to create a physical model of the aortic valve that can replicate different pathologies that would allow surgical trainees to practice the repair procedures. Boodhwani and El Khoury summarized the main aortic valve insufficiency pathologies in Figure 2.7 (Boodhwani & El Khoury, 2009). This summary provided a range of possible pathologies that could be used in the aortic valve training model.


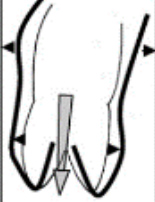
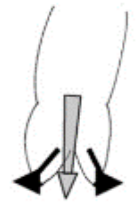

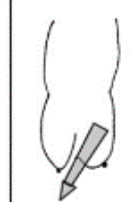

AI Class	Type I Normal cusp motion with FAA dilatation or cusp perforation				Type II Cusp Prolapse	Type III Cusp Restriction
	1a	1b	1c	1d		
Mechanism						
Repair Techniques (Primary)	STJ remodeling <i>Ascending Aortic Graft</i>	Aortic Valve sparing: <i>Reimplantation or Remodeling with SCA</i>	SCA	Patch Repair <i>Autologous or bovine pericardium</i>	Prolapse Repair <i>Free Margin Plication Triangular Resection Free Margin Resuspension</i>	Leaflet Repair <i>Shaving Decalcification Patch</i>
(Secondary)	SCA		STJ Annuloplasty	SCA	SCA	SCA

Figure 2.7. Aortic valve insufficiency classification (Boodhwani & El Khoury, 2009)

AI : aortic insufficiency; FAA: functional aortic annulus; LCC: left coronary commissure; NCC: noncoronary commissure; RCC: right coronary commissure; SCA: sub-commissural annuloplasty; STJ: Sinotubular junction; VAJ: Ventriculo-aortic junction.

Aortic valve-sparing surgeries (Figure 2.8) that do not involve aortic valve cusp diseases are mainly divided into the aortic valve reimplantation technique (reimplantation) and aortic root remodelling technique (remodeling). Both techniques can be used successfully to treat aortic root aneurysms using tubular Dacron™ (DuPont, Wilmington, DE, USA) grafts. The reimplantation technique focuses on excising the sinuses and the aortic valve from the aortic root while also detaching the coronary arteries.

Then, the aortic valve is implanted inside a Dacron graft. On the other hand, the remodelling technique uses a tailored graft to remodel the aortic root. Reproducing aortic valve sparing surgeries can be challenging given the complex nature of the surgical steps (David, 2016).

The purpose of my work was to create a 3D model of the aortic root that can be used for surgical skills training. The reimplantation and the remodelling surgeries involve excising and suturing aortic tissues as well as graft insertion. These tasks can be done on my 3D model. Please refer to Chapter 5 for more details.

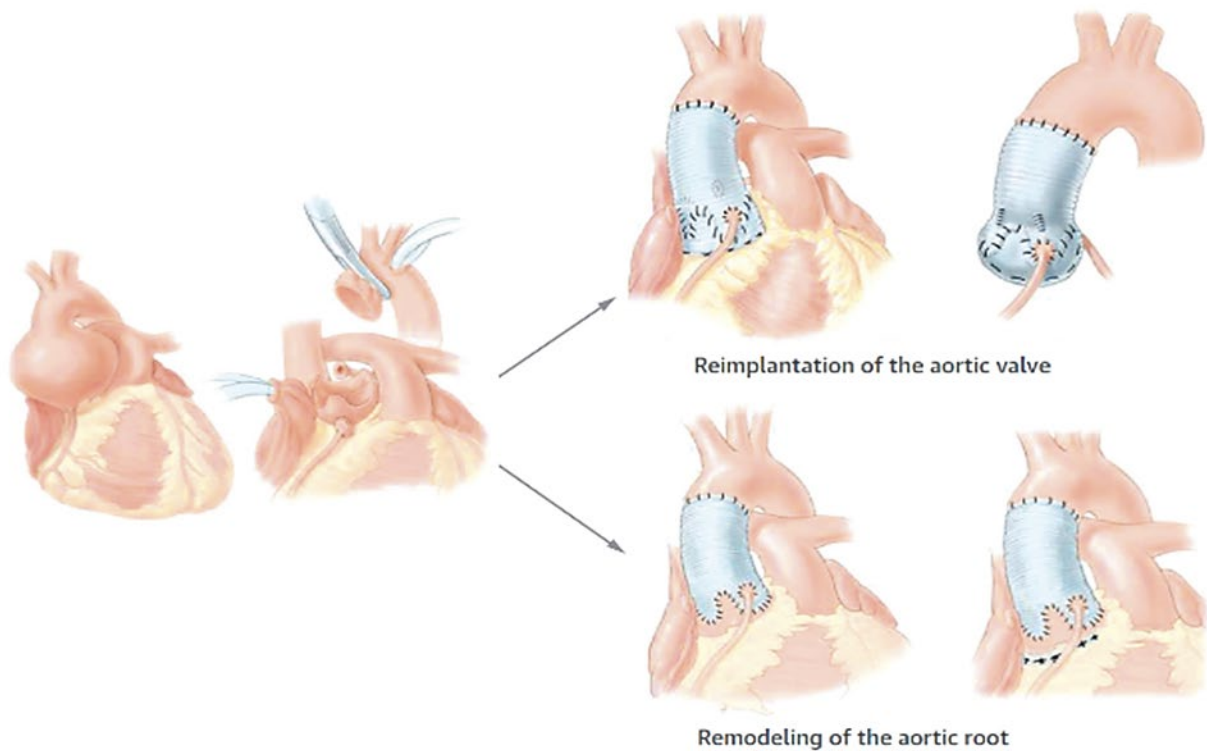


Figure 2.8. Aortic valve sparing surgical repair strategies (David, 2016).

2.3. Manufacturing Methods Background

2.3.1. Additive Manufacturing

Additive Manufacturing (AM) is a process that involves generating 3D parts by adding layers upon layers of materials. The process relies on Computer-Aided Design (CAD) models as an input to create the desired geometries. The CAD models provide cross-sectional geometric information that is essential for the layered-based approach of AM. Hence, the contour and layer/slice thickness are produced accordingly. AM is a very flexible process since it can be done at any stage of the product development cycle without affecting other processes. Many build materials can be used for AM, but those materials are proprietary and usually associated with specific machines. This can impose some limitations on using AM for the time being. Future developments can overcome this limitation especially if the AM market can attract suppliers of novel build materials. The fundamental principles of AM include two steps: 1) generating a single layer based on contour and slice thickness, 2) joining each layer with the preceding layer.

These fundamental principles are carried out by five main AM processes that include the following:

- Polymerisation / Stereolithography
- Laser sintering / Laser melting
- Layer-laminate manufacturing
- 3D Printing
- Fused laser manufacturing

The standard layer thickness in AM is about 0.1 mm. However, small layer thickness such as 16 μm can be achieved as well. High precision AM processes require more build time. The type of build materials can affect the layer thickness (hard metals require more processing and greater input energy).

The main differences among AM commercial machines can be addressed by the following questions:

- How is each layer made?
- How successive layers are merged?
- What material is processed?

For example, layer generation requires an energy source. For instance, laser sintering 3D printers use laser sources to process metals, while FDM 3D printers use an electric heating system to process polymers.

The following section includes a summary of the main AM processes used in this research specifically polymers-based AM processes (Gebhardt, 2011).

2.3.1.1. Polymerization

The polymerization AM process is defined as using ultraviolet radiations to solidify selectively or cure the monomeric liquid resin. This liquid resin can include epoxy, vinyl or acrylate. Polymerization (also known as photopolymerization) includes several processes such as laser-stereolithography, polymer printing and jetting and digital light processing. The main differences in these processes are in the layer generation (contouring)

and how the UV radiations of the curing process are applied. The curing process can affect the part processing time. For example, some processes produce green parts that are not fully cured and require a post-curing oven to solidify fully. In contrast, some processes apply full curing during the part building process. The type of materials used in the AM process can play a key role in the stability of the model and post-processing. Polymerization-based AM processes require support to fix the model on the building platform and ensure a connection with all design components. Moreover, preventing warping and distortion is also required and can be achieved by using the same support. The consequences of this requirement are that the support needs to be included in the CAD model at the design stage and manually or automatically removed in post-processing.

2.3.1.2. Extrusion – Fused Layer Modeling

Fused Layer Modeling or Fused Deposition Modeling (FDM) is an AM process that uses deposited strings of pasty building materials to create the part layer by layer. Building materials include PLA, ABS and PC-ABS. Other materials include coloured and special grade materials for medical applications. This process requires support that can be removed either manually or automatically using a special washing device. Moreover, instead of a laser source, FDM uses an electric heating system to heat the materials before they are deposited by the nozzle. The produced parts show anisotropic behaviour and are affected by positioning during the buildup process. FDM processed parts can be used as concept models, functional prototypes or as final parts.

2.3.1.3. The Benefits of Additive Manufacturing

1. Just in Time Manufacturing.

The process flow is quite simple as it only requires sending an STL file of the CAD design to the AM contractor. This contrasts with the conventional manufacturing methods, which require more preparations, such as creating drawing files and procuring the raw materials separately. Therefore, AM provides the convenience to manufacture any part anywhere without the restrictions of the conventional machine shop.

2. Patient-Specific Models – Excellent for Surgical Planning on Complex and Unique Cases.

Currently, 3D-printed cardiac models are based on patient-specific data for pre-operation planning in preparation for valve replacement operations. For instance, Jung et al. 3D printed a patient-specific aortic valve for aortic stenosis cases (Jung et al., 2016). Additionally, Ripley et al studied a population of 16 patients to produce 3D printed models that can be used for transcatheter aortic valve replacement (TAVR) pre-planning and predict paravalvular aortic regurgitation (PAR) (Ripley et al., 2016). Figure 2.9 shows samples of those 3D-printed valves.

Additive manufacturing is mainly used for surgical planning in many cases. This may result in creating 3D printed models with specific design intentions such as measuring the diameter of the aortic root before and after the operation. On the other hand, additive manufacturing using mould casting has yet to be explored for the aortic valve. The limited

control over the mechanical properties of AM materials, in general, is one of the major challenges in developing training models (O'Brien et al., 2016). Some researchers attempted to address this challenge by 3D printing using dual materials. However, there is not enough information regarding how to fine-tune and control the properties of the materials of such a method. Another closely related challenge is capturing the geometry of the aortic valve leaflets. Due to their small and delicate structures, they are challenging to measure, model, and manufacture.



3D printed aortic valve showing right coronary artery and the left main artery (Ripley et al, 2016)



Aortic Valve Stenosis (Jung et al., 2015)

Figure 2.9. 3D printed aortic valves.

3. Incorporation of Multiple Materials in One Build.

Another advantage of AM is the ability to use multi-materials during the manufacturing process. This could provide more flexibility in the manufacturing process as it is not necessary to do extra steps to produce the model.

2.3.1.4. The Limitations of Additive Manufacturing

1. Inadequate Material Behaviour for Current Additive Manufacturing Materials.

The limited options of compliant materials are a key limitation when using the AM method. Also, the mechanical properties of AM materials are strain-softening at higher strain values (around 10%) (Wang et al., 2016). On the other hand, the biological tissues exhibit strain-hardening behaviours due to the presence of collagen fibres (Wang et al., 2016). Although AM materials can mimic the behaviours of biological tissues at lower strain values (less than 3%), their usage can be limited if the application requires a high degree of fidelity, such as in creating patient-specific models for pre-operational planning (Wang et al., 2016).

2. Anisotropy of Failure Properties.

The AM process is based on building a layer on top of another layer to manufacture a part. This process introduces many parameters that control the quality of the manufacturing such as the build orientation, layer thickness, percent infill support, and infill pattern. Also, other parameters are usually outside the control of the user such as the filament properties and 3D printers' specifications (e.g., dimensions, electronics etc.).

For example, each filament would be manufactured according to certain guidelines by the manufacturer resulting in specific materials properties (e.g., hardness, stiffness and tensile strength). Thus, modifying those properties is not typically done by the user. All the controllable parameters can influence the mechanical properties of the AM part. Behzad et al. demonstrated that there was a significant difference in strength between 0.2 mm and 0.4

layer thicknesses in which the 0.2 mm layer was stronger (Rankouhi et al., 2016). Also, Kim and Oh showed that the build orientation can significantly impact the tensile strength of the additive manufactured part for several AM processes (Kim & Oh, 2008). Therefore, the build quality can vary greatly depending on the parameters used. This can make the failure of the part anisotropic and unpredictable. An example of 3D printing part failure is the layers splitting due to poor layer thickness and temperature control.

3. High Cost Per Model.

The high-cost aspect of the AM is most apparent when using specialized printers and materials. For instance, using a hobby-grade 3D printer can be relatively inexpensive for printing PLA (polylactic acid, generic non-specialized material) since it was possible to procure the filament and the printer for less than C\$1000. However, a single TangoPlus Fullcure 930 (similar to the material tested in Chapter 4) cartridge was significantly more expensive at about C\$1800. Also, the printer cost was significantly more expensive since the TangoPlus material can only be used by mid-range printers provided by Stratasys. The starting price for those mid-range printers was C\$20,000 according to the Computer-Aided Technology website (*3D Printer Price - Stratasys 3D Printers*, 2020).

Thus, for practicality, it was more cost-effective to request AM services from a company for small AM jobs than to purchase a mid-range 3D printer. The average cost per model varies depending on factors, such as the material used and volume of production. For the typical volumes required for cardiac tissues, the cost was around C\$200 per model according to Oliveri et. al. (Oliveri et al., 2016). Moreover, the cost for AM the models in

this research was around C\$280 per model. These costs were significantly more expensive compared to models produced using casting.

4. Patient-Specific Models – Additive Manufacturing Limitations.

Patient-specific models are not as comprehensive as they tend not to have key structures such as the leaflets. The typical spatial resolution range for CT scans commonly used for cardiovascular structures ranges from 0.3 to 0.7 mm (S.-J. Yoo et al., 2016). The CT scans cannot adequately capture the delicate structures such as the leaflets and the chords due to the technology limitations as these structures require higher resolution (S.-J. Yoo et al., 2016). Also, patient-specific models are labour-intensive to create. The CT scans need to be segmented to extract the geometry of the cardiac tissues. The segmentation process requires knowledge of the cardiac tissues to identify the geometries correctly. This process involves an extensive trial and error approach to adequately produce a segmented model. Due to the technical limitations of the CT scans, the walls of the cardiac structures are very challenging to capture and they require additional interpolations and processing (S.-J. Yoo et al., 2016). After that, the model needs to be converted to STL format in preparation for the printing. This conversion process would require CAD knowledge as the segmented model may require further modifications. The amount of manual work and technical expertise required to produce a patient-specific model as well as the high production cost are critical limitations of this method.

2.3.2. Casting of Models

The casting manufacturing process involved the use of moulds that are filled with liquid materials that undergo the solidification process. After the solidification process is complete, the final part is obtained. Casting uses a wide range of materials from metals to plastics. In this research, the materials used were silicone, polyurethane and urethane. Since casting materials showed promising results after the cutting and puncture tests, it is essential to produce a fully functional aortic valve model using a variety of casting materials.

2.3.2.1. Benefits of Casting of Models

1. Large Volume for A Low Cost – High Volume Production for Trainees.

The materials cost to produce the casted models is relatively inexpensive compared to the AM process. This enables high production strategies for a different level of production volume requirements. For instance, for low production volumes, several moulds can be additively manufactured to be used to simultaneously cast several models at the same time. The curing time depends on the casting materials used. For example, it takes around 18 to 24 hours for the silicone A10 (used in this research) to cure. However, this method is not ideal for large production volumes as the demoulding time can be relatively long. On the other hand, injection moulding can be used for high production volumes. Also, injection moulding would produce more models at a lower cost compared to AM.

2. Potential for Very High Volumes.

Casting has the potential to develop into injection moulding for very high production volumes. The same flexibility is not currently possible for AM. Yoo et al. reported that they typically use three 3D printed patient-specific models for pre-operative assessment of congenital heart diseases (S.-J. Yoo et al., 2016). Patient-specific AM models such as those developed by Yoo and colleagues are important for pre-operative assessment, which does not necessarily require large production volumes. On the other hand, a generic aortic valve AM model would be used to develop competence in more general procedures in which a large production volume is highly beneficial.

AM cost per case can be very expensive. If the same process can be done by casting, then the potential for very high-volume production can be investigated to reduce the costs and increase the quantity of the models for the trainees.

3. Flexible materials options.

Casting materials have a wide selection of compliant materials that can provide more flexibility in the model design. This was in contrast to AM in which the compliant materials options were limited.

2.3.2.2. Limitations of Casting of Models

1. Less Flexible for Changing Part Design Than Additive Manufacturing.

Perhaps the major limitation of casting is that it is not flexible to make changes to the part after making the mould. Therefore, if the mould design was not modular, then it is necessary to make a new mould each time any modification is required. In contrast, in AM, it is possible to make any changes to the model without any changes to the process. Designing a modular mould could help in overcoming the need to produce new moulds for each design update. This was done in this research by creating a modular design for the upper section of the mould assembly.

2. Limitations Due to The Production Process (Make A Negative to Cast).

Casting relies on making a negative mould to hold the liquid cast material. If the casted part includes internal structures, then the complexity of the process will increase rapidly. For example, in the aortic valve model case, the mould design included negative and positive interlocking parts.

The internal parts had to be secured to allow for the successful flow of the casting material. If a mould release agent was not applied or the structures were very delicate, then the demoulding process becomes particularly challenging leading to damaged casted parts. Therefore, casting requires careful considerations of how to design the mould to allow for an easy and successful demoulding process.

3. No Patient-Specific Models.

It is certainly possible to additively manufacture complex shapes without any major issues. Also, this could be applicable for the mould design in casting since the mould can be additively manufactured too. However, a complex mould does not necessarily enable a streamlined casting process as relatively simple designs could. For instance, patient-specific models tend to be of high fidelity to capture all information on the pathology. This would require creating a complex mould that requires a series of small interlocking internal sections to produce the cast. This process can be time-consuming as the mould need to be designed and tested to ensure adequate results. Thus, creating a one-off complex patient-specific pathology using casting is not ideal. Conversely, AM is more suitable for the complex nature of patient-specific models. That is, no additional procedural steps are required in many cases for complex parts.

Therefore, the aim of the work in this project was to further evaluate the two manufacturing processes to determine which process provides a better training model. On a per-model basis, we compared the ease of production and cost of production. Then we requested feedback from cardiac surgical residents on the two different models for their training purposes. To test the materials with the surgeons, it was necessary to produce several aortic valve models using different materials. The approach was to produce the models using the softest materials in each material group. This was done to create a baseline regarding which approach to focus on in the future.

Chapter 3

3. Development of Aortic Model and Manufacturing Process

3.1. Introduction

This chapter included details regarding the complete design to manufacturing cycle to produce the aortic valve training model. The chapter was divided into three parts including creating an aortic valve model using patient-specific information (Part 1), creating a general model of the aortic valve (Part 2) and the manufacturing processes involved in producing the aortic valve models (Part 3).

In Part 1, the patient-specific model was initially realized by processing Computed Tomography (CT) scans data via the segmentation process. Image segmentation was used to extract the necessary geometric information of the contrasted blood inside the heart. The result of the analysis was an unprocessed STL model that served as the foundation of the CAD reconstruction process of the aortic valve and its surrounding regions of interest. After that, the unprocessed model was processed in SpaceClaim (SpaceClaim, Concord, MA, USA) software to reverse engineer the surfaces to create an editable CAD model.

Patient-specific aortic valve models are useful, but they represent specific cases. Also, manipulating reverse engineered geometries was challenging. Therefore, investigating another method to create an aortic valve CAD model was carried out.

This second method had to provide a general simplified CAD model. Part 2 included details about the process of creating a general CAD model, such as the geometric information required and the CAD construction process. Since the aortic valve is a complex organic structure, it was challenging to represent the valve geometry using prismatic shapes. Therefore, NURBS (Non-Uniform Rational Basis Spline) curves were used instead of the parametric approach to approximate the shapes of the surfaces. By reviewing the aortic valve insufficiency pathologies, it was possible to recreate them in the CAD model by modifying the dimensions.

It is currently possible to additively manufacture a component using a low-hardness polymer, and additive manufacturing is valuable for creating complex shapes and being able to make single prototypes. However, the cost of manufacturing is relatively high, so it was important to explore options for alternate manufacturing including casting techniques. The main manufacturing method was additive manufacturing. However, the role of this method changed throughout the research. Part 3 provided a full explanation of this transformation including details about casting, which was the final method of choice.

3.1.1. Part 1: Patient-Specific Aortic Valve Model

3.1.1.1. Medical Imaging Techniques

Acquiring the geometric information of the aortic valve is a key step in the modelling process. This is because surgeons need to assess the geometry of the valve before doing any repairs. Since the aortic valve is a relatively compliant cardiac tissue inside the heart,

using conventional measuring methods is not ideal. Thus, medical imaging techniques were used to obtain the geometry of the aortic valve. This was realized by processing Computed Tomography (CT) scans data via the segmentation process. Image segmentation can extract the necessary geometric information of the contrasted blood inside the heart. This information included the volume of the blood inside the aortic tissue regions as well as the major diameters of the main junctions (STJ and VAJ) surrounding the aortic root. The result of the analysis was an unprocessed STL model. An unprocessed model contains many sharp spikes and rough edges that need to undergo a smoothing process. The unprocessed STL model served as the foundation of the CAD reconstruction process of the aortic root and its surrounding regions including the ascending aorta, coronary arteries and left ventricle. After that, the unprocessed model was processed using Geomagic (3D Systems, Rock Hill, SC, USA) and SpaceClaim (Ansys, Canonsburg, PA, USA) software to reverse engineer the surfaces to create an editable CAD model. This process involved smoothing the spikes and rough edges around the model to prepare the model for reverse engineering. Since the aortic valve is a complex organic structure, it was challenging to represent the valve geometry using prismatic shapes. Therefore, NURBS curves were used instead of the parametric approach to approximate the shapes of the surfaces.

Several medical imaging techniques can be used to capture the valve geometry including the following:

- **Transthoracic Echocardiogram (TTE)** is a basic ultrasound test that is used to diagnose heart structures and diseases. The ultrasound waves will produce an echo

that can be converted into imaging data with the help of a sonographer and a computer system.

- **Transesophageal Echocardiography (TEE)** is similar to TTE in principle, but the method of the test is different. That is, the doctor would insert a probe going through the patient's esophagus. Then, the probe would take high-quality ultrasound images of many of the small structures inside the heart such as the coronary arteries using an ultrasound transducer. TEE is usually reserved as an additional step if TTE is not enough for the diagnosis.
- **Computed Tomography (CT)** uses ionizing radiation (X-ray) passing through a part to obtain its image. The image file creates a map of Hounsfield. They are commonly used in medical diagnosis. CT scans have superior spatial contrast resolution especially with the aid of radio-opaque injectable materials. However, they are not as superior when it comes to capturing dynamic objects (temporal resolution).
- **Magnetic Resonance Imaging (MRI)** uses a strong magnetic field and radio waves to create images of the structures of organic pathology inside the body. The protons in the water and fats inside the body will act as signals that can be converted into images. MRI has relatively low spatial contrast resolution compared to CT. However, MRI offers a superior temporal resolution.

3.1.1.2. DICOM Files

Digital Imaging and Communication in Medicine (DICOM) is the file exchange format standard of radiology and other related fields. The objective of using DICOM is to streamline the communication process of accessing diagnostic and therapeutic information across a wide network of practitioners from different fields such as radiology and cardiology (Mildenberger et al., 2002). DICOM files cannot be used in their raw form as CAD models because they are a data set of pixel intensities rather than geometric shapes. A processing stage must take place to convert DICOM files into an editable CAD format.

This can be achieved by using a wide variety of open source and commercial DICOM editors. Figure 3.1 shows a DICOM image of a CT scan of the aortic valve (Bennett et al., 2012).



Figure 3.1. CT scan of aortic valve. Right (*R*), left (*L*), and noncoronary (*N*) cusps. LA = left atrium, RVOT = right ventricular outflow tract (Bennett et al., 2012).

3.1.1.3. Hounsfield Units

In CT scans, as the x-ray beam passes through the material, the x-ray will experience a reduction in intensity due to scattering or deflection from interacting with the material. This phenomenon is known as attenuation (McKetty, 1998). This attenuation can be used to identify the tissues in a CT scan by using Hounsfield units. R. Brooks proposed these units by deriving a relationship between the attenuation of the matter to be measured and the attenuations of both water and air (Brooks, 1977).

The Hounsfield unit formula is the following (Hurrell et al., 2012):

$$H = 1000 \times \frac{H_m - H_w}{H_w - H_a}$$

Where H: Hounsfield unit; H_m : attenuation of the unknown material; H_w : attenuation of water, which is 0; H_a : attenuation of air, which is -1000.

The Hounsfield units can vary widely according to the tissue type. For example, the approximate Hounsfield units for fat is -100 while it is +1000 for cortical bone (Hurrell et al., 2012).

3.1.2. Part 2: General CAD Model

The second modelling approach was to design a general aortic root model. The initial proposed model resembled a cylinder. This representation followed Kerchove and El Khoury's simplified anatomy of the key sections of the aortic root (Khoury & Kerchove,

2013). Also, this design was made after consulting Dr. Dominic Parry (Cardiologist at Hamilton General Hospital). Figure 3.2 shows the initial aortic valve design considering all the necessary information that was relevant to a cardiac surgeon. This was done after meeting with Dr. Parry to know more about the design and model expectations. The geometry of the model was also inspired by Swanson and Clark's paper (Swanson & Clark, 1974). This paper provided extensive information regarding all the key dimensions of the aortic tissues including the inner structures, such as the aortic valves. Figure 3.3 shows an approximation of the major dimensions of the aortic tissues.

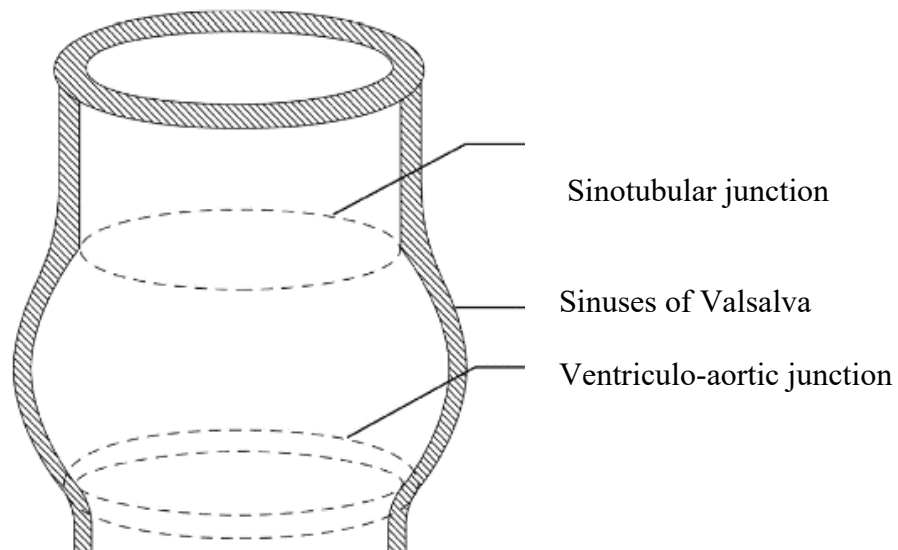


Figure 3.2. Simplified aortic root diagram (Kerchove and El Khoury 2013).

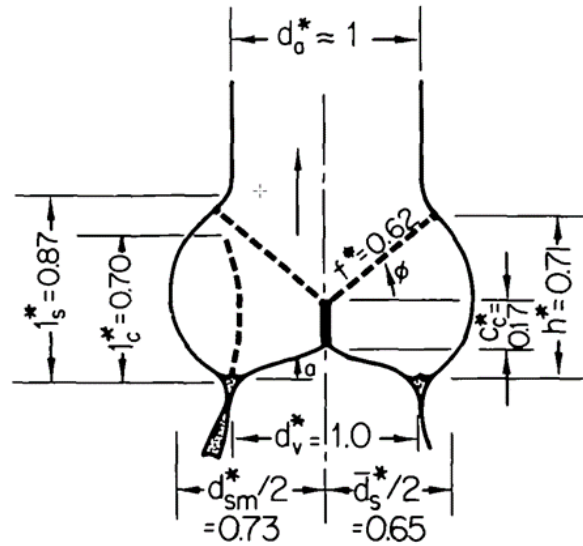


Figure 3.3. Aortic valve geometry approximation (Swanson and Clark, 1974).

Geometric information definitions:

l_s : length of the sinus of Valsalva

l_c : length of the center

d_s : diameter of the sinus of Valsalva

d_{sm} : Maximum diameter of the sinus of Valsalva

d_a : diameter of the aorta

d_v : diameter of the ventricular tract

C_c : Coaptation center

h : height from ventricular tract base plane to top of the annulus fibrosis.

f : Free edge

ϕ : Free edge angle

α : Leaflet angle

*: Dimensionless quantity referred to d_v .

The dimensions were referred to as the diameter of the ventricular tract because it is the inlet tract. Also, it did not experience large variations under different pressures. The values of d_v ranged from 22 mm to 28 mm.

3.1.3. Part 3: Aortic Valve Model Manufacturing Processes

The third stage of the project was to manufacture test models for surgical training as developed in Part 2. The original concept at the outset of this project was to develop models for additive manufacturing with compliant materials. However, the cost of 3D printing is relatively expensive. The purpose of this work was to review the considerations for two different manufacturing options (additive manufacturing versus casting) and to obtain initial feedback from surgical residents on the aortic training models resulting from each process. It is critical to investigate different manufacturing methods to determine what is best in achieving the desired geometry and mechanical properties of the training model. Also, the cost and the volume of the production are important factors as well. For these reasons, it was necessary to compare AM against the casting.

3.2. Materials and Methods

3.2.1. Part 1: Patient-Specific Aortic Valve Model

3.2.1.1. Medical Imaging Segmentation

Major challenges in capturing the geometry of delicate structures such as the aortic valve include the lack of available CAD models and adequate measurement methods. It is possible to get meaningful geometric information about the aortic valve using medical imaging such as CT and MRI scans. An example of a CT scan of the aortic valve can be seen in Figure 3.4. Medical imaging segmentation is the process of extracting geometric information from a DICOM file. The segmentation process involves using different computational approaches to analyze the variations in the contrast levels in the DICOM file slices.

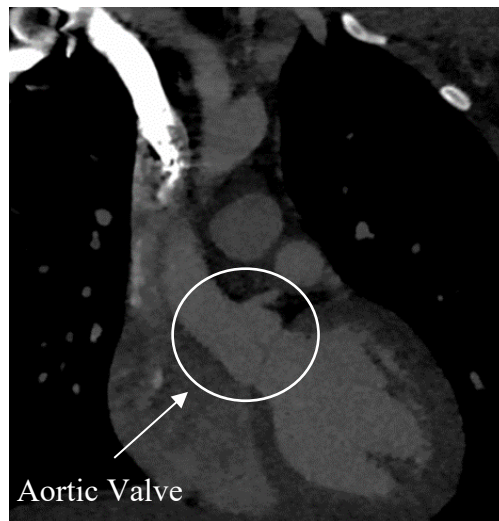


Figure 3.4. CT scan of the aortic valve (coronal plane).

The medical imaging data for this thesis project were obtained from Dr. Zahra Motamed and Dr. Dominic Parry. The software used to process these data was VMTK lab (v. 1.3, Orobix Bergamo, Italy). The CT device was SIEMENS SOMATOM Definition Flash with a slice thickness of 0.75 mm and a cross-plane resolution of 0.3 mm.

A major limitation of using the CT scan was that thicknesses of the aortic tissues cannot be determined from the images directly. To get clear scans of the internal structures of the body, a contrasting agent (radio-opaque) is injected into the body. Then, the CT scan would be performed.

The results would show the internal structures as represented by the blood volume-occupying them. This is similar to attempting to reverse engineer a water bottle by only considering the water inside it. It is possible to get the overall shape of the bottle, but not the thickness of the walls of the bottle.

To start, I imported the DICOM slices into the VMTK lab software. The slice planes were manipulated to identify possible starting points for a source seed, which is the starting position of the segmentation process. To improve the accuracy of the process, suitable threshold values for the contrast were selected by testing. For soft tissues, the threshold for the Hounsfield units was found to be in the range of 50 to 500. Other segmentation parameters were chosen according to the developer tutorials and trial and error approach.

The parameters were the following:

- Segmentation initialization type: Colliding Fronts
- Iterations: 300
- Propagating scaling: 0.3
- Scaling factor: 0.4
- Advection scaling: 1
- Deviating from sigma: 0

Next, the segmentation results were exported as an STL file and were smoothed by Geomagic Studio 12. This process started by importing the STL file and running the “*mesh doctor*” option to automatically clean the mesh and remove any isolated small facets around the model. Then using Geomagic smooth functions, the model was processed further to make it suitable for CAD reconstruction. Figure 3.5 shows the initial segmentation results.

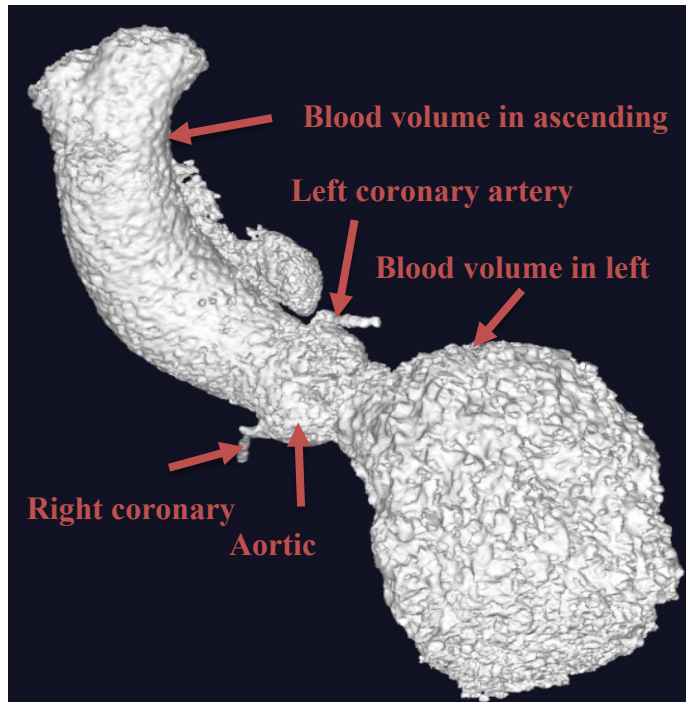


Figure 3.5. Initial aortic tissues segmentation in VMTK Lab software.

3.2.1.2. CAD Reconstruction Process

I used the segmentation results that I did previously as a baseline model for curves extractions for the geometry reconstruction process. The reverse engineering principles used in this step were focused on utilizing the curves obtained from the STL facets to create blended geometries. This method uses parallel planes that intersect the scanned surface in different locations. Other approaches involved using NURBS reverse engineering functions in SpaceClaim to extract surfaces from the segmentation results. Figure 3.6 shows an overview of the steps needed to use the skin surface function of SpaceClaim (v 1.9). The aortic root was intersected by using a pattern of ten parallel planes. The distance between the planes was 2 mm.

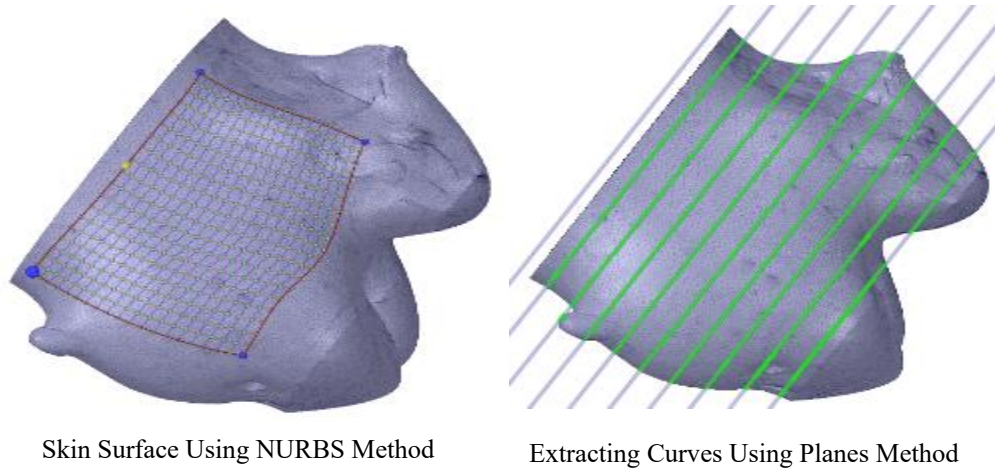


Figure 3.6. Aortic valve reverse engineering techniques.

The direction of the planes was normal to the aortic root. After that, the skin surface function was used by selecting two planes that were intersecting the aortic root. If the planes do not directly intersect the object, the skin function operation will not work using this plane-intersection approach. Then, the mesh sample size was selected to be 20 nodes as it was suitable to sufficiently capture the geometry of the aortic root. The plane-intersection approach was an automated method to generate the skin surface of the aortic root. It was possible to manually create a network of meshes on the surface of the aortic root to produce similar results. However, the manual approach was more laborious.

The other reverse engineering approach attempted was extracting curves from the aortic root. This was done using the same pattern of intersecting planes but without the skin surface function. This method produced curves that were used in a blending operation to recreate the aortic root profile. The purpose of this method was to create a parametric design that could be modified by changing the parameters of certain curves to simplify the design.

3.2.2. Part 2: General CAD Model

SpaceClaim (v R19) was used to design the CAD models. The approach was to design the aortic dimensions mainly using the data from the literature (Swanson & Clark, 1974). The major dimensions of the model were simplified as much as possible. That is, the STJ and VAJ had the same dimensions at 25 mm. Also, the middle section of the model had a diameter of 35 mm. The thicknesses of the major sections of the model were 0.5 mm for the leaflets, 2 mm for the walls of the sinuses and 3 mm for the walls of the aorta. Those dimensions were based on the values of the porcine aortic tissues reported by Sauren and colleagues (Sauren et al., 1983).

Several other dimensions were chosen for the aortic valve leaflet thicknesses for ease of manufacturing in the subsequent stages. Those dimensions were 0.75 mm and 0.9 mm. In addition, the dimensions between the aortic root, which is the middle section in the design, and the outer sections were both 15 mm. The height of the aortic root was 25 mm. The aortic tissues model went through three design iterations that are discussed in the following sections.

3.2.2.1. First Design Iteration

The first iteration was the simplest in design and followed the basic cylindrical shape. This design did not include any realistic sinuses and the heights of the upper and lower sections of the model were relatively short but would enable the trainees to perform basic surgical

processes (cutting and suturing) on a structure that had the same basic geometry as the normal aorta.

3.2.2.2. Second Design Iteration

The second iteration of the aortic tissue model was produced to make the model more realistic. The curvature of the aorta was similar to that of the patient-specific model. Also, more realistic sinuses of Valsalva and simple coronary arteries were added to the design. The coronary arteries dimensions were 4 mm for the inner diameters, 6 mm for the outer diameters and the lengths were about 30 mm.

3.2.2.3. Third Design Iteration

Following the surgical residents' feedback and to make it easier to manufacture the models via casting, a third design iteration was carried out. The major design change in this iteration was simplifying the ascending aorta design. Another modification was changing the orientation of the coronary arteries so that they align correctly when mounted on a testing platform. The upper section of the model was extended by 51 mm and the lower section by 22 mm compared to the first iteration. This was chosen to allow for more materials to be utilized by the surgical trainees. The simplified design led to an easier manufacturing process as discussed in Part 3.

The final design modification was related to the leaflets. The latest iteration included a smoother design compared to the previous iterations. This was done to add more realism to

the leaflets. Also, more height (about 5 mm) was added in the middle section of the leaflet following the surgeons' recommendations.

3.2.3. Part 3: Aortic Valve Model Manufacturing Processes

3.2.3.1. Additive Manufacturing Models

The process of creating the aortic training model by additive manufacturing (AM) is relatively simple because it uses a commercial manufacturing process. Several models were created by AM with compliant material TangoPlus A27. The models were developed by CAD (as described in Part 2) to enable a functional tricuspid aortic valve in a realistic aortic geometry. The design guiding dimensions were obtained from Swanson and Clark's paper (Swanson & Clark, 1974). The AM models were initially printed at Proto 3000 and subsequently at Niagara College. The benefit of the AM process was the creation of the aortic structures using a relatively simple process and the ability to make the model in a morphology that is similar to the native aorta. There were some drawbacks including material behaviour (see results from surgeon feedback) and a relatively high cost per unit produced. This step involved saving the CAD design STL file and sending it to Proto3000 (Vaughan, ON) and Niagara College (Welland, ON) to complete the production of the models. Figure 3.7 shows a sample of the 3D printed models supplied by Niagara college.



Figure 3.7. AM model with fixture.

3.2.3.2. Casting Moulds Design

The casting manufacturing processes required the development of multi-part moulds to produce the aortic valve model. The external parts of the mould were relatively simple to capture as moulded sections, but complex internal structures, such as the aortic valve leaflets were more challenging.

Figure 3.8 shows the first iteration of the mould design including the casted model. This iteration did not include realistic sinuses or coronary arteries. Also, the lengths of the upper and lower sections of the model were relatively short compared to future iterations.



Figure 3.8. Aortic valve model made from Silicone A10 (Si A10) with 3D printed casting mould (PETG material).

Casting Mould Main Components:

The following were the components of the mould design:

1. Upper outer section: the outer boundaries of the upper section of the model
2. Lower outer section: the outer boundaries of the lower section of the model
3. Upper internal section: the internal boundaries of the upper section
4. Lower internal section: the internal boundaries of the lower section
5. Handle: to secure the internal upper section to the outer upper section during the casting process.

3D printer information:

The modified mould was printed using a Prusa MK3 FDM 3D printer. The material was PLA. The layer thickness was 0.2 mm for the outer sections and 0.15 mm for the inner sections.

3.2.3.3. Educational Model Design

The educational model consists of the aortic valve model and a fixture to hold the model in place during training. The first fixture design iteration was not ideal for training (training setup in Figure 3.7). Although it can hold the aortic valve model in place, the fixture design does not resemble a chest cavity. A new design iteration has been conceptualized after the surgeons' feedback. The new design is a box-like structure that enables holding the aortic valve model closer to what the surgeons see in real surgery with the patient prone on the surgical table. This can be achieved by slightly modifying the positions of the coronary arteries and create a box-like enclosure for the aortic valve model. Figure 3.9 shows a visualization of the modified educational model setup.

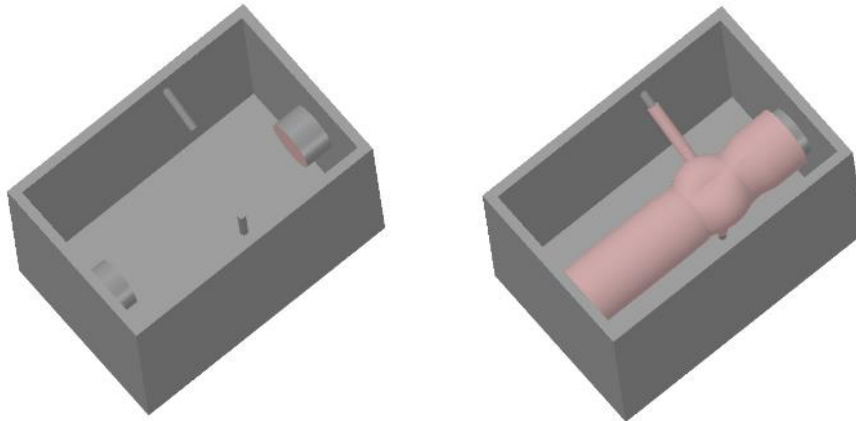


Figure 3.9. Aortic valve model training box.

3.3.Results and Discussion

3.3.1. Part 1: Patient-Specific Aortic Valve Model

3.3.1.1. Medical Imaging Segmentation Results

The scanned data of the aortic tissues were edited to isolate the aortic root and the aorta from the left ventricle. The timing of the CT scan in the cardiac cycle made the segmentation process challenging. For instance, identifying the line of separation between the aortic valve leaflets and the left ventricle was filled with blood. Therefore, a complete segmentation of the leaflets was not possible. Figure 3.10 A shows the rough edges aorta model that resulted from the segmentation process. The aorta model was considered rough at that stage because of the state of the model surface that was filled with spikes. Rough surfaces were challenging to reverse engineer because they require additional processing for their curves and resulting geometries. Thus, it was essential to minimize surface roughness and make the model surface as smooth as possible. Figure 3.10 B shows the final smoothed model of the aorta. After that, the model was used as the baseline of the CAD reconstruction process. The purpose of this step was to derive a suitable model for reverse engineering. Achieving this required a trial and error-based approach to arrive at the presented models. Some of the limitations of this approach were the relatively low resolution of the scanned data, the CT scan timing (relative to the cardiac cycle) and orientation (relative to the anatomy of the heart). Better CT scan timing and orientation can make identifying the aortic valve regions easier.

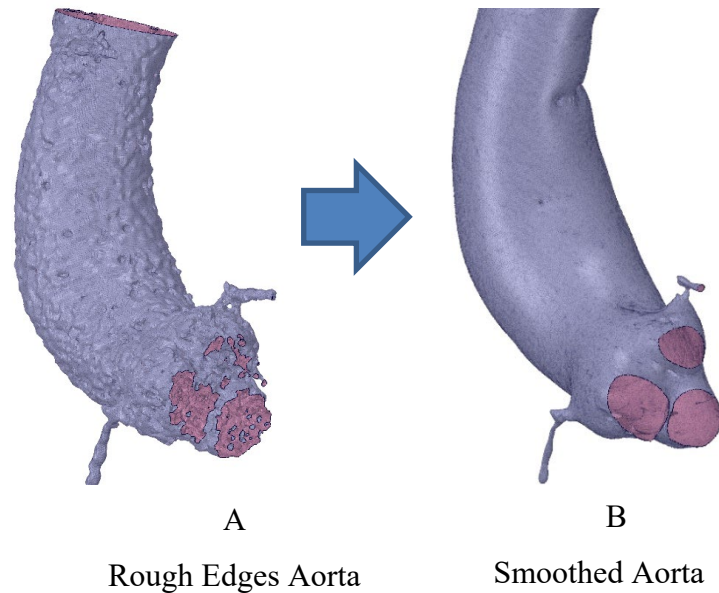


Figure 3.10. Segmentation results.

On the other hand, many of the other controlled processes can be optimized to obtain superior results. For instance, conducting more trials to maximize the volume of segmented results will provide more raw data that cover more areas around the regions of interest. Also, choosing more conservative parameters for the smoothing process can increase the model dimensional accuracy. The trade-off in using conservative parameters is that the post-processing stage would be more laborious. For instance, extracting curves from rough edges would require more editing compared to smooth edges.

Creating a CAD model from the segmented results was challenging especially since the volume extracted from the scans was for the blood rather than the actual tissues. The timing of the CT scan and the image quality can impact the amount of volume extracted. This was observed when analyzing the leaflet geometries.

For instance, identifying the coaptation areas and the leaflet boundaries was not possible due to the small size of the leaflets relative to the scanning resolution. Therefore, it was proposed that a relatively simple CAD model constructed from geometric information from the literature could serve as the standard model for the surgical training setup.

3.3.1.2. CAD Reconstruction Results

The smooth aorta model could be 3D printed as it was. However, editing the model was very challenging and was a problem for subsequent geometric changes to model pathologies of the aorta and aortic root. For instance, changing the diameter of the STJ without affecting the geometry of the overall model was difficult. It is possible to edit STL models that are made of meshes and facets, but the options to do so are often limited to simple operations such as intersect, combine and scale. To do more complex operations such as editing specific parameters of the model, creating a parametric model was proposed. The rationale was that reverse-engineering the smooth model would produce a model that could be edited relatively easier compared to the STL model. Also, some of the missing parts could be approximated to complete the model.

Figure 3.11 shows the results of the CAD reconstruction process. The ascending aorta and the aortic valve were reconstructed from the scan results. In addition, an outer shell was constructed around the aortic valve to resemble the inner structures of the aortic root, since this structure could not be obtained directly from the CT segmented results.

The final result was produced in SpaceClaim by saving the CAD model as an STL file. The STL file needed more processing to make sure that it was a watertight or gap-free model in preparation for 3D printing. This was done using the STL editing capabilities of SpaceClaim. The check facets and auto fix functions on the cleanup tab were used to clean the model.

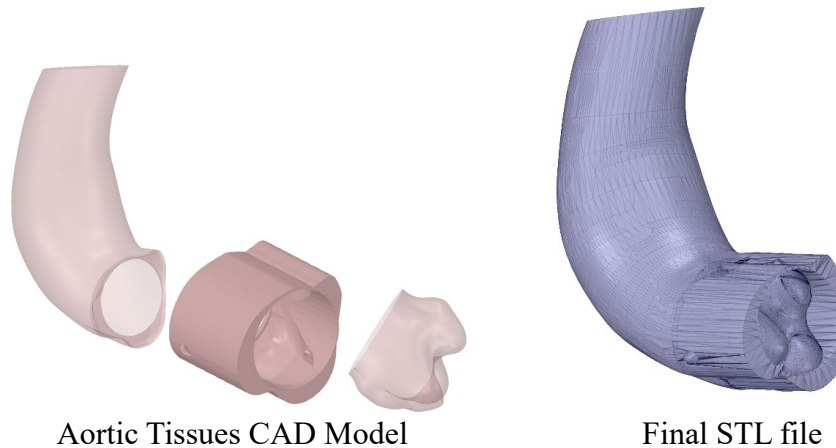


Figure 3.11. CAD reconstruction results.

Increasing the complexity of the design could produce more accurate results. However, this would increase the design modification time and the computation requirement to process the models. For instance, increasing the sample size of the meshes in the skin surface reverse engineering function would increase the complexity of the model and increase the load on the computer. Also, generating more planes would produce more intersecting curves that require manual editing.

3.3.2. Part 2: General CAD Model

The initial design gained positive responses from the cardiac surgeons (Figure 3.12), and their feedback led to the development of the second CAD model (Figure 3.13). This model included a more realistic sinus of Valsalva as well as the coronary arteries.

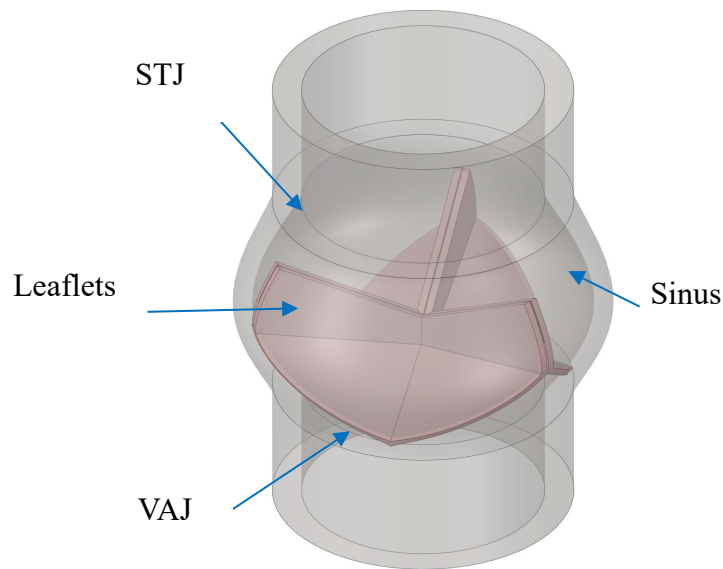


Figure 3.12. First aortic valve CAD design iteration. STJ: Sinotubular junction; VAJ: Ventriculo-aortic junction.

The aortic valve model v2 was not completely parametric. This is due to the inability to parametrize some of the design steps in SpaceClaim. It was perhaps possible to overcome this limitation by using some of the programming options available in SpaceClaim. However, this would make the design customization process more complicated especially for a layperson using the model. After consulting cardiac surgeons at Hamilton General Hospital, it was decided that a parametric model was not essential at that point in the project.

The design iterations were done after going through a series of materials testing and manufacturing as discussed in later chapters. Thus, the modifications performed were the results of these activities especially cardiac surgeons' consultations after every iteration. For instance, having a realistic curvature for the ascending aorta was not necessary at that stage. Moreover, the locations of the coronary arteries were incorrectly oriented compared to how they are aligned during real surgery.

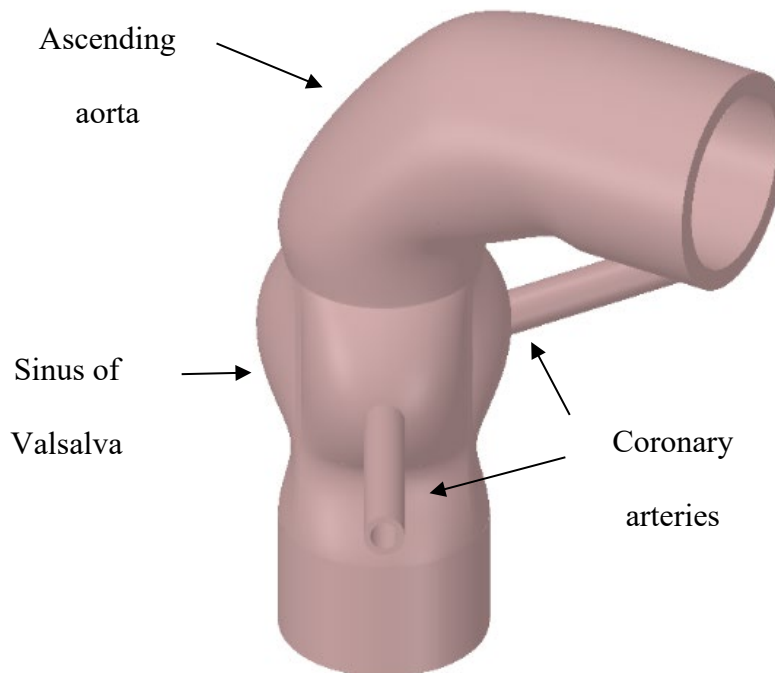


Figure 3.13. Second design iteration.

The third and final iteration incorporated all the feedback from the surgeons (Figure 3.14). The ascending aorta was simplified and extended, the coronary arteries were aligned properly, and the design of the leaflet was modified.

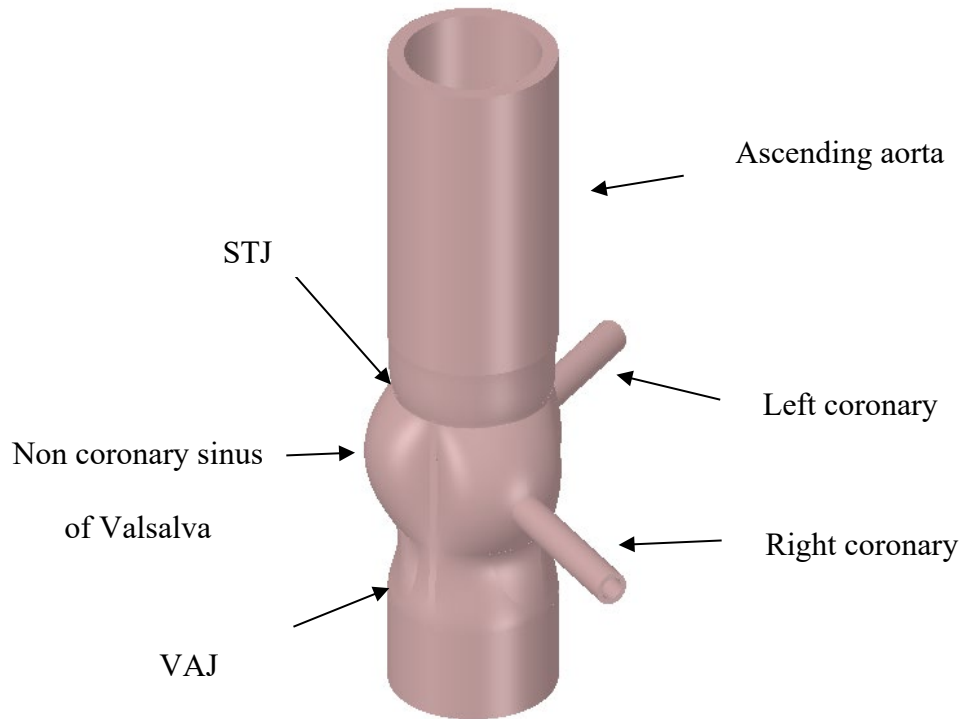


Figure 3.14. Third design iteration. STJ: Sinotubular junction; VAJ: Ventriculo-aortic junction.

3.3.3. Part 3: Aortic Valve Model Manufacturing Processes

The main advantage of using AM is the ease of production. However, this advantage can be overshadowed by relatively higher production costs and limited materials options.

- 1. Costs:** The cost analyses only compared the costs of the final production steps. The costs of creating the CAD model and optimization of the casting moulds were not included to simplify the analyses.

- **AM:** The cost of 1 Kg of TangoPlus was about C\$500 (Proto3000, 2020). Also, the cost per model was about C\$280 (assuming special quantity pricing for 26 models). As a result, AM was the more expensive option compared to casting.
- **Casting:** 1 Kg of silicone (the best material tested) was about C\$75 (plasticworld.ca). Also, a complete mould set was 3D printed for about C\$50. Assuming a total processing time of one hour for the whole casting operation using one mould, the estimated cost per model was C\$100 including the 3D printing and labour fees. The cost could be lowered for each subsequent cast using the same mould. Also, it is possible to use multiple moulds at the same time to lower labour costs. Therefore, casting showed greater cost-saving potential compared to AM. A labour cost of C\$46 per hour was assumed in the casting cost estimations.

2. Ease of Manufacturing:

- **AM:** Manufacturing the aortic valve models using AM was relatively easier compared to casting. In the AM case, the only requirement was to supply the CAD file to the manufacturing partner to complete the process.
- **Casting:** The casting process required optimization of the mould design to ensure producing complete models. Also, there were other factors that affected the casting process, such as the active pouring time of the casting materials, curing time of the cast and the use of demoulding agents.

After finally optimizing all these parameters, the casting process became easier. However, more work was required for casting compared to AM.

3. Materials Flexibility:

- **AM:** Compliant materials selections were extremely limited for AM. It is possible to use multiple materials to achieve more realistic models. However, the types of tissues of interest in this research were soft compliant tissues. Therefore, AM was not an ideal option compared to casting in this case. This does not mean that AM is not a suitable option for cardiac skills training, but our mechanical test results demonstrate that the currently available mechanical properties do not yet mimic real tissue response.
 - **Casting:** Casting offered more flexibility in terms of materials options especially for compliant materials. Also, it is possible to adjust the hardness of the casting materials using thickening or thinning agents. The results from our mechanical tests demonstrate that the casting materials respond to surgical procedures such as cutting and suturing with similar forces to the aortic tissues.
- **Design flexibility:**
- **AM:** Making any changes to the aortic valve model can be easily accommodated by the AM process. Also, generally, complex shapes can be 3D printed without issues. Major design flexibility in AM is the possibility to

create patient-specific models. This patient-specific model manufacturing option is not ideal for casting.

- **Casting:** Making any changes to the design of the aortic valve model would require creating a new mould and going through an optimization process to make sure that an adequate cast can be manufactured without any issues. Also, complex shapes are more challenging to manufacture using casting.

The following table summarizes the pros and cons of each manufacturing process:

Table 3-1. Summary of the pros and cons of AM and casting.

Criteria	AM	Casting
Costs	★ (Expensive)	★★★ (inexpensive)
Ease of manufacturing	★★★ (Easy)	★★ (Depends on production volume)
Materials flexibility	★ (Limited options, difficult to control the properties of the materials)	★★★ (Many options, possible to control the properties of the materials)
Design flexibility	★★★ (Very flexible)	★ (Inflexible)

Ultimately, choosing the best method depends on the objective of the training. If the training focuses on patient-specific cases, then AM is the better option. However, if the training models are castable, then casting is the better option as it can provide greater cost savings. Regarding the training setup, it is possible to optimize the design by eliminating the box in favour of removable fixtures. The latest design iteration had four-pin fixtures to hold the model in place. These fixtures could be made removable by 3D printing them as attachments. This would add more flexibility to the design while minimizing the costs. The downside is that the model would become harder to align correctly and the absence of a suitable structure for the attachments could become an issue. Testing the training box with the surgeons will be conducted as a future step. Figure 3.15 shows the casting results.

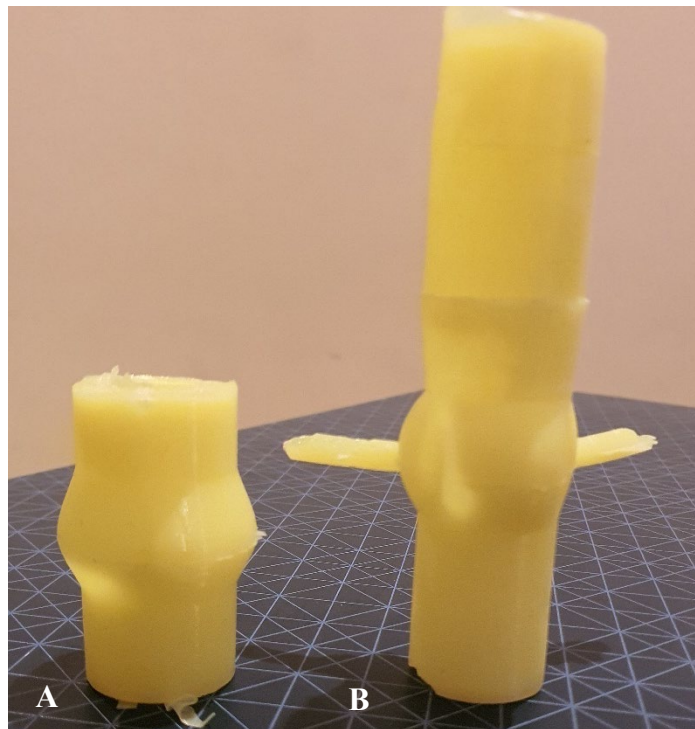


Figure 3.15. Aortic valve model casts; A. First iteration; B: Second iteration.

3.4. Conclusion

The quality of the acquired geometry is subject to the capabilities of the imaging technique used. Each technique has advantages and disadvantages depending on the type of information needed. For measuring the dimensions of the cardiac tissues, CT and MRI scans tend to be the best scanning methods. Performances of imaging techniques are often compared against each other to validate the best method of acquiring geometric information. Although significant advancements have been made in the field of imaging technology, there are still limitations in obtaining images of small soft tissues, such as the aortic valve with sufficient resolution.

For pre-operation planning, Aortic valve patient-specific CAD models are derived from patient-specific scan data. This approach does not aim to produce a parametric model that can be manipulated to produce different pathologies and models with different scales. These models have many advantages including realistic representation of the pathology and relatively cost-effective production costs. However, sometimes the training objective is to get accustomed to many different cases that do not have any existing models. These cases can benefit from using a generic CAD model that can represent different pathologies in different scales. The principle of making these generic models is to use geometric information from the literature to create parametric models. Although these generic CAD models might be less accurate in comparison to patient-specific models, they can offer relatively cost-effective valuable training opportunities.

The first step toward creating educational cardiac tools was successfully realized. Several CAD models of the aortic valve were developed using different approaches (patient-specific and general models). Three design iterations were performed to create an adequate aortic valve model. The first design iteration included simplified geometries that resembled a cylinder. The second iteration was the most complex as it included realistic sinuses as well as realistic ascending aorta. After consulting with surgical residents, it was found that the second iteration was overly complex and a simplified version of it was more desirable. Thus, a third design iteration was carried out resulting in a more streamlined design. The major modifications included simplifying the ascending aorta, change the alignment of the coronary arteries and modifying the design of the leaflets.

Aortic valve models were successfully manufactured using AM and casting. While AM offered more flexibility in the design process and ease of use, it suffered from the lack of materials options, and it was a very expensive manufacturing process. On the other hand, the casting process was cheap and flexible in terms of materials options. However, the upfront optimization process to design the mould and the need to repeat this process for each new design update were the major drawbacks of this process.

The long-term costs saving of the casting process made it the better option in this comparison. AM was essential as a supporting manufacturing method to create the mould for the casting. However, using it as the main method of manufacturing was very expensive compared to casting.

A training box was designed to conceptualize all the necessary training elements including the aortic valve 3D printed model and a box that mimics the chest cavity. Also, the orientation of the model was updated to enable a more realistic representation of the positioning of the aortic valve inside the body.

For future steps, it is possible to only focus on a limited number of aortic valve pathologies by creating several moulds for them. These moulds could be optimized to be used in an injection moulding process. The first pathology of choice was selected as the ascending aorta aneurysm. The casting mould was modified to include the upper inner section of the pathology. Therefore, completing the mould design is a future step. Also, the training box design requires performance evaluation from cardiac surgeons. This could be carried out as part of the training sessions discussed in Chapter 5.

Chapter 4

4. Mechanical Testing of Aortic Tissues and Manufacturing

Materials

4.1. Introduction

The purpose of Chapter 4 was to provide details regarding the aortic valve model materials selection process. This process involved conducting mechanical testing of aortic tissues and manufacturing materials.

The process of tissue testing involved testing biological materials from porcine and equine aortic tissues as well as synthetic materials such as silicon and 3D printed compliant materials termed “rubber-like”. The goal of the testing was to determine the mechanical behaviour in response to surgical tools during testing. Also, the testing results were used to determine a suitable material for manufacturing the aortic valve model.

The second step was to determine the mechanical behaviour of the aortic valve tissues during surgical repairs. Even though data for the mechanical properties of the aortic valve exists in the literature, they are based on standard tensile and flexural tests and do not provide information related to the mechanical behaviour of the tissues in response to cutting and suturing during surgical repairs. This was achieved by testing the tissues using a mechanical testing system. Three different types of tissues were compared in this test.

These tissues include porcine tissues, soft 3D printing materials, and latex castings. This test was essential because the goal was to produce a model that resembles aortic valve tissues rather than being a replacement to the real tissue in which identical properties may be required.

The main topics in this section included:

- Review of material properties of aortic valve tissues
- Mechanical behaviour of tissues under cutting and puncturing by surgical tools:
 - Needle driving forces.
 - Suturing forces
- Tissues testing using surgical tools (suturing needles and scalpel blade)

To create a useful surgical skills training setup, the mechanical properties of the materials of the model should mimic the interactions between the surgeons and the aortic valve. This interaction involves cutting the cardiac tissues using surgical tools, suturing, and manipulating the tissues to be able to inspect and measure cardiac structures.

A first step to understanding the material properties needed for the project was to refer to porcine aortic valve data in the literature. Kalejs conducted a series of material properties testing on aortic valves using the universal tensile testing system (Kalejs, 2014). The sample included in those experiments were from natural porcine valves and a variety of bioprosthetic valves.

The results of the experiments can be seen in Table 4.1 in the form of recommended design limits. One of the goals of this thesis project was to produce a 3D printed physical model of the aortic valve for surgical skills training using materials that can mimic the mechanical behaviour of real tissues during surgical repairs. This suggested that it was not necessary to replicate the properties of the same materials as a porcine valve or even bio-prosthetic as the goal was not to design an aortic valve replacement model.

Table 4-1. Recommended mechanical properties of aortic valve leaflet (Kalejs, 2014).

	Native Porcine valve	Prosthetic valves	
	Modulus of elasticity (MPa)		
	(Optimal value)	Min	Max
Circumferential	9.7	9.0	29.5
Radial	1.0	0.8	15.8
	Ultimate stress (MPa)		
Circumferential	2.3	2.3	8.9
Radial	0.5	0.4	5.2
	Ultimate strain (%)		
Circumferential	44.8	28.7	64.9
Radial	95.6	53	95.6

“Optimal” was defined by Kalejs as values from natural porcine valves.

Another approach to obtaining the properties of the materials was to conduct flexural properties testing. Ragaert et al. created an indentation test of the porcine aortic valve by puncturing the valve tissues until rupture with a ball-headed rod (Ragaert et al., 2012).

A limitation is that the mechanical properties obtained from this test are not representative of the forces experienced by the surgeon in a surgical training environment that includes surgical tools and haptic feedback. Additional experiments are needed to investigate the interaction between surgeons and cardiac tissues.

Haptic feedback can provide essential information for the aortic valve model. Surgical cutting forces and medical clamping/suturing can give insights that can lead to selecting suitable materials for surgical training. Moreover, quantifying the forces required for cutting and suturing aortic tissue could help in developing haptic feedback models for virtual training environments. Currie and colleagues evaluated conventional and robotic-assisted mitral valve annuloplasty repairs done by novice and expert cardiac surgeons (Currie et al., 2013). The testing setup included a porcine mitral valve, customized mount and 6 axis force/torque sensors (Figure 4.1). The conventional repairs forces range was from 1.6 N to 3.6 N and the robotic assistance forces range was from 4.1 N to 11.5 N.

Kitagawa and colleagues compared different suture techniques applied by expert and novice surgeons using hands, laparoscopic instruments and robotic suture tying approaches (Kitagawa et al., 2002). The testing setup was a knot tying tension (Figure 4.2). The forces applied varied depending on the suture type and approach used. Attending surgeon suturing data was provided as a sample. The results were similar for the laparoscopic instruments and hand tying approaches. The applied forces were between 0.5 N and 3.5 N. For the robotic suturing approach, the forces were between 0.5 N and 7.5 N.

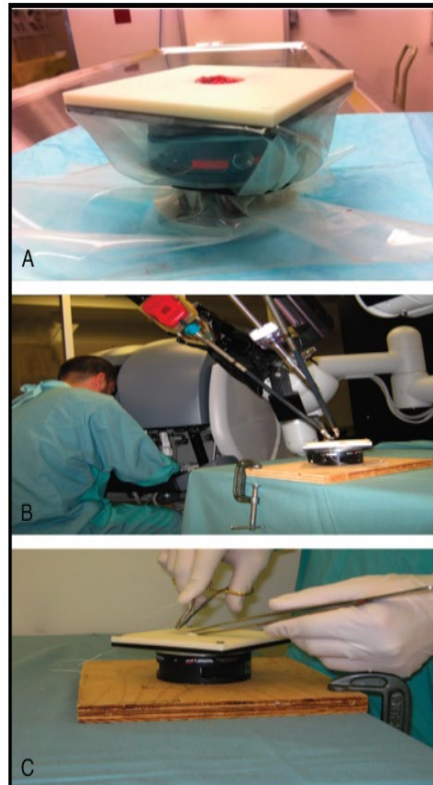


Figure 4.1. Mitral valve repair test bed (Currie et al. 2013).
A, Mitral valve annuloplasty test-bed. **B,** Mitral valve annuloplasty test-bed within the operative field of the da Vinci robot. **C,** Mitral valve annuloplasty test-bed used for conventional valve repair.

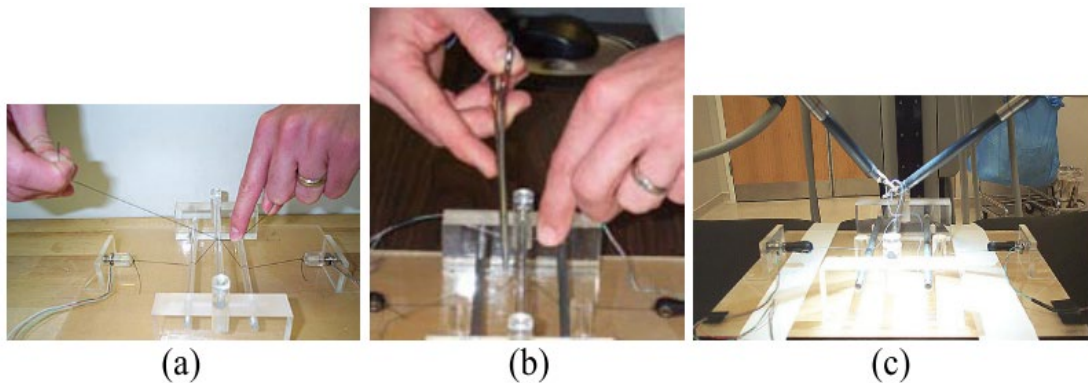


Figure 4.2. Analysis of suture manipulation forces (Kitagawa et al. 2002).
 A tension measurement device is used to measure the forces applied to sutures, (a) by hand, (b) by instrument, and (c) using the robot.

Based on these foregoing studies, more data are needed on the forces required for surgical procedures on natural aortic tissues such as needle driving and cutting with surgical scissors. Moreover, it is important to compare the mechanical response of any synthetic materials that are to be used in the synthetic models. As an analogue for surgical training, porcine tissues are a viable option in modelling certain cardiovascular conditions that are found in humans, such as calcific aortic valve disease and graft and flap techniques for surgical repairs (Swindle et al., 1988; Tsang et al., 2016). However, there are limited data regarding the force measurements of surgical tools used in aortic valve surgical repairs. Therefore, I used porcine aortic tissues as the baseline of the material testing in comparison to synthetic materials including silicone, polyurethane, urethane, and commercial 3D printed compliant polymers (TangoPlus™, Agilus30™ and Digital Material).

4.2. Materials and Methods

To manufacture an aortic root training model, it was essential to know more about the mechanical properties of the manufacturing materials and how they would behave during a surgical simulation. An important aspect of the model was that it should be manufactured using relatively compliant material as close as possible to porcine aortic tissues. This was to increase the fidelity of the model. Several manufacturing materials were chosen based on one of two manufacturing methods including casting and 3D printing materials. Then, samples of those materials were tested and compared against biological aortic tissues obtained from pigs and horses. The following sections include details about the materials tested and the testing protocols.

4.2.1. Materials Tested

All the materials are listed in Table 4-2. The organic tissues were obtained after receiving approval from the Animal Research Ethics Board at McMaster University (AUP #17-01-01). The porcine samples were obtained from surgical training sessions at Hamilton General Hospital. The pig hearts obtained were intact and from healthy pigs. Also, the equine heart tissues were obtained from the Ontario Veterinary Clinic courtesy of Dr. L. Arroyo. All the tissues were intact and healthy. The training sessions done by Yoo et al. suggested that the TangoPlus material was suitable for surgical training for cardiac surgery (S. J. Yoo et al., 2017). The average shore hardness value for the TangoPlus was around A27. This information was used as the main criterion to choose all the materials. The rationale was to choose compliant materials that could feel like porcine aortic tissues under surgical cutting and suturing. Among all the known additive manufacturing materials at the time, TangoPlus was the most compliant. Also, relatively stiffer rubber-like additive manufacturing materials were chosen. The second choice was Agilus30, which had an average shore hardness of A32.5, and the final choice was a special TangoPlus mix called digital material with an average shore hardness value of A40. Regarding the casting materials, the most compliant material was the silicon with a shore hardness of A10 (SiA10). The other casting materials were silicone with a shore hardness of A20 (SiA20), rubber-like polyurethane with a shore hardness of A20 (RuA20) and urethane with a shore hardness of A30 (RuA30). The selection process was similar to what was done in the additive manufacturing materials. The materials were chosen based on the shore hardness values that were similar to the TangoPlus or more compliant.

The materials tested were the following:

Table 4-2. Tests materials.

Material Group	Description	Comments
Biological	Porcine aortic tissues	Primary reference aortic tissue material obtained from 6 months old pigs
	Equine aortic tissues	Used as a reference only due to its relatively high stiffness compared to porcine tissues.
Additive Manufacturing	TangoPlus™	TangoPlus Fullcure 930 the most compliant AM material tested. Shore value of A26-28 (Stratasys, 2020c) Average shore scale A value of 27
	Agilus30™	Relatively harder than TangoPlus. Shore value of A30-35 (Stratasys, 2020a) Average shore scale A value of 32.5
	Digital Material A40 (TangoPlus mixed with Vero white plus)	The hardest AM material was tested. Shore value of A35-45 (Stratasys, 2020b). Average shore scale A value of 40
Casting	Silicone A10	The most compliant material in all the tests with a shore value of 10. Acronym: Si A10
	Silicone A20	Silicone with a shore value of A20. Acronym: Si A20
	Rubber-like polyurethane A20	Polyurethane with a shore value of A20. Acronym: Ru A20
	Rubber-like Urethane A30	Urethane was the hardest casting material tested at A30. Acronym: Ru A30

The casting materials were obtained from Polytek (Polytek, Easton, PA, USA) and Plastic World (Plastic world, North York, ON). Figure 4.3 shows the casting material samples.

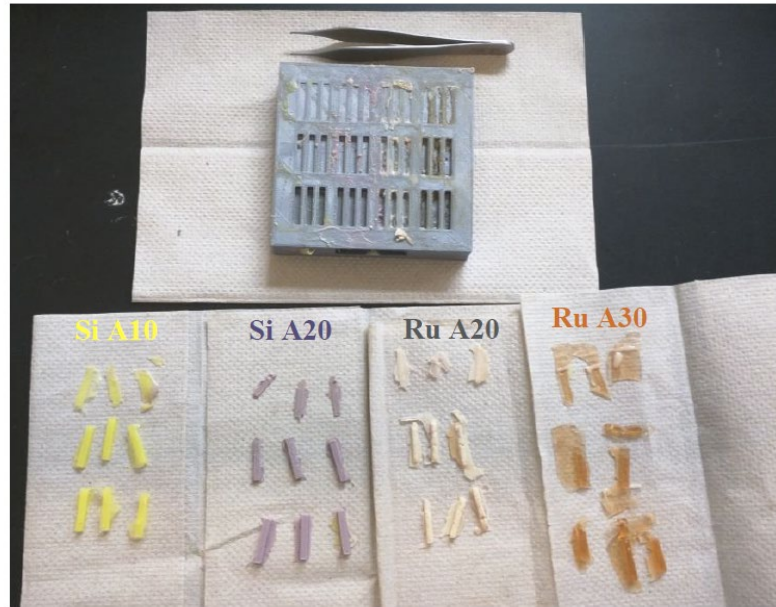


Figure 4.43. Test samples of casting materials as described in Table 1.
SiA10 = Silicone A10 (Shore A hardness A10);
SiA20 = Silicone A20; Ru A20 = Rubber-like polyurethane A20;
RuA30 = Rubber-like urethane A30.

4.2.2. Testing Protocols

The tissue testing involved mounting a custom-made fixture to help with the tissue's placement on the material testing machine (Electropuls E1000, Instron). A pair of clamps were used to secure the samples in place directly under the surgical tools. To hold the surgical tools on the material test machine, a custom-made surgical tools holder was designed and manufactured.

The testing included the following tools (Figures 4.4, 4.5 and 4.6):

- Custom-made fixture to mount the sample on the material test machine (courtesy of Jared Daley). Figure 4.4 shows an image of the setup.
- Custom-made surgical tools holder to hold the instrument on the material test machine (Figure 4.5).
- Custom-made sample aligner.
- Bulldog clamps, forceps, and surgical needle drivers
- Porcine aortic tissue, equine aortic, and synthetic material samples
- Surgical needle 2-0 Ethibond Excel 2-0 SH 26 mm 1/2c taper (Ethicon, USA)
- Surgical needle 2-0 Ethibond Excel 2-0 V5 17 mm 1/2c taper (Ethicon, USA)
- Scalpel blade No. 11 (ALMEDIC, Canada)

All samples were prepared for testing by forming them into rectangular test strips. For the biological samples, this required cutting strips (about 4 mm x 20 mm where possible as some samples were very small) from the aortic valves and aorta wall. This was sometimes challenging given the behaviour of the tissue to retract and curl. Care was taken to keep the tissue moist with saline. The aortic tissue samples were placed in sealable baggies with saline-moistened gauze and then frozen until the day of testing. On the day of testing, the sample was removed from the freezer and allowed to thaw while keeping them moist with saline. The casting materials were cast into rectangular forms (0.5, 2, and 3 mm thicknesses x 20 mm x 3 mm, Figure 4.3). For the 3D printed materials, special orders were made for test strips of each material (0.5, 2, and 3 mm thicknesses x 20 mm x 3 mm).

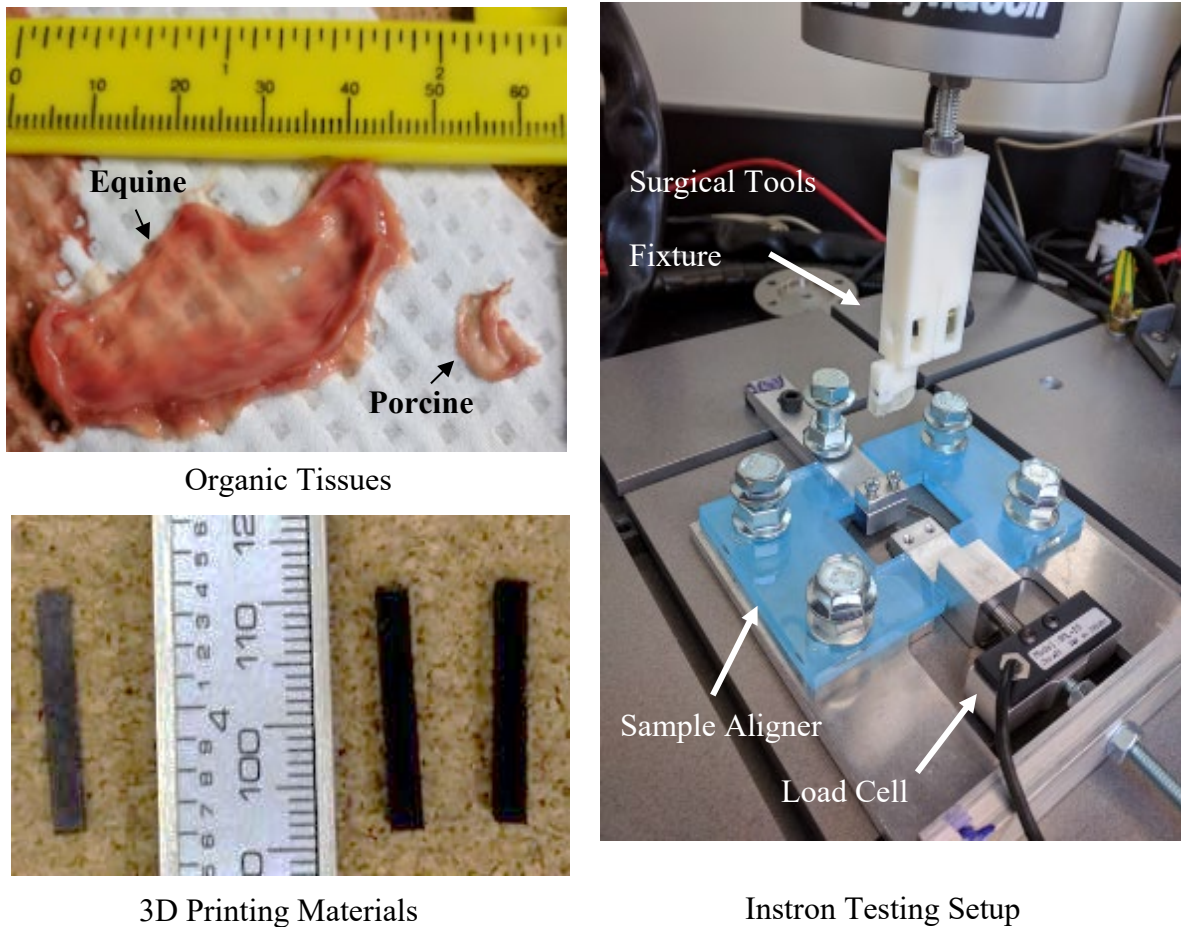


Figure 4.4. Instron testing setup and testing materials.

After consulting with the cardiac surgeons, surgical needle 2-0 (taper and tapered cut) and scalpel blade No. 11 were chosen for the surgical puncture and cutting testing procedures. Since the Instron material test machine did not have a specialized fixture for holding the surgical tools, a custom-made surgical tools holder was produced for this purpose. The surgical tools holder was able to successfully hold the surgical needle and the scalpel blade on the Instron machine.

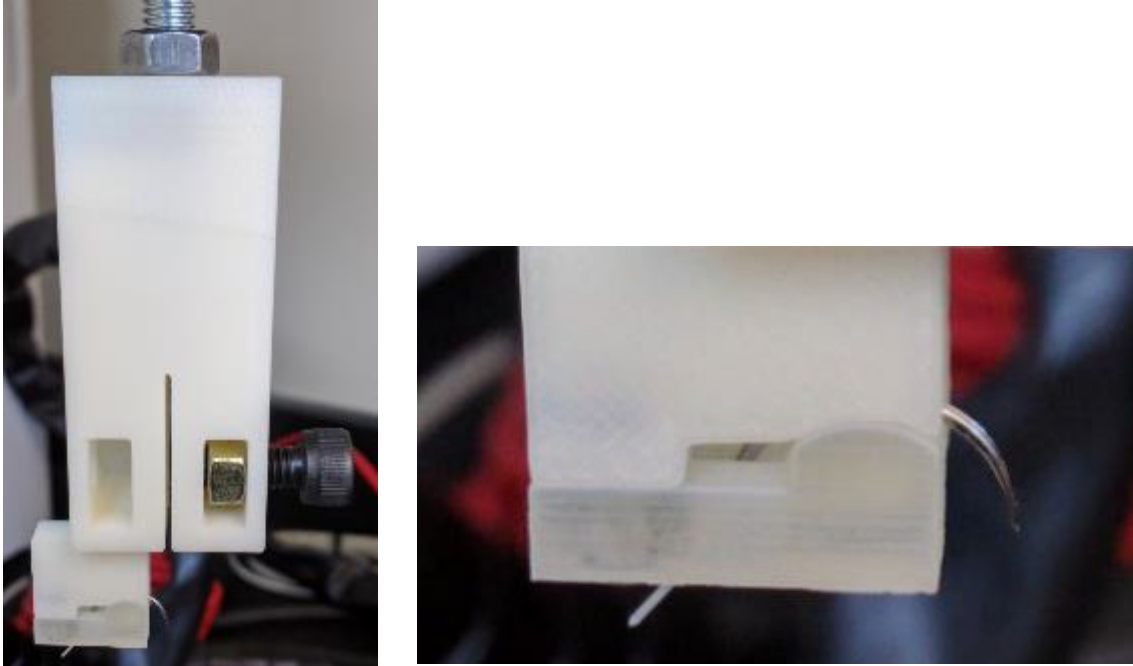


Figure 4.5. Surgical tools holder.

The samples were gripped by the bulldog clamps and a tensile load of 1 N was applied to a set load. The tensile load was measured for each sample by a load cell (Interface SML-25, Interface, Scottsdale, AZ) in line with the sample, and the load information was recorded through a National Instruments DAQ (National Instruments USB-6009) through a custom LabVIEW program. The tensile load of 1 N was consistently applied to all samples prior to the puncture or cutting tests. In some cases, the load had to be re-applied as the sample relaxed after the initial load application.



A



B



C

Figure 4.6. Surgical tools used for the testing; A: Surgical needle 2-0 Ethibond Excel 2-0 V5 17 mm, Scalpel blade No. 11; B: Surgical needle 2-0 Ethibond Excel 2-0 SH 26 mm; C: Needle holder and tweezers.

For mechanical testing, a 250 N load cell (Dynacell model 2527-131, Instron) was used. Load and deflection data were recorded by the Wave Matrix software (Firmware v. 12.1, Instron).

The first step in preparing the testing was to perform a calibration for load and deflection. The load value was set to zero via calibration and an upper and lower limit of 25 N was set for safety. Then, the surgical tool was placed slightly on top of the sample highlighting the digital position starting value. After that, the digital position value was calibrated.

The second step was to create a method that can be used repeatedly to do the testing. This was done by choosing the ramp waveform method with a ramp rate of 1 mm/s for all the steps. The test methodology consisted of three steps including downward movement, upward movement and final stopping position. The downward movement maximum travel distance was set at -6 mm. This was to account for the elongation experienced by the samples before the actual puncturing and cutting moments. The same value was chosen for the upward movement to return to the same starting position. Also, the waveform end action in step two was set to end the test, so there was no need to choose any additional parameters for step three.

4.3. Results and Discussion

The results were processed after obtaining the data in the form of spreadsheets from Wave Matrix software. The data were analyzed in Excel (Microsoft 365) to determine the key data points of interest. For the needle puncturing tests, the key point of interest was chosen based on the maximum force value right before a sudden decrease in the force due to the puncturing action (Figure 4.7). The force and displacement values were obtained from that point. Similarly, the blade test results were obtained using the same method of locating the maximum force before any significant drop in the value of the forces (Figure 4.8). Since the surgical tools starting positions were above the samples, the final displacements values needed adjustments. Recording of displacement was started at the point that the load started to rise above the noise values. This was not always easy as the data were inherently noisy due to the very low load values. Generally, this resulted in omitting the first 1 mm of the displacement values. This process was done for all the tests for all the materials. Statistical analysis was carried out to compare all the data against the porcine aortic tissues. Force and displacement data were compared between the manufacturing materials and the porcine tissues by analysis of variance (ANOVA) at $\alpha = 0.05$

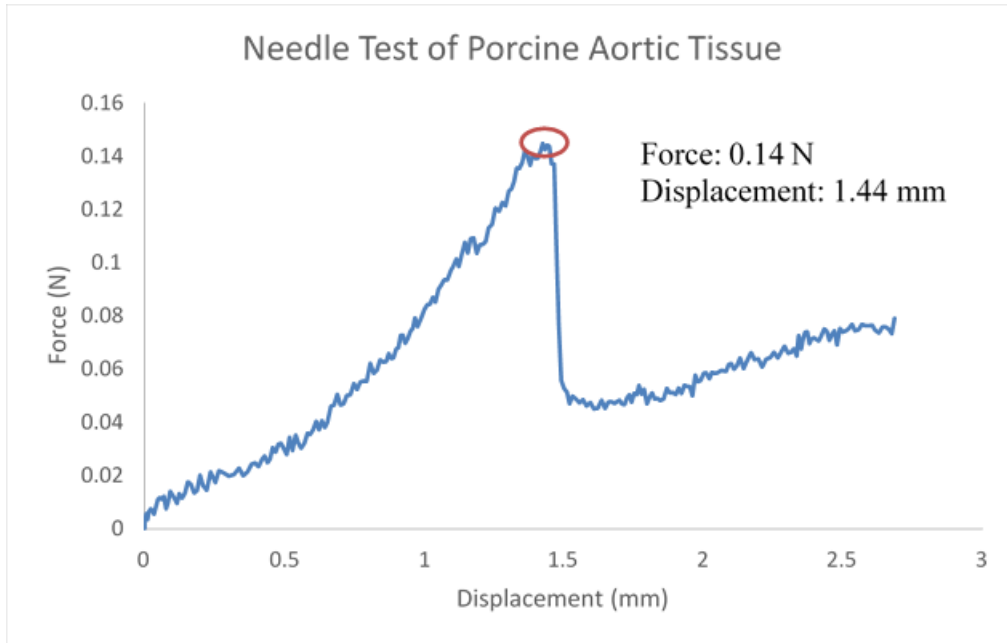


Figure 4.7. Needle test sample result.

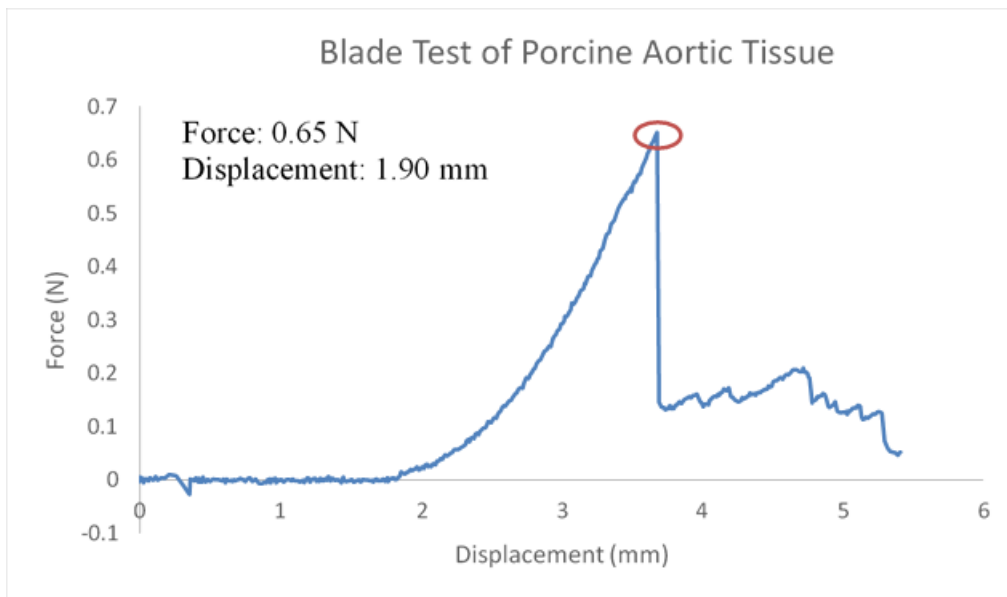


Figure 4.8. Blade test sample result.

The biological tissues were separated based on their source due to differences in tissue thickness and were grouped into three groups: aortic valve ($t = 0.5$ mm), aortic wall ($t = 3$ mm), aortic sinus wall ($t = 2$ mm). The synthetic cast samples and 3D printed samples were manufactured to have equivalent thicknesses (0.5 mm, 2 mm, 3 mm).

The following sections include the results of each group:

4.3.1. Needle and Blade Tests of $t = 0.5$ mm Group

The results shown in Figures 4.9 and 4.10 compare different tests against the porcine aortic tissue values (shown with lighter colours). For the needle tests, the maximum puncture force was for the digital material A40, and the lowest was for the silicone A10. The maximum displacement was for the Agilus30 material. For the cutting tests with the scalpel blades, the highest cutting force was for the equine tissues, and the lowest was for the silicone A10. The equine tissues also had the highest displacement at failure force.

Conducting statistical analysis using a confidence interval of 95% on the data showed that there were significant differences among the results of the needle tests and blade tests as well.

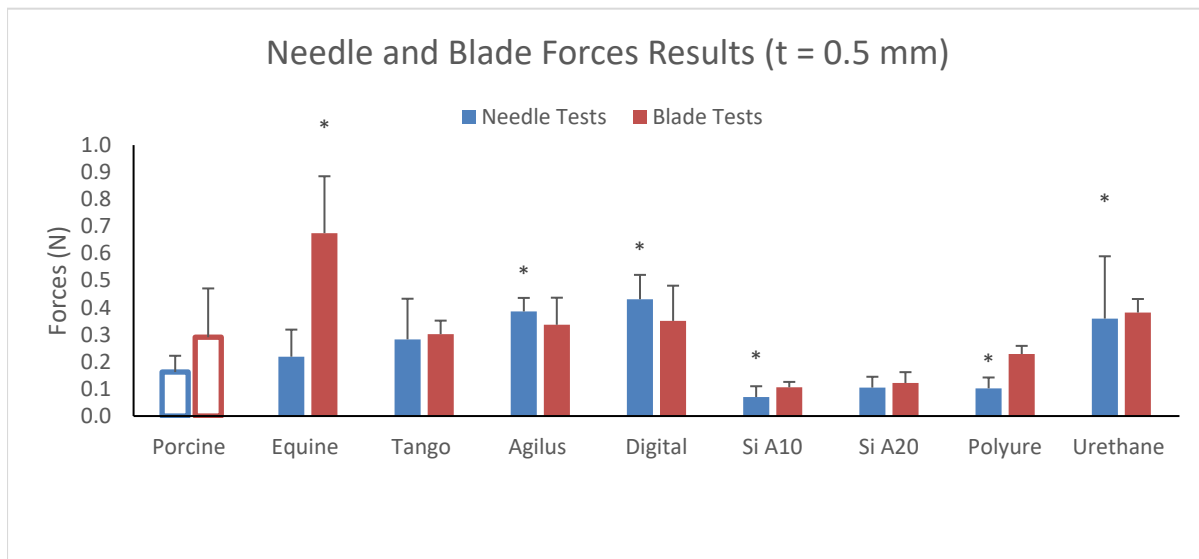


Figure 4.9. Comparison of forces for needle puncture and scalpel blade cutting tests for each of the materials tested at 0.5 mm. All testing forces were compared to porcine aortic tissue. *Statistically greater than the porcine aortic tissue.

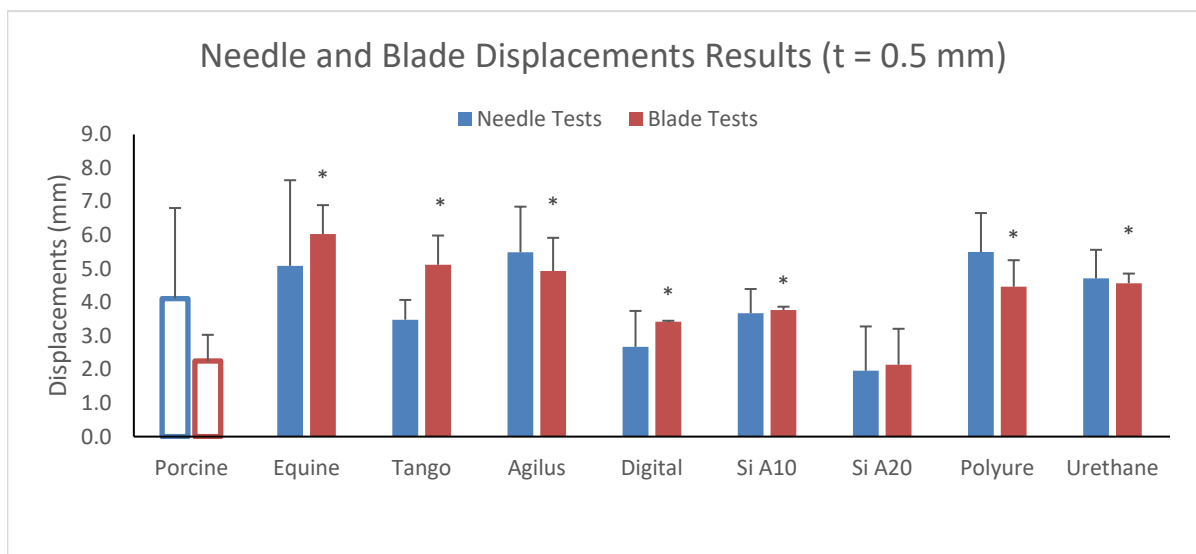


Figure 4.10. Comparison of displacement at max force for needle puncture and scalpel blade cutting tests for each of the materials tested at 0.5 mm thickness. All displacements were compared to porcine aortic tissue. *Statistically greater than the porcine aortic tissue.

A more detailed analysis comparing each sample to the porcine tissues revealed the following:

4.3.1.1. Needle tests:

For the force analyses, the silicone A10, polyurethane, Agilus30 and the digital material had significantly greater needle puncture forces than the porcine aortic tissue (Table 4.3, Figure 4.9). For the displacement analyses, there were no significant differences for any of the materials compared to porcine tissues (Table 4.3, Figure 4.10).

4.3.1.2. Blade tests:

For the force tests, the only significant differences were found in the comparison between equine and porcine samples. Cutting forces for the equine aortic tissues were significantly greater than the porcine tissues (Table 4.4, Figure 4.9). For displacement, all the materials tested had significantly greater displacement than the porcine samples except for the silicone A20 materials (Table 4.4, Figure 4.10).

Figures 4.11 and 4.12 shows samples of the needle and blade tests of the 0.5 mm group.

Table 4-3. Needle puncture tests for $t = 0.5$ mm.

	Material	n	Cutting Force (N)	<i>p</i> Value for Force	Displacement (mm)	<i>p</i> Value for Displacement
Bio	Porcine aortic tissues	6	0.17 ± 0.06	-	4.11 ± 2.70	-
	Equine aortic tissues	15	0.22 ± 0.10	.181	5.09 ± 2.55	.443
AM	TangoPlus	5	0.29 ± 0.15	.086	3.49 ± 0.59	.624
	Agilus30	3	0.39 ± 0.05	.001	5.49 ± 1.36	.440
	Digital Material	3	0.44 ± 0.09	.001	2.68 ± 1.07	.415
Cast	Silicone A10	6	0.07 ± 0.04	.005	3.68 ± 0.72	.711
	Silicone A20	3	0.11 ± 0.04	.140	1.97 ± 1.32	.243
	Polyurethane	6	0.10 ± 0.04	.040	5.51 ± 1.16	.272
	Urethane	4	0.36 ± 0.23	.066	4.72 ± 0.85	.680

Table 4-4. Blade cutting tests for $t = 0.5$ mm.

	Material	n	Cutting Force (N)	<i>p</i> Value for Force	Displacement (mm)	<i>p</i> Value for Displacement
Bio	Porcine aortic tissues	8	0.3 ± 0.18	-	2.26 ± 0.78	-
	Equine aortic tissues	11	0.68 ± 0.21	< .001	6.04 ± 0.86	< .001
AM	TangoPlus	3	0.31 ± 0.05	.925	5.13 ± 0.87	< .001
	Agilus30	3	0.34 ± 0.1	.689	4.94 ± 0.99	.001
	Digital Material	3	0.36 ± 0.13	.608	3.43 ± 0.03	.032
Cast	Silicone A10	3	0.11 ± 0.02	.109	3.77 ± 0.1	.027
	Silicone A20	3	0.13 ± 0.04	.141	2.15 ± 1.07	.145
	Polyurethane	3	0.23 ± 0.03	.502	4.47 ± 0.79	< .001
	Urethane	2	0.39 ± 0.05	.508	4.57 ± 0.29	< .001

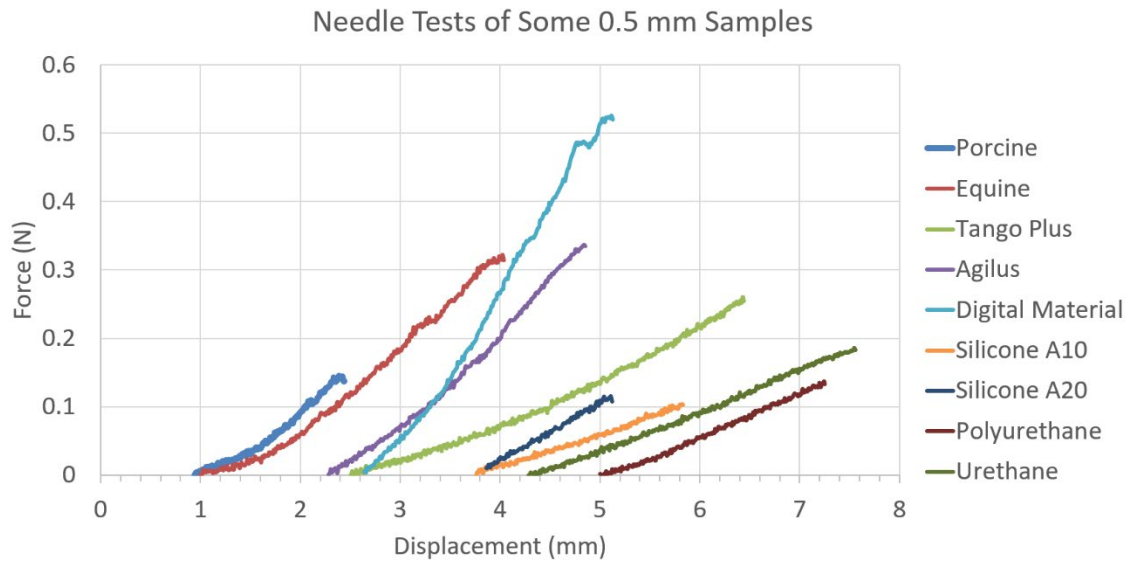


Figure 4.11. Representative needle tests of some 0.5 mm samples [Note: starting point for each displacement has been purposely altered to show the different groups.]

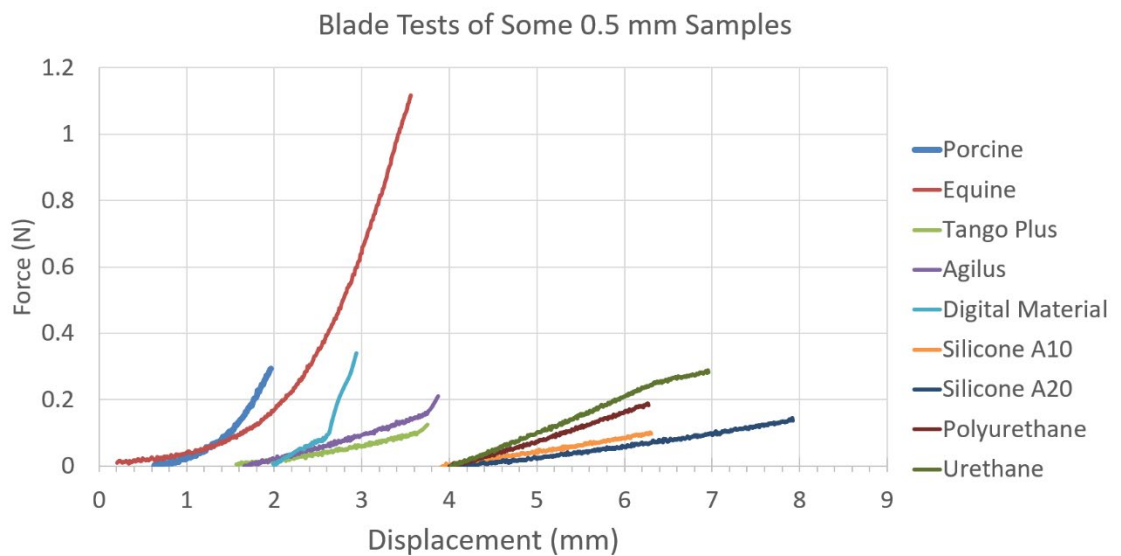


Figure 4.12. Blade tests of some 0.5 mm samples [Note: starting point for each displacement has been purposely altered to show the different groups.]

4.3.2. Needle and Blade Tests of $t = 2$ mm Group

In this thickness range, the difference between the AM group and the casting group became more noticeable. For example, in the needle tests, the maximum puncture force was recorded for the digital material at about 1.14 N, while the minimum force was for the polyurethane. Also, in the blade tests, the maximum cutting forces were for the digital material and the minimum forces were for the silicone A10. The differences in the displacement values among the samples were not significant.

4.3.2.1. Needle Tests:

The force required to puncture the material by the needle was significantly greater for all 2 mm thick materials compared to the puncture force for the porcine aortic sinus wall (Table 4.5, Figure 4.13). For needle displacement, there were no statistical differences of any material compared to the porcine sample displacement value (Table 4.5, Figure 4.14).

4.3.2.2. Blade Tests:

The AM materials showed significantly greater values in both force and displacement compared to the porcine tissues (Table 4.6, Figure 4.13 and 4.14). For casting materials, only the urethane samples showed significantly greater values in both force and displacement compared to the porcine tissues (Table 4.6, Figure 4.13 and 4.14). The polyurethane displacement was significantly greater than the porcine values (Table 4.6, Figure 4.14).

Table 4-5. Needle puncture tests t = 2 mm.

	Material	n	Cutting Force (N)	P-Value for Force	Displacement (mm)	P-Value for Displacement
Bio	Porcine aortic tissues	6	0.24 ± 0.06	-	6.08 ± 1.51	-
AM	TangoPlus	9	0.49 ± 0.25	.033	4.46 ± 2.19	.139
	Agilus30	3	1.07 ± 0.05	< .001	6.74 ± 0.26	.489
	Digital Material	4	1.14 ± 0.23	< .001	4.39 ± 1.04	.090
Cast	Silicone A10	6	0.37 ± 0.06	.004	5.07 ± 1.46	.267
	Silicone A20	3	0.41 ± 0.06	.003	4.10 ± 0.59	.071
	Polyurethane	3	0.25 ± 0.04	.886	5.58 ± 0.71	.615
	Urethane	3	0.39 ± 0.02	.003	5.23 ± 0.51	.386

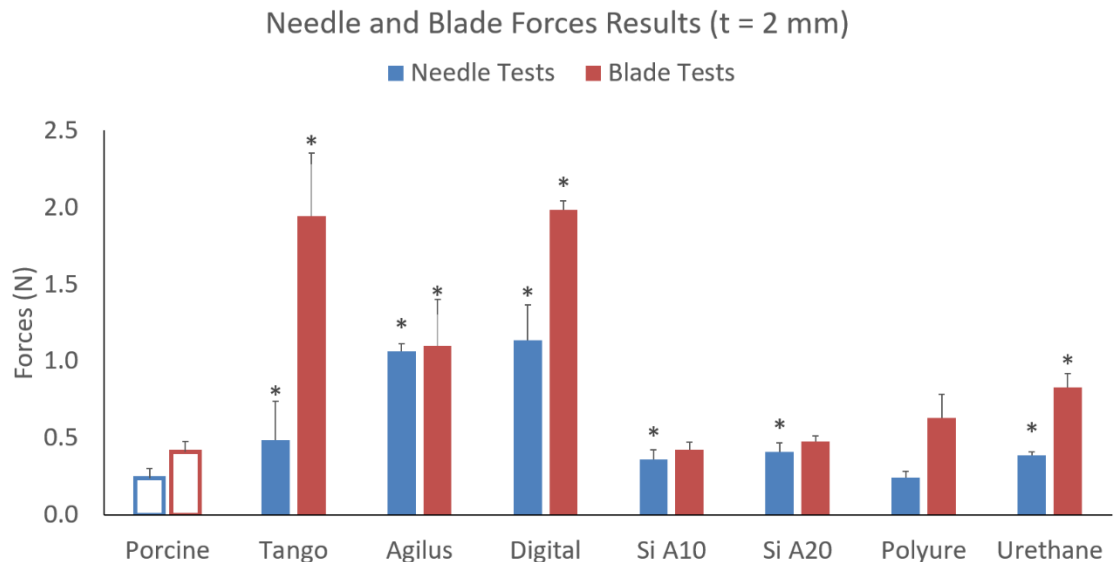


Figure 4.13. Comparison of forces for needle puncture and scalpel blade cutting tests for each of the materials tested at 2 mm. All testing forces were compared to porcine aortic tissue. *Statistically greater than the porcine aortic tissue.

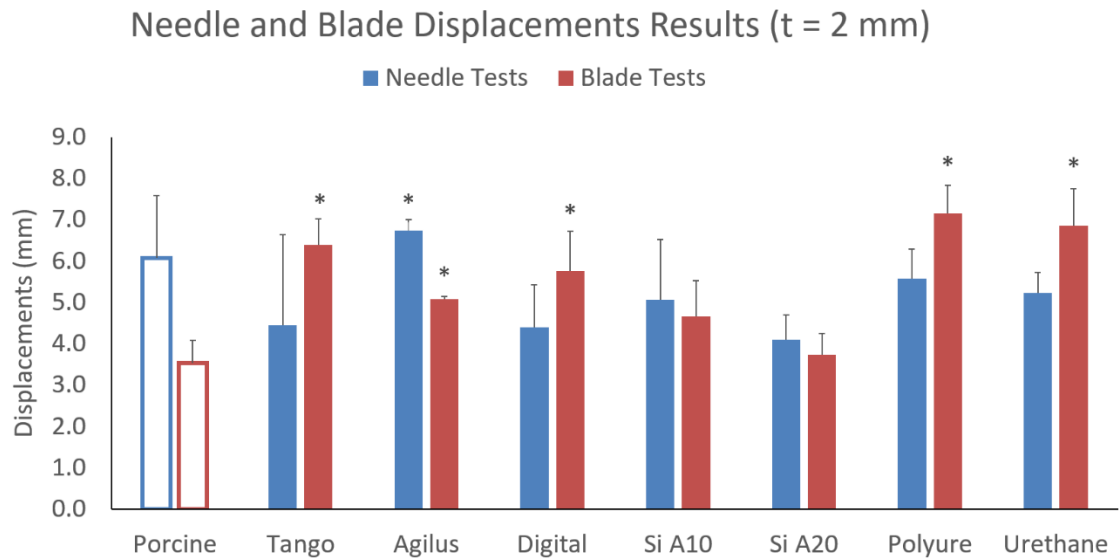


Figure 4.14. Comparison of displacement at max force for needle puncture and scalpel blade cutting tests for each of the materials tested at 2 mm thickness. All displacements were compared to porcine aortic tissue. *Statistically greater than the porcine aortic tissue.

Table 4-6. Scalpel blade cutting tests t = 2 mm.

	Material	n	Cutting Force (N)	P-Value for Force	Displacement (mm)	P-Value for Displacement
Bio	Porcine aortic tissues	3	0.41 ± 0.07	-	3.54 ± 0.54	-
AM	TangoPlus	2	1.95 ± 0.41	.006	6.38 ± 0.64	.012
	Agilus30	3	1.11 ± 0.30	.017	5.08 ± 0.07	.008
	Digital Material	3	1.99 ± 0.06	< .001	5.77 ± 0.96	.024
Cast	Silicone A10	3	0.43 ± 0.05	.762	4.66 ± 0.86	.127
	Silicone A20	3	0.48 ± 0.04	.210	3.74 ± 0.50	.649
	Polyurethane	4	0.64 ± 0.15	.056	7.15 ± 0.69	.001
	Urethane	3	0.83 ± 0.09	.003	6.86 ± 0.90	.005

4.3.3. Needle and Blade Tests of $t = 3$ mm Group

This group contained the largest recorded cutting force at about 5.35 N, and it was for cutting the digital material samples using the blade. It was also observed that the values of the forces of the AM materials tended to be significantly greater than the values of the porcine tissues.

4.3.3.1. Needle Tests:

The AM materials showed significantly greater forces compared to the porcine tissues (Table 4.7, Figure 4.15). The silicon A20, polyurethane and urethane showed significantly greater displacement values compared to the porcine tissues (Table 4.7, Figure 4.16). The only samples that were not significantly different compared to the porcine tissues were the silicon A10 samples.

4.3.3.2. Blade Tests:

The AM group showed significant differences in both the force and displacement values compared to the porcine tissues (Table 4.8, Figure 4.15 and 4.16). Similar to the needles tests observations, all the casting materials showed significant differences in displacement values compared to the porcine tissues except for the silicone A10 (Table 4.8, Figure 4.16). The A10 silicone did not show any significant differences in both the forces and displacement values compared to the porcine tissues (Table 4.8, Figure 4.15 and 4.16).

Table 4-7. Needle tests t = 3 mm.

	Material	n	Cutting Force (N)	P-Value for Force	Displacement (mm)	P-Value for Displacement
Bio	Porcine aortic tissues	4	0.44 ± 0.13	-	7.66 ± 0.7	-
AM	TangoPlus	9	1.00 ± 0.23	.001	6.62 ± 1.95	.329
	Agilus30	4	1.68 ± 0.23	<.001	6.46 ± 0.77	.192
	Digital Material	3	1.64 ± 0.41	.002	8.13 ± 0.64	.404
Cast	Silicone A10	6	0.47 ± 0.10	.666	6.11 ± 1.37	.071
	Silicone A20	3	0.52 ± 0.09	.411	3.63 ± 0.04	<.001
	Polyurethane	6	0.34 ± 0.04	.084	6.42 ± 0.76	.030
	Urethane	3	0.48 ± 0.09	.708	4.83 ± 0.52	.002

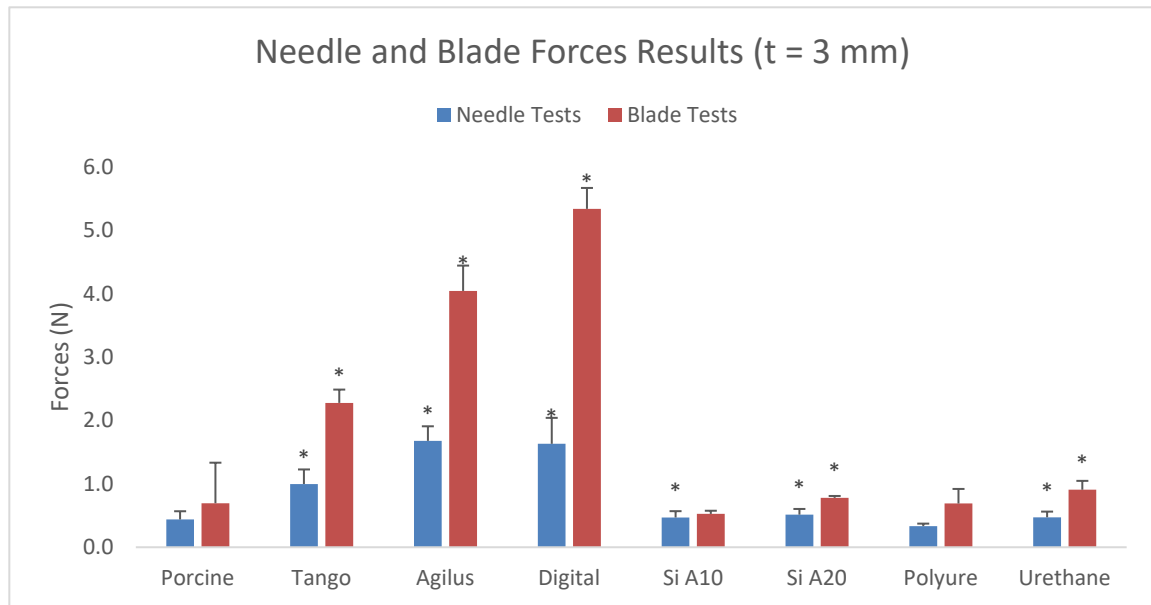


Figure 4.15. Comparison of forces for needle puncture and scalpel blade cutting tests for each of the materials tested at 3 mm. All testing forces were compared to porcine aortic tissue. *Statistically greater than the porcine aortic tissue.

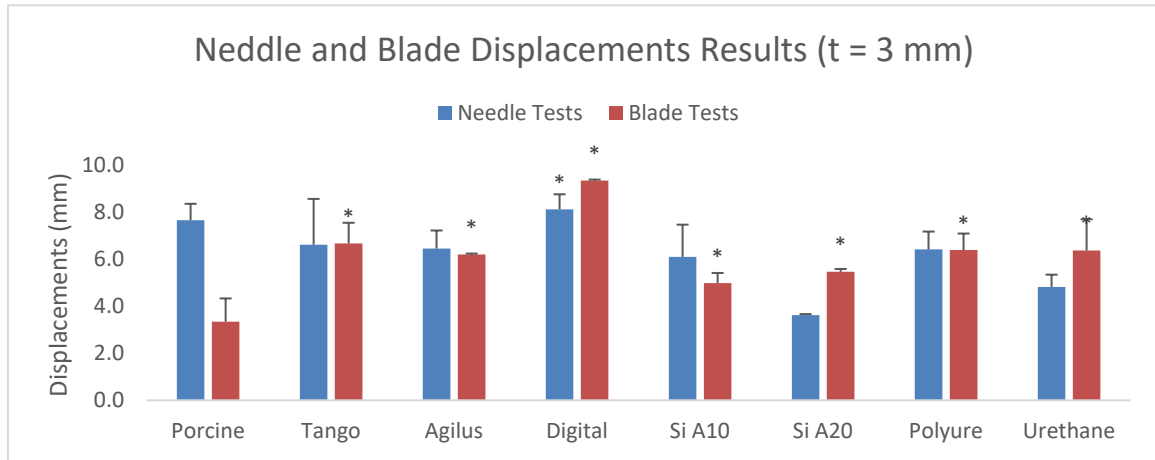


Figure 4.16. Comparison of displacement at max force for needle puncture and scalpel blade cutting tests for each of the materials tested at 3 mm thickness. All displacements were compared to porcine aortic tissue. *Statistically greater than the porcine aortic tissue.

Table 4-8. Blade tests t = 3 mm.

	Material	n	Cutting Force (N)	P-Value for Force	Displacement (mm)	P-Value for Displacement
Bio	Porcine aortic tissues	3	0.70 ± 0.64	-	3.35 ± 0.99	-
AM	TangoPlus	4	2.28 ± 0.21	.005	6.68 ± 0.88	.005
	Agilus30	3	4.05 ± 0.40	.001	6.21 ± 0.04	.007
	Digital Material	3	5.35 ± 0.33	< .001	9.35 ± 0.04	< .001
Cast	Silicone A10	3	0.53 ± 0.05	.671	4.99 ± 0.43	.057
	Silicone A20	3	0.78 ± 0.03	.652	5.47 ± 0.12	.021
	Polyurethane	4	0.70 ± 0.23	.990	6.40 ± 0.70	.005
	Urethane	3	0.91 ± 0.14	.600	6.38 ± 1.33	.034

4.3.4. Needle Tests of Manufactured Models

Additional tests were done on the synthetic materials for manufacturing the aortic valve region of the models. After the initial testing, we realized that we would not be able to reliably manufacture the region of the aortic valves at 0.5 mm thickness (either by casting or additive manufacturing) without defects (e.g., tears or gaps in the structure). Tests were performed on two additional thicknesses for the cast materials and 3D printed materials – 0.75 mm and 0.9 mm. Those models had different thicknesses for aortic valve manufacturing that were not represented in the previous tests. This was done to gain more information about the actual materials used in the models rather than only relying on the previous test values. For instance, it was not possible to manufacture aortic valve models with 0.5 mm thickness.

Also, the updated value of 0.75 mm was the minimum threshold for the AM, but such thickness was not ideal for casting. Therefore, another iteration was carried out to test 0.9 mm thickness for the aortic valve for casting.

The results of the analysis showed that there were no significant differences among the samples tested and the porcine tissues (Tables 4.9 and 4.10, Figures 4.17 to 4.20).

Table 4-9. Needle tests t = 0.75 mm.

	Material	n	Needle Puncture Force (N)	P-Value for Force	Needle Test Displacement (mm)	P-Value for Displacement
Bio	Porcine aortic tissues	6	0.17 ± 0.06	-	4.45 ± 2.39	-
Cast	TangoPlus	3	0.17 ± 0.01	.957	6.24 ± 0.47	.231
	Silicone A10	3	0.12 ± 0.01	.207	6.38 ± 0.69	.206

Table 4-10. Needle tests t = 0.9 mm.

	Material	n	Puncture Force (N)	P Value for Force	Displacement	P-Value for Displacement
Bio	Porcine aortic tissues	6	0.17 ± 0.06	-	4.45 ± 2.39	-
Cast	Silicone A10	3	0.13 ± 0.01	.298	7.04 ± 0.02	.112
	Polyurethane	3	0.11 ± 0.01	.139	7.02 ± 0.02	.114

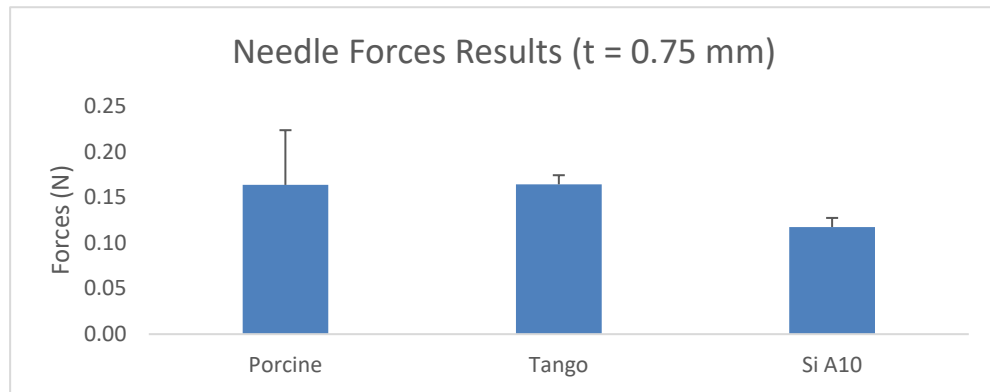


Figure 4.17. Comparison of forces for needle puncture and scalpel blade cutting for TangoPlus and silicone A10 at 0.75 mm. All testing forces were compared to porcine aortic tissue.

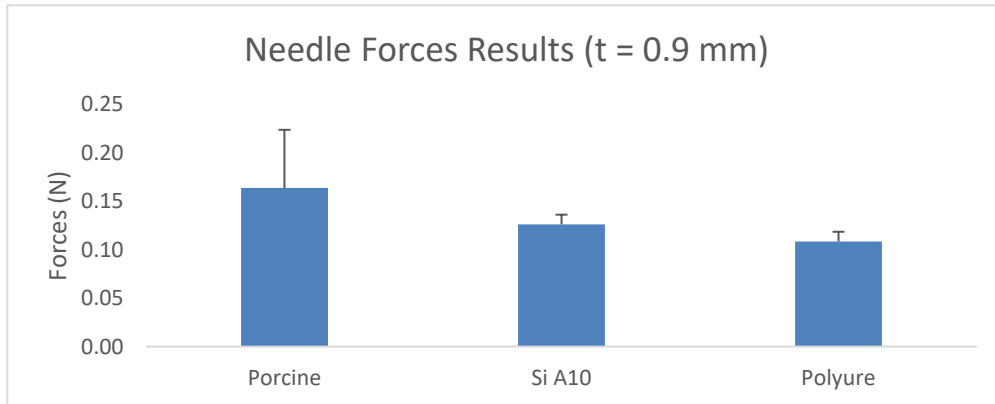


Figure 4.18. Comparison of forces for needle puncture and scalpel blade cutting tests for silicone A10 and polyurethane at 0.9 mm. All testing forces were compared to porcine aortic tissue.

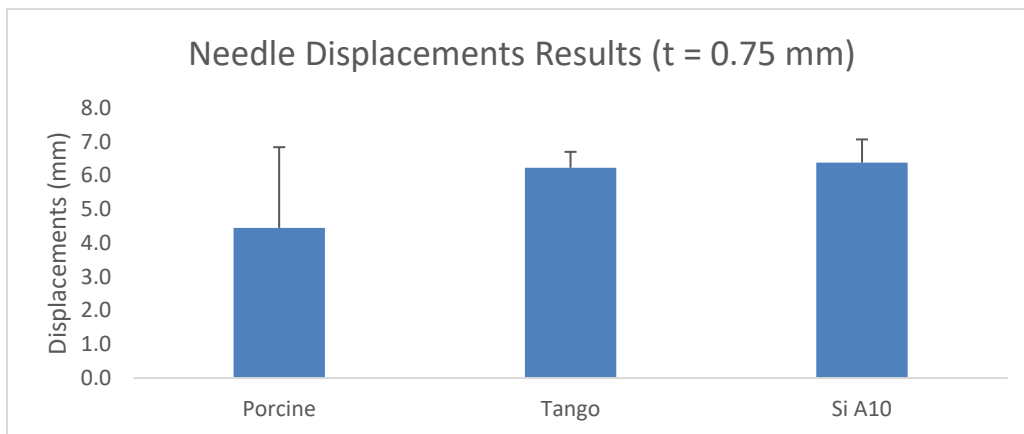


Figure 4.19. Comparison of displacement at max force for needle puncture and scalpel blade cutting tests for TangoPlus and silicone A10 at 0.75 mm thickness. All displacements were compared to porcine aortic tissue.

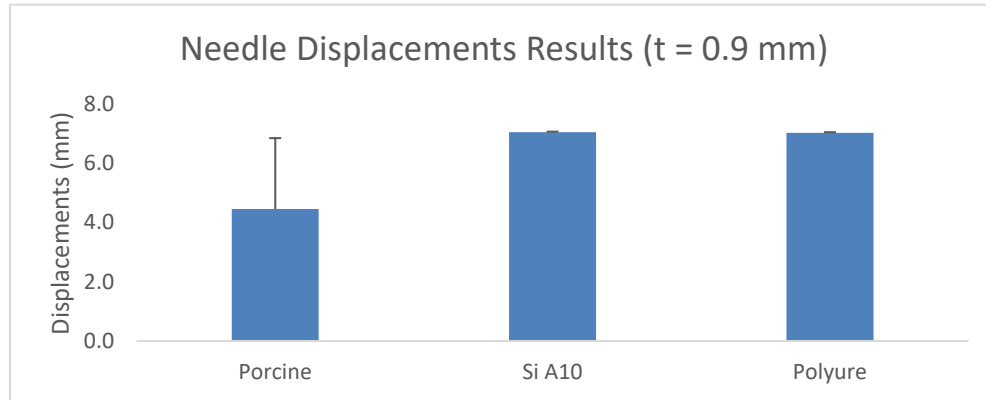


Figure 4.20. Comparison of displacement at max force for needle puncture and scalpel blade cutting tests for silicone A10 and polyurethane at 0.9 mm thickness. All displacements were compared to porcine aortic tissue.

4.4. Discussion

The purpose of this study was to compare the response (maximal force and displacement) of materials to surgical cutting procedures including needle puncture and scalpel blade cutting. The key findings were that the casting materials (silicone and polyurethane) were more likely to be similar to the porcine aortic tissues in all the tests performed regardless of the thickness of the sample tested. On the other hand, the compliant AM materials were less likely to be similar to the porcine tissues as the sample thickness increases.

The expectation was that the harder materials, in general, would be less likely to be similar to the porcine tissue. The results supported this assumption when it came to the AM materials.

However, that was not the case for all the casting materials, especially for polyurethane. In that case, greater hardness was not directly associated with greater forces for needle puncturing or scalpel cutting.

Comparing all the test results to the range of forces used in mitral valve annuloplasty surgical repairs reported by Currie and colleagues showed that only AM materials were within that range from 1.6 N to 11.5 N (Currie et al., 2013). Those AM materials were the samples with 2 and 3 mm thicknesses. The comparison was done to give a sense of the forces exerted by the surgeons using surgical tools during heart valve repair operations.

The experiment limitations include tissue relaxation, sample size and surgical tools movements. For example, sometimes the samples could not be fully stretch due to their small size leading to relatively higher cutting forces compared to fully stretched samples. Also, sample sizes were relatively small at three samples on average per tissue type. Some results showed noisy data that were likely the results of the movements of the surgical tools while cutting through the samples. For instance, the data may show more than one point with high force values, one occurred at the first contact and the other at the cut-through moment. Choosing the correct maximum puncturing force, in this case, depends on the test's observations (e.g., for thick samples, the puncturing force occurred at higher displacement values compared to thinner samples). This made detecting the puncturing and cutting points more challenging for some of the tests.

Regarding the synthetic testing materials, the AM materials were harder and significantly more expensive than the casting materials. The testing results showed that casting should be considered first to manufacture the aortic valve models.

4.5. Conclusions

Manufacturing the aortic valve model requires choosing suitable materials that can mimic the behaviour of real tissues during surgical training. Investigating this was done via mechanical tests with cutting by scalpel and puncture tests with needles. The AM materials were relatively stiffer than the casting materials.

Therefore, the forces required to penetrate or cut the AM samples were significant compared to those required for the casting materials. The results showed that the best candidates for manufacturing materials were casting materials especially silicone A10. This was largely due to having similar values.

The tests only considered one scenario in which the samples were directly cut or punctured. However, surgical repairs training would involve suturing and constant manipulation of the model. Therefore, it is suggested to explore other testing scenarios for future tests. For example, a scenario that can test the competency of the surgical suture could provide more insight regarding the selection of the materials. Also, other factors need to be considered such as ease of manufacturing, cost and surgeons' feedback.

Chapter 5

5. Educational Model Evaluation

5.1. Introduction

Surgical simulation training exists to provide solutions for many surgical training challenges. For instance, simulation training offers a viable alternative to training on live patients, which is undesirable and risky. Moreover, simulation training could offer cost saving potentials depending on the situation. Training activities tend to require repetition (more time compared to regular activities) and are prone to mistakes that could lead to failures. Therefore, using specialized equipment or designated areas, such as operation rooms for training is not as cost-effective as simulation training (Munro, 2012). Also, it has been estimated that only 25% is attributed to manual dexterity in successfully performed operation, while 75% is attributed to decision making (Spencer, 1978). Thus, acquiring decision-making skills is critical. Simulation surgical training could offer many different scenarios to safely acquire those decision-making skills.

At its core, simulation surgical training is about increasing the competency of the surgeons. The surgeons need to translate their theoretical knowledge into repeatable skills to achieve competency. Miller's pyramid for assessing clinical competence consists of four stages including 1) knows, 2) knows how, 3) shows how, and finally 4) does (Miller, 1990). Figure 5.1 shows an illustration of the steps (Okoro et al., 2010).

It is critical to measure the technical ability of surgeons at each step. Structured simulation training could provide the tools to fulfill this need.

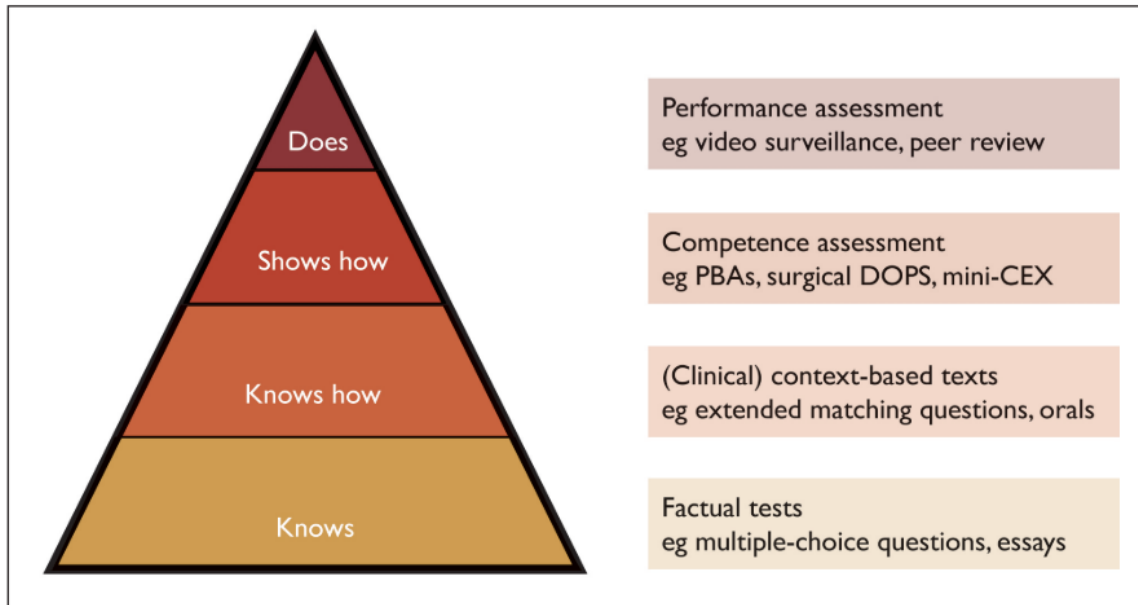


Figure 5.1. Miller's pyramid for assessing clinical competence (Miller, 1990; Okoro et al., 2010).

For laparoscopic suturing training, Korndorffer and colleagues determined that simulation training using the video trainer suturing model was effective in increasing the operative performance of the trainees (Korndorffer et al., 2005). The study was done using a live porcine model and synthetic model that included an instructional video for the surgical simulation. The assessment process was carried out using the completion time and accuracy of the sutures. The study compared the performances of the two groups. The control group only used the porcine model, while the video trainer group used both the porcine and synthetic model for the training.

Fann and colleagues reported that there was a need for simulation surgical training in the surgical training curriculum (Fann et al., 2010). Their study was regarding coronary artery anastomosis and consisted of a boot camp training session using a synthetic anastomosis task station and porcine model. The surgeons trained on the anastomosis task station then performed on the porcine model. Senior surgeons evaluated the performance of trainee surgeons. The evaluation methods included surveys and a technical rating scale. The surveys included questions about the fidelity of the synthetic model and the training experience in general. The rating scale included numerical weight (poor = 3, average = 2 and good = 1) for specific training tasks, such as the graft orientation, appropriate spacing, use of forceps and needle transfer. The study concluded that the training improved the surgeons' skills (Fann et al., 2010).

Yoo and colleagues conducted training sessions using 3D printed patient congenital heart diseases. All the surgeons found the training helpful in improving their surgical skills (S. J. Yoo et al., 2017). The evaluation method was done by an expert surgeon. Also, a questionnaire regarding the fidelity of the model was used.

An example of the current state of surgical training tools for cardiac surgery was a training model developed by Loo and colleagues (Figure 5.2). The model was low fidelity adequately realistic multi-station surgical training tool. The box-like tool can mimic cannulation, coronary artery bypass grafting, aortic graft replacement, aortic valve replacement, and mitral valve annuloplasty surgical tasks.

The surgical training set is made of polyester fabrics, holster-like holders and Velcro attachments. The aortic valve chamber was 3D printed to mimic the actual dimensions of the valve (Loor et al., 2016). The educational model cost was around US\$700 with a selling price of about US\$1200.

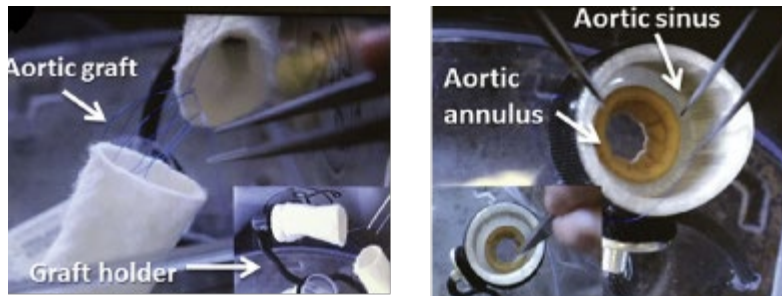


Figure 5.2. Surgical training setup showing aortic valve and aortic graft stations (Loor et al., 2016).

Surgical training educational models are limited and overly simple. The Loor and colleagues' educational model did not have high fidelity structures of the cardiac tissues such as the aortic valve and the mitral valve. The model approximates the size of these tissues by using 3D-printed rings. The educational model was not pressure tested, did not have key cardiac regions such as the left ventricle and focuses on surgical replacement tasks rather than surgical repairs of the valves. Also, specific aortic valve anomalies such as the bicuspid aortic valve were not available.

Aims of this chapter:

- Get feedback from surgical trainees on the utility of the training model.
- Assess if the model helps to improve trainee skills development using a validated assessment method in collaboration with Dr. Matt Sibbald from the Centre for Surgical Simulation at McMaster University.

5.2. Materials and Methods**5.2.1. An Initial Assessment with Surgical Trainees on Models and Materials**

The first type of assessment was to ask the surgical residents directly about the model. The objective was to get the surgeons' impression regarding the morphology of the aortic valve model as well as the suitability of the model for training. Showing the models to the residents was the most critical step to validate the model and the materials selections. An evaluation session was planned in collaboration with Dr. Matt Sibbald from the Centre for Surgical Simulation at McMaster University. The introductory session was held at Hamilton General Hospital with a group of cardiac surgical residents to test the models.

The residents were provided with four types of aortic valve models, including the following (Figure 5.3):

- Silicone aortic valve version1
- Polyurethane aortic valve version1
- Two TangoPlus aortic valves (versions 1 and 2)

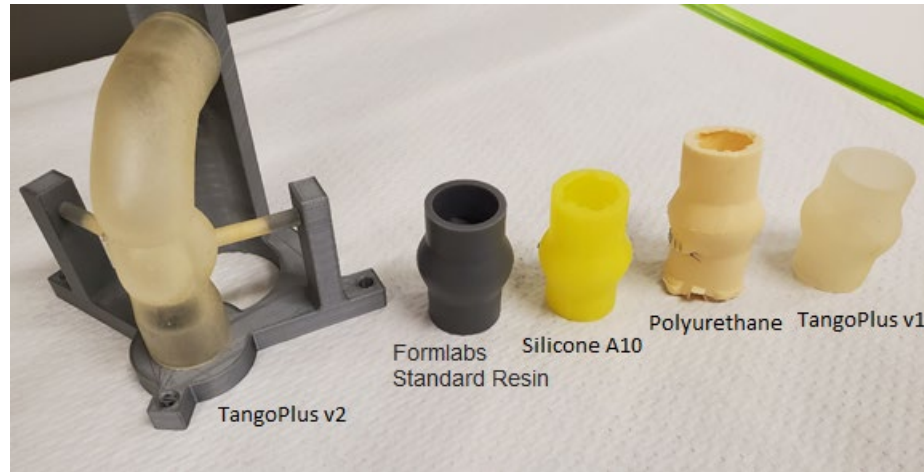


Figure 5.3. Aortic valve models used in the initial assessment session.

The assessment method was done by giving the surgical residents the models and then asking them questions and for feedback while they inspected the models.

The questions were the following:

- What do you think about the geometry of the aortic valve model?
- What do you think about the materials of the models? Does the material mimic real tissue?
- What would you like to see as a new or updated feature in the model?
- Can you please rank the models according to your preference?

The session included surgical residents with three different skill levels including the following:

- **Level 1:** Interns or new to surgery. The focus of this group was to test the model for basic suturing practice. Their practice did not involve complicated processes, such as cutting the ascending aorta and suturing it back to its place. They received guidance from the other residents.
- **Level 2:** Junior surgical residents: They focused on sectioning the aortic valve model to do a surgical repair process. The process was done by cutting the ascending aorta and suturing it back to its place in the model. Also, members of this group assisted each other throughout the repair process.
- **Level 3:** Senior surgical residents: Their primary role was to give guidance and feedback to all the other residents. They performed some surgical tasks such as cutting and suturing to sample the aortic valve models and show the other residents how to do the surgical skills properly. They also provided feedback on the type of modifications and pathologies they would like to see mimicked in the surgical model.

5.2.2. Plans Developed for Trainee Skills Assessment Using Model Vs. Standard Training

Note: We encountered some challenges in this last section. Our clinical collaborator, Dr. Parry, moved out of the country in 2019 and so we had to re-establish local clinical connections, which caused a delay in the setup of the skills training.

Ultimately, due to the COVID-19 pandemic, this part had to be cancelled before we could perform the actual skills training and we were unable to perform the testing or gather skills outcomes data. Recommendations are made for continuing this assessment in the future.

The proposed plan consisted of two primary methods of testing including 1) comparing the performances of two groups using different training methods, and 2) measuring the outcomes of the training sessions using both quantitative and qualitative measurement criteria.

5.2.2.1. Two Groups Method

This method consists of two groups doing surgical skills training using different methods. The first group would train using porcine tissues only. On the other hand, the second group would train using both porcine tissues and the aortic valve synthetic model. The objective is to validate if the synthetic aortic valve model would have a positive impact on surgical skills training compared to the standard training.

5.2.2.2. Outcome Measures Method (test using a synthetic aortic model):

Outcomes measures would be performed using a senior surgeon. In the training session done for the initial assessment mentioned in the previous section, senior surgical residents were evaluating the performance of junior residents. Examples of measuring methods include time, qualitative (functional performance), objective structured assessment of

technical skills (OSATS), hand motion analysis and live and video assessments by expert surgeons (Lodge & Grantcharov, 2011). The time measuring method is simply measuring the completion time for the training. Qualitative assessment includes testing the model after the training to check for performance measures, such as testing for leaking (examples can be seen in Figure 5.4). Hand motion analysis uses hand tracking devices to measure hand motion. OSATS is a 5 points global rating assessment that includes 7 categories as seen in Figure 5.5. Senior surgeons can use OSATS for both live and video assessments of the trainees.

OSATS have been found to be reliable and valid to assess surgical skills (Faulkner et al., 1996; Martin et al., 1997; Price et al., 2011; Reznick et al., 1997). Also, some researchers created modified global rating scales based on OSATS (Fann et al., 2010; Hance et al., 2005; Sidhu et al., 2007).

Subject study No.:	Judge:				
Lab date (dry/wet):	Date of assessment:				
End-product rating scale					
Suture spacing	1 Bites inconsistent in size and depth, with wide gaps	2	3	4	5 Consistently equal and appropriate spacing
Suture eversion	1 Inadequate	2	3	4	5 Superior performance
Quality of anastomotic heel	1 Inadequate	2	3	4	5 Superior performance
Quality of anastomotic toe	1 Inadequate	2	3	4	5 Superior performance
Total score: /20					
Notes:					

Figure 5.4. Qualitative rating scale (Price et al., 2011).

Respect for tissue	1 Frequently used unnecessary force on tissues and or caused damage by inappropriate use of instruments	2	3 Careful handling of tissue but occasionally caused inadvertent damage	4	5 Consistently handled tissues appropriately with minimal damage
Time and motion	1 Many unnecessary moves	2	3 Efficient time/motion, but some unnecessary moves	4	5 Clear economy of movement and maximum efficiency
Instrument handling	1 Repeatedly made tentative or awkward moves with instruments by inappropriate use of instruments	2	3 Competent use of instruments but occasionally appeared stiff or awkward	4	5 Fluid moves with instruments and no awkward moves
Knowledge of instruments	1 Frequently asked for wrong instrument or used inappropriate instrument	2	3 Knew names of most instruments and used appropriate instrument	4	5 Obviously familiar with the instruments and their names
Flow of operation	1 Frequently stopped operating and seemed unsure of next move	2	3 Demonstrated some forward planning with reasonable progression of procedure	4	5 Obviously planned course of operation with effortless flow from one move to the next
Use of assistants	1 Consistently placed assistants poorly or failed to use assistants	2	3 Appropriate use of assistants most of the time	4	5 Strategically used assistants to the best advantage at all times
Knowledge of specific procedure	1 Deficient knowledge. Needed specific instruction at most steps	2	3 Knew all important steps of the operation	4	5 Demonstrated familiarity with all steps of the operation

Figure 5.5. OSATS global rating scale (Martin et al., 1997; Price et al., 2011).

The following subsections include suggestions for measuring the outcomes of training based on skills:

5.2.2.2.1. Sectioning and closure procedure:

This is similar to what was done in the initial assessment training session. That is, the surgical trainees sectioned the models by cutting the ascending aorta from the model. The closure step was to try and adequately reattach the ascending aorta back to its original place in the model. Thus, a level 1 resident would train on how to make proper sutures while inspecting the geometry of the model. On the other hand, level 2 and 3 surgical residents could completely remove the ascending aorta and the lower portion of the model (VAJ) to reattach them back to the aortic root. The work of all the trainees could be evaluated by a senior surgeon. The measuring methods would include:

- A. OSATS evaluation,
- B. completion time for the trainee, and
- C. fluid leaking test of the repaired model.

5.2.2.2.2. Dacron Graft Repair Procedures (David, 2016):

Dacron graft procedures referred to the two main aortic valve-sparing operations mentioned in Section 2.2.3. including the aortic valve reimplantation and the aortic root remodelling. Both operations are complex, but the reimplantation method is easier to teach compared to the remodelling (David et al., 2015). Also, the same paper stated that starting with the reimplantation method was the better approach for young surgeons. Both operations share

common steps, such as excising the damaged aortic sinuses and removing the coronary arteries from the aortic root. However, the reimplantation method requires reimplanting the aortic valve inside a tailored Dacron graft. On the other hand, the remodelling method requires suturing the graft to the remaining aortic root tissues. Dr. Parry's goal was to enable the training of these complex procedures using the surgical training model developed in our research.

A level 2 surgical resident could train on the aortic valve model following the reimplantation method, while a level 3 surgical resident could train on the remodelling method. A senior surgeon would guide and evaluate all the trainees. Aortic valve-sparing operations are used to treat aortic valve insufficiency, which is a leaking issue caused by the improper aortic valve leaflet functions causing the blood to flow back (leaking) to the left ventricle. Therefore, conducting a pressurized test to test the leakage of the model could prove to be a mechanism to validate the competency of the surgical repairs. However, the current aortic valve models were not optimized to be pressure tested. The evaluation method would be done using OSATS, time of repair completion and an end of repair test (qualitative assessment). Also, the assessment method could be done live or via video depending on the options available.

5.2.2.2.3. Additional Outcomes Measuring Methods:

Another plan to measure the outcomes of the training is using questionnaires similar to what was done in the literature (Fann et al., 2010; Loor et al., 2016; Olivieri et al., 2016; S.

J. Yoo et al., 2017). Those questionnaires would include questions about the training outcomes and the fidelity of the training model.

Finally, checklists could be used to measure the outcomes of the training (Figure 5.6). This was done by Martin and colleagues (Martin et al., 1997). The checklist could include inspection and selection tasks that need to be done during the training.

Examples of survey questions from Yoo and colleague (S. J. Yoo et al., 2017):

- How many years have you performed cardiovascular surgery?
- Did the models provide you with the necessary information regarding the major pathological findings?
- How would you grade the overall quality of the models you operated on?
- Was the consistency and elasticity of the model material similar to that of the human myocardium?
- Was the model material acceptable for an appropriate surgical simulation? Did you find this Hands-on Surgical Simulation Session helpful in improving your surgical skills?
- Would you consider including similar Hands-on Surgical Simulation Sessions in the training programs for residents and fellows?

Item	Not Done/ Done Incorrectly	Done correctly
CONTROL OF HEMORRHAGE		
1. Applies pressure to stop bleeding first	0	1
2. Asks assistant to suction field	0	1
3. Inspects injury by carefully releasing IVC	0	1
4. Ensures all equipment needed for repair is at hand before starting	0	1
5. Control of bleeding point (use de Bakey forceps / Satinsky clamp or prox / distal pressure)	0	1
REPAIR		
6. Select appropriate suture (4.0 / 5.0 / 6.0 polypropylene)	0	1
7. Select appropriate needle driver (vascular)	0	1
8. Select appropriate forceps (de Bakey)	0	1
9. Needle loaded 1/2 – 2/3 from tip 90% of time	0	1

Figure 5.6. Example of a checklist (Martin et al., 1997).

5.3. Results and Discussion

The surgical residents were asked to determine the best materials that could resemble a real tissue. The evaluation methods included cutting parts of the samples and attempting to reattach the removed parts via suturing.

The result of the evaluation concluded that the best material was the silicone A10 and the worst was the TangoPlus model. This can be seen in Figure 5.7, ranked from the best (left end) to the worst model (right end).

The session included surgical residents at different proficiency levels ranging from intern to senior. The intern surgical residents were interested in practicing suturing techniques on the model regardless of the dimensional accuracy or the pathology. Also, the junior surgical residents were mainly interested in the geometry of the model. On the other hand, senior surgical residents were interested in the idea of having models with different pathologies. This demonstrated that surgical residents at different proficiency levels had different training needs and challenges that they needed to tackle.

Regarding the expectations of the future, it is reasonable to assume that the model can be beneficial in improving the surgical skills of the trainees. This was after examining the literature provided in this chapter earlier as well as at the beginning of this thesis. For instance, the TangoPlus material used in the aortic valve 3D printed model was similar to those used in Yoo and colleague studies (S. J. Yoo et al., 2017). Almost all the trainees found the TangoPlus material as either acceptable (40%) or highly acceptable (50%) for surgical simulation. The results presented in this chapter and those mentioned in Chapter 4 suggested that the silicone A10 could provide a better simulation experience compared to that of using AM materials including TangoPlus.



Testing Silicone A10



Testing TangoPlus



Training Setup



Figure 5.7. Models evaluation by surgical residents.

Also, the aortic model geometry was based on realistic dimensions obtained from the literature (Swanson & Clark, 1974). Considering the materials used in manufacturing the model whether AM materials or casting, the model would not be considered as a low fidelity model. The model by Loor and colleagues was of low fidelity and was reported to be both adequately realistic and suitable to be included in cardiovascular training programs (Loor et al., 2016). Thus, it is expected that the aortic valve model would also be viewed positively by the surgeons.

Ribeiro and colleagues conducted a systematic review of simulation-based skill training for trainees in cardiac surgery and reported that simulation training was associated with improved learning outcomes even with low fidelity training simulators (Ribeiro et al., 2018). Therefore, it is expected that the aortic valve model would improve the surgical skills of the trainees.

Aortic valve sparing surgeries are complex and challenging to be reproduced (David, 2016). Those surgeries are the treatment of choice (instead of valve replacement) for certain conditions, such as the aortic root aneurysm (David et al., 2015). Also, one of the issues in performing these surgeries was excessive bleeding (in aortic valve remoulding in particular). This was likely due to long suture lines (David et al., 2015).

Dr. Parry mentioned the need to produce training models for aortic valve sparing surgeries. This suggests that there is a need to have simulation training for these surgeries to make them more reproducible and minimize their risks. It is expected that the aortic valve model would positively contribute to aortic valve sparing surgeries training.

5.4. Conclusions

Preliminary testing of the aortic valve training model was carried out with a group of cardiac surgical residents at Hamilton General Hospital. The group consisted of surgical residents of various levels of proficiency ranging from interns to seniors. The surgical residents were given several aortic valve models to test including silicone, polyurethane and TangoPlus models. The models were ranked according to the surgical residents' preferences with the silicone model being the best, followed by the polyurethane and then the TangoPlus model, respectively. The surgical residents demonstrated various training needs including simple models for interns, a geometrically competent model for junior surgical residents and pathology-based models for senior surgical residents.

Additionally, the plans proposed in Section 5.2.2. need to be explored to validate and document the training outcomes of the aortic valve model. The simulation training tests were planned in collaboration with Dr. Matt Sibbald (Director of the Centre for Simulation-Based Learning, Faculty of Health Sciences, McMaster University). When the COVID-19 pandemic is resolved and access to hospitals is permitted again, then the training plans should resume using the proposed assessment techniques.

Using all the measuring methods including measuring methods include time, qualitative, OSATS, hand motion analysis and live and video assessments by expert surgeons would maximize the data gathering of the training sessions. However, hand motion analysis would require specialized tracking equipment and simply measuring the time is not enough to adequately measure the outcomes of the training (Lodge & Grantcharov, 2011).

Martin and colleagues reported that using a global rating was more reliable than using task-specific checklists (Martin et al., 1997). Therefore, using OSATS as the foundation of the training assessment is an adequate starting point. The expert surgeons can then use OSATS to evaluate the performance of the trainees including time-based assessment as a secondary objective. Additionally, a qualitative assessment should be done to check for any leaking in the models after the surgical repairs. The availability of live training sessions could be challenging during certain times, such as during the COVID-19 pandemic. Therefore, video assessment using OSATS can provide a solution to this issue.

Chapter 6

6. Conclusion and Future Work

6.1. Recommendations

6.1.1. Aortic Valve CAD Design

In designing the aorta CAD model, I had to use three different software packages, including VMTK LAB, Geomagic Studio and SpaceClaim, to process the data from image segmentation to CAD model. The reverse engineering process for the patient-specific aortic valve CAD model was complicated. Therefore, it is recommended to use a comprehensive CAD processing system, if available, to process the data to minimize the processing time. Also, having high-quality CT scans with the correct timing of the valve opening and closing actions within the cardiac cycle is essential to produce optimum CAD models.

Regarding the general aortic valve CAD model, using a parametric-based CAD software package can reduce the processing time. I used SpaceClaim, which is a direct modelling CAD package to do the CAD reconstruction and modelling processes. The advantage of this direct modelling approach was the ease of reverse engineering and the direct editing of the model. However, creating parametric relations between the design entities required additional linking steps. Therefore, it is recommended that the designer considers the advantages and disadvantages of each modelling approach based on the complexity of the model.

6.1.2. Tissues Testing

Initially, the sample mounting process on the Instron machine was relatively long. This was due to using a pair of two metal blocks, including four bolts to secure the samples. Eventually, I designed a small fixture to hold a pair of bulldog clamps to hold the samples in place. This significantly increased the mounting time for the samples. Thus, I recommend designing custom-made tools to enhance the materials testing experience.

Regarding the sample width and length, I recommend increasing both these dimensions to allow for more flexibility in positioning the samples. It was particularly challenging to stretch some of the samples due to their short length. Also, due to the limited ranges of motion of the fixture platform, it was sometimes difficult to position the samples directly under the surgical tool point of contact. This was mainly due to the short width of the samples.

After doing the training session with the cardiac surgeons, I realized that an additional testing method could be investigated to add more value to the selection criteria of the aortic valve model materials. This method involves pulling the sutures to test the structural integrity of the materials of the models. This could be done by preparing some samples that include sutures beforehand and then pulling them using a hook-like fixture using the Instron machine.

6.1.3. Aortic Valve Manufacturing

For direct AM, preparing the STL file was the most critical step before sending the file to the AM partners. Therefore, making sure that the STL model was watertight and ready for printing was essential. Also, knowing the limits of the AM capabilities beforehand can save some time and money. For example, AM of 0.5 mm aortic valve thickness was not successful. This was due to the difficulties in removing the support materials from the model.

For casting, several models were developed to optimize this process. The critical features that directly impacted the quality of the casts were the internal coaptation spacing between the aortic valve leaflets, the viscosity and working time of the casting materials, the use of a mould release agent, proper material exit points and proper sealing between removable sections.

The optimal coaptation spacing highly depends on the capabilities of the 3D printer. I tried some moulds with 0.1 mm spacing, and the results were unsuccessful since the leaflets were joined. Then, I tried increasing the spacing from 0.1 to 0.5 mm, and I was able to cast complete models with separated leaflets successfully. The use of a mould release agent was particularly essential for all the casting materials. It was possible to cast some of the materials without any release agents such as the A10 and A20 silicone, but it was not possible for the polyurethane.

Understanding the working time of the casting materials helped in limiting material waste and ensured adequate coverage of all the mould sections. Initially, all the materials seeped through the mould. Still, after several iterations, I determined that the best approach was the incremental filling of all the sections depending on the working time of the materials (e.g., 1 hour for A10 silicone and 4 min for polyurethane). Proper sealing was achieved using bolts, nuts and mould release agents. In some moulds, allowing a coated layer to form between the sections proved to be beneficial as a sealing method.

6.1.4. Educational Model Testing

Unfortunately, due to COVID-19, it was not possible to conduct training sessions with cardiac surgical residents to test the final educational model. However, it was recommended by the residents that the box or the aortic valve fixture should mimic the same position as the aortic valve during surgeries, as shown in Figure 3.9. Also, senior residents were interested in seeing an educational model with a simple pathology. The educational models were not tested using a pressurized system, so investigating this is included as a future step.

I recommend further investigating casting methods as it offers a wide range of materials selections that can be calibrated.

6.2. Future Work

6.2.1. Aortic Valve CAD Design

Currently, the surgical residents were interested in simplified representations of pathologies. So, it is possible to explore more methods in this area. This will lead to the creation of a library of different pathologies that could be used for training. Also, it is equally important to investigate how to create patient-specific models easily by non-CAD specialists.

6.2.2. Tissues Testing

Using different testing protocols such as cutting speed, cutting angles and preloading conditions can expand the scope of the testing. Also, using the suture pulling testing method mentioned in Section 6.1.2. will provide more insights regarding the aortic valve materials selection.

6.2.3. Aortic Valve Manufacturing

Creating a pathology-based mould is the next manufacturing step. The candidate pathology is the aortic valve aneurysm between the ascending aorta and the STJ. After that, an injection moulding manufacturing method will be investigated.

6.2.4. Aortic Valve Educational Model Validation

Training sessions need to be conducted to validate the model and measure the outcomes of the training. These sessions could be done using the two-groups method and the outcomes measuring method. The measuring methods that would be used include OSTAS, repair time of completion and end of repair quality test.

References

3D Printer Price. (2020). COMPUTER AIDED TECHNOLOGY. Retrieved September 01, 2020, from <https://www.cati.com/3d-printing/3d-printer-price/>).

Aortic root surgery. (2015). Retrieved August 30, 2020, from Mayo Clinic. <https://www.mayoclinic.org/tests-procedures/aortic-root-surgery/care-at-mayo-clinic/pcc-20383400>

Augoustides, J. G. T., Szeto, W. Y., & Bavaria, J. E. (2010). Advances in aortic valve repair: Focus on functional approach, clinical outcomes, and central role of echocardiography. In *Journal of Cardiothoracic and Vascular Anesthesia* (Vol. 24, Issue 6, pp. 1016–1020). Elsevier Inc. <https://doi.org/10.1053/j.jvca.2010.08.007>

Badash, I., Burt, K., Solorzano, C. A., & Carey, J. N. (2016). *Innovations in surgery simulation : a review of past , current and future techniques*. 4(23), 1–10. <https://doi.org/10.21037/atm.2016.12.24>

Baker, C. J., Sinha, R., & Sullivan, M. E. (2012). Development of a cardiac surgery simulation curriculum: From needs assessment results to practical implementation. *Journal of Thoracic and Cardiovascular Surgery*, 144(1), 7–15. <https://doi.org/10.1016/j.jtcvs.2012.03.026>

Bennett, C. J., Maleszewski, J. J., & Philip, A. (2012). CT and MR Imaging of the Aortic Valve : *Radiographics*, 32, 1399–1420. <https://doi.org/10.1148/rg.325115727/-/DC1>.

Boodhwani, M., & El Khoury, G. (2009). *Aortic valve repair*. <https://doi.org/10.1053/j.optechstcvs.2009.11>.

Brooks, R. A. (1977). A quantitative theory of the hounsfield unit and its application to

- dual energy scanning. *Journal of Computer Assisted Tomography*, 1(4), 487–493.
<https://doi.org/10.1097/00004728-197710000-00016>
- Brujic, D., Ainsworth, I., & Ristic, M. (2011). Fast and accurate NURBS fitting for reverse engineering. *International Journal of Advanced Manufacturing Technology*, 54(5–8), 691–700. <https://doi.org/10.1007/s00170-010-2947-1>
- Charitos, E. I., & Sievers, H.-H. (2013). Anatomy of the aortic root: implications for valve-sparing surgery. *Annals of Cardiothoracic Surgery*, 2(1), 53–56.
<https://doi.org/10.3978/j.issn.2225-319X.2012.11.18>
- Currie, M. E., Trejos, A. L., Rayman, R., Chu, M. W. A., Patel, R., Peters, T., & Kiaii, B. B. (2013). Evaluating the effect of three-dimensional visualization on force application and performance time during robotics-assisted mitral valve repair. *Innovations: Technology and Techniques in Cardiothoracic and Vascular Surgery*, 8(3), 199–205. <https://doi.org/10.1097/IMI.0b013e3182a3200e>
- David, T. E. (2016). Aortic Valve Sparing in Different. *Journal of the American College of Cardiology*, 68(6), 654–664. <https://doi.org/10.1016/j.jacc.2016.04.062>
- David, T. E., Coselli, J. S., Khoury, G. El, Miller, D. C., & Svensson, L. G. (2015). Aortic Valve Repair. *Seminars in Thoracic and Cardiovascular Surgery*, 27(3), 271–287.
<https://doi.org/10.1053/j.semtcvs.2015.10.010>
- De Raet, J. M., Arroyo, J., Büchner, S., Siregard, S., Andreas, M., Halvorsen, F., Grabosch, A., & Stubbendorff, M. (2013). How to build your own coronary anastomosis simulator from scratch. *Interactive Cardiovascular and Thoracic Surgery*, 16(6), 772–776. <https://doi.org/10.1093/icvts/ivt075>

- Enter, D. H., Lou, X., Hui, D. S., Andrei, A. C., Barner, H. B., Sheen, L., & Lee, R. (2015). Practice improves performance on a coronary anastomosis simulator, attending surgeon supervision does not. *Journal of Thoracic and Cardiovascular Surgery*, *149*(1), 12–16. <https://doi.org/10.1016/j.jtcvs.2014.09.029>
- Fann, J. I., Calhoun, J. H., Carpenter, A. J., Merrill, W. H., Brown, J. W., Poston, R. S., Kalani, M., Murray, G. F., Hicks, G. L., & Feins, R. H. (2010). Simulation in coronary artery anastomosis early in cardiothoracic surgical residency training: The Boot Camp experience. *Journal of Thoracic and Cardiovascular Surgery*, *139*(5), 1275–1281. <https://doi.org/10.1016/j.jtcvs.2009.08.045>
- Faulkner, H., Regehr, G., Martin, J., & Reznick, R. (1996). Validation of an objective structured assessment of technical skill for surgical residents. *Academic Medicine : Journal of the Association of American Medical Colleges*, *71*(12), 1363–1365. <https://doi.org/10.1097/00001888-199612000-00023>
- Feins, R. H., Burkhart, H. M., Conte, J. V., Coore, D. N., Fann, J. I., Hicks, G. L., Nesbitt, J. C., Ramphal, P. S., Schiro, S. E., Shen, K. R., Sridhar, A., Stewart, P. W., Walker, J. D., & Mokadam, N. A. (2017). Simulation-Based Training in Cardiac Surgery. *Annals of Thoracic Surgery*, *103*(1), 312–321. <https://doi.org/10.1016/j.athoracsur.2016.06.062>
- Fonseca, A. L., Reddy, V., Longo, W. E., & Gusberg, R. J. (2014). Graduating general surgery resident operative confidence: Perspective from a national survey. *Journal of Surgical Research*, *190*(2), 419–428. <https://doi.org/10.1016/j.jss.2014.05.014>
- Gebhardt, A. (2011). *Understanding Additive Manufacturing*.

<https://doi.org/10.3139/9783446431621>

Gibson, I., Rosen, D., & Stucker, B. (2015). Additive manufacturing technologies: 3D printing, rapid prototyping, and direct digital manufacturing, second edition. In *Additive Manufacturing Technologies: 3D Printing, Rapid Prototyping, and Direct Digital Manufacturing, Second Edition*. <https://doi.org/10.1007/978-1-4939-2113-3>

Hance, J., Aggarwal, R., Stanbridge, R., Blauth, C., Munz, Y., Darzi, A., & Pepper, J. (2005). Objective assessment of technical skills in cardiac surgery. *European Journal of Cardio-Thoracic Surgery*, 28(1), 157–162.

<https://doi.org/10.1016/j.ejcts.2005.03.012>

Heart, I. J. C., Saliba, E., Sia, Y., & Hamamsy, I. El. (2015). The ascending aortic aneurysm : When to intervene ? *IJCHA*, 6, 91–100.

<https://doi.org/10.1016/j.ijcha.2015.01.009>

Hossien, A. (2015). Comprehensive middle-fidelity simulator for training in aortic root surgery. *Journal of Surgical Education*, 72(5), 849–854.

<https://doi.org/10.1016/j.jsurg.2015.04.024>

Hossien, A., Gesomino, S., Maessen, J., & Autschbach, R. (2016). The Interactive Use of Multi-Dimensional Modeling and 3D Printing in Preplanning of Type A Aortic Dissection. *Journal of Cardiac Surgery*, 31(7), 441–445.

<https://doi.org/10.1111/jocs.12772>

Hurrell, M. A., Butler, A. P. H., Cook, N. J., Butler, P. H., Ronaldson, J. P., & Zainon, R. (2012). Spectral Hounsfield units: A new radiological concept. *European Radiology*, 22(5), 1008–1013. <https://doi.org/10.1007/s00330-011-2348-3>

- Izawa, Y., Hishikawa, S., Muronoi, T., Yamashita, K., Maruyama, H., Suzukawa, M., & Lefor, A. K. (2016). Ex-vivo and live animal models are equally effective training for the management of a penetrating cardiac injury. *World Journal of Emergency Surgery*, *11*(1), 1–10. <https://doi.org/10.1186/s13017-016-0104-3>
- Jung, J. I., Koh, Y.-S., & Chang, K. (2016). 3D Printing Model before and after Transcatheter Aortic Valve Implantation for a Better Understanding of the Anatomy of Aortic Root. *Korean Circulation Journal*, *46*(4), 588. <https://doi.org/10.4070/kcj.2016.46.4.588>
- Kalejs, M. (2014). *OPTIMAL MECHANICAL PARAMETERS FOR STRUCTURAL COMPONENTS OF HEART VALVE BIOPROSTHESES AND SELECTION OF A MATCHING SUBSTITUTE Summary of the Doctoral Thesis*. Rīga Stradiņš University.
- Khoury, G. El, & Kerchove, L. De. (2013). Principles of aortic valve repair. *The Journal of Thoracic and Cardiovascular Surgery*, *145*(3), S26–S29. <https://doi.org/10.1016/j.jtcvs.2012.11.071>
- Kim, G. D., & Oh, Y. T. (2008). A benchmark study on rapid prototyping processes and machines: Quantitative comparisons of mechanical properties, accuracy, roughness, speed, and material cost. *Proceedings of the Institution of Mechanical Engineers, Part B: Journal of Engineering Manufacture*, *222*(2), 201–215. <https://doi.org/10.1243/09544054JEM724>
- Kitagawa, M., Okamura, A. M., Bethea, B. T., Gott, V. L., & Baumgartner, W. A. (2002). *Analysis of Suture Manipulation Forces for Teleoperation with Force Feedback*.

2488, 155–162. https://doi.org/10.1007/3-540-45786-0_20

Korndorffer, J. R., Dunne, J. B., Sierra, R., Stefanidis, D., Touchard, C. L., & Scott, D. J.

(2005). Simulator training for laparoscopic suturing using performance goals translates to the operating room. *Journal of the American College of Surgeons*, 201(1), 23–29. <https://doi.org/10.1016/j.jamcollsurg.2005.02.021>

Lodge, D., & Grantcharov, T. (2011). Training and assessment of technical skills and

competency in cardiac surgery. *European Journal of Cardio-Thoracic Surgery*, 39(3), 287–293. <https://doi.org/10.1016/j.ejcts.2010.06.035>

Loor, G., Doud, A., Nguyen, T. C., Antonoff, M. B., Morancy, J. D., Robich, M. P.,

Odell, D. D., Yarboro, L. T., Vaporciyan, A. A., & Roselli, E. (2016). Development and Evaluation of a Three-Dimensional Multistation Cardiovascular Simulator. *Annals of Thoracic Surgery*, 102(1), 62–69.

<https://doi.org/10.1016/j.athoracsur.2015.12.070>

Martin, J. A., Regehr, G., Reznick, R., Macrae, H., Murnaghan, J., Hutchison, C., &

Brown, M. (1997). Objective structured assessment of technical skill (OSATS) for surgical residents. *British Journal of Surgery*, 84(2), 273–278.

<https://doi.org/10.1002/bjs.1800840237>

McKetty, M. H. (1998). The AAPM/RSNA Physics Tutorial for Residents: X-ray

Attenuation. *Radiographics*, 18(1), 151–163.

<https://doi.org/10.1148/radiographics.18.1.9460114>

Mildenberger, P., Eichelberg, M., & Martin, E. (2002). Introduction to the DICOM

standard. *European Radiology*, 12(4), 920–927.

<https://doi.org/10.1007/s003300101100>

Miller, G. E. (1990). The assessment of clinical skills/competence/performance. In *Academic Medicine* (Vol. 65, Issue 9, pp. S63–S67).

<https://doi.org/10.1097/00001888-199009000-00045>

Mokadam, N. A., Fann, J. I., Hicks, G. L., Nesbitt, J. C., Burkhart, H. M., Conte, J. V., Coore, D. N., Ramphal, P. S., Shen, K. R., Walker, J. D., & Feins, R. H. (2017). Experience With the Cardiac Surgery Simulation Curriculum: Results of the Resident and Faculty Survey. *Annals of Thoracic Surgery*, *103*(1), 322–328.

<https://doi.org/10.1016/j.athoracsur.2016.06.074>

Munro, M. G. (2012). Surgical Simulation: Where Have We Come From? Where Are We Now? Where Are We Going? *Journal of Minimally Invasive Gynecology*, *19*(3),

272–283. <https://doi.org/10.1016/j.jmig.2012.01.012>

Nishimura, R. A. (2002). Aortic Valve Disease. *Circulation*, *106*(7), 770–772.

<https://doi.org/10.1161/01.CIR.0000027621.26167.5E>

O'Brien, E. K., Wayne, D. B., Barsness, K. A., McGaghie, W. C., & Barsuk, J. H. (2016).

Use of 3D Printing for Medical Education Models in Transplantation Medicine: a Critical Review. *Current Transplantation Reports*, *3*(1), 109–119.

<https://doi.org/10.1007/s40472-016-0088-7>

Okoro, T., Sirianni, C., & Brigden, D. (2010). The Concept of Surgical Assessment: Part 1 – Introduction. *The Bulletin of the Royal College of Surgeons of England*, *92*(9),

322–323. <https://doi.org/10.1308/147363510x527664>

Olivieri, L. J., Su, L., Hynes, C. F., Krieger, A., Alfares, F. A., Ramakrishnan, K.,

- Zurakowski, D., Marshall, M. B., Kim, P. C. W., Jonas, R. A., & Nath, D. S. (2016). “Just-In-Time” Simulation Training Using 3-D Printed Cardiac Models After Congenital Cardiac Surgery. *World Journal for Pediatric and Congenital Heart Surgery*, 7(2), 164–168. <https://doi.org/10.1177/2150135115623961>
- Online 3D Printing Services. (2020). 3D HUBS. Retrieved August 30, 2020, from <https://www.3dhubs.com/3d-printing/>
- Park, I. K., Yun, I. D., & Lee, S. U. (1999). Constructing NURBS surface model from scattered and unorganized range data. *Proceedings - 2nd International Conference on 3-D Digital Imaging and Modeling, 3DIM 1999*, 312–320. <https://doi.org/10.1109/IM.1999.805361>
- Price, J., Naik, V., Boodhwani, M., Brandys, T., Hendry, P., & Lam, B. K. (2011). A randomized evaluation of simulation training on performance of vascular anastomosis on a high-fidelity in vivo model: The role of deliberate practice. *Journal of Thoracic and Cardiovascular Surgery*, 142(3), 496–503. <https://doi.org/10.1016/j.jtcvs.2011.05.015>
- Proto3000. (2020). *Proto3000*. Retrieved August 01, 2020, from <https://proto3000.com/>
- Qayumi, K., Pachev, G., Zheng, B., Ziv, A., Koval, V., Badiei, S., & Cheng, A. (2014). Advances in Medical Education and Practice Dovepress status of simulation in health care education: an international survey. *Advances in Medical Education and Practice*, 5–457. <https://doi.org/10.2147/AMEP.S65451>
- Ragaert, K., De Somer, F., Somers, P., De Baere, I., Cardon, L., & Degrieck, J. (2012). Flexural mechanical properties of porcine aortic heart valve leaflets. *Journal of the*

Mechanical Behavior of Biomedical Materials, 13, 78–84.

<https://doi.org/10.1016/j.jmbbm.2012.04.009>

Rankouhi, B., Javadpour, S., Delfanian, F., & Letcher, T. (2016). Failure Analysis and Mechanical Characterization of 3D Printed ABS With Respect to Layer Thickness and Orientation. *Journal of Failure Analysis and Prevention*, 16(3), 467–481.

<https://doi.org/10.1007/s11668-016-0113-2>

Regehr, G., & Macrae, H. (1997). *Technical Skill via an Innovative “Bench Station” Examination*. 9610(97).

Reznick, R., Regehr, G., MacRae, H., Martin, J., & McCulloch, W. (1997). Testing technical skill via an innovative “bench station” examination. *American Journal of Surgery*, 173(3), 226–230. [https://doi.org/10.1016/S0002-9610\(97\)89597-9](https://doi.org/10.1016/S0002-9610(97)89597-9)

Ribeiro, I. B., Ngu, J. M. C., Lam, B. K., & Edwards, R. A. (2018). Simulation-Based Skill Training for Trainees in Cardiac Surgery: A Systematic Review. *Annals of Thoracic Surgery*, 105(3), 972–982. <https://doi.org/10.1016/j.athoracsur.2017.11.036>

Ripley, B., Kelil, T., Cheezum, M. K., Goncalves, A., Di Carli, M. F., Rybicki, F. J., Steigner, M., Mitsouras, D., & Blankstein, R. (2016). 3D printing based on cardiac CT assists anatomic visualization prior to transcatheter aortic valve replacement. *Journal of Cardiovascular Computed Tomography*, 10(1), 28–36.

<https://doi.org/10.1016/j.jcct.2015.12.004>

Sauren, A. A. H. J., van Hout, M. C., van Steenhoven, A. A., Veldpaus, F. E., & Janssen, J. D. (1983). The mechanical properties of porcine aortic valve tissues. *Journal of Biomechanics*, 16(5), 327–337. [https://doi.org/10.1016/0021-9290\(83\)90016-7](https://doi.org/10.1016/0021-9290(83)90016-7)

- Schachner, T., Bonaros, N., Ruttmann, E., Höfer, D., Nagiller, J., Laufer, G., & Bonatti, J. (2007). Training models for coronary surgery. *Heart Surgery Forum*, *10*(4), 215–217. <https://doi.org/10.1532/HSF98.20070704>
- Schubert, S. A., & Ghanta, R. K. (2016). Aortic Valve Anatomy: Implications for Transcatheter Aortic Valve Replacement. In *Catheter Based Valve and Aortic Surgery* (pp. 1–10). Springer New York. https://doi.org/10.1007/978-1-4939-3432-4_1
- Sidhu, R. S., Park, J., Brydges, R., MacRae, H. M., & Dubrowski, A. (2007). Laboratory-based vascular anastomosis training: A randomized controlled trial evaluating the effects of bench model fidelity and level of training on skill acquisition. *Journal of Vascular Surgery*, *45*(2), 343–349. <https://doi.org/10.1016/j.jvs.2006.09.040>
- Spencer, F. (1978). Teaching and measuring surgical techniques – the technical evaluation of competence. *Bulletin of the College of Surgeons*, *63*, 9–12.
- Stratasys. (2020a). *Agilus30*. Retrieved August 18, 2020, from <https://www.stratasys.com/materials/search/Agilus3030>
- Stratasys. (2020b). *Digital Materials*. Retrieved August 18, 2020, from https://www.stratasys.com/-/media/files/material-spec-sheets/mss_pj_digitalmaterialsdatasheet_0617a.pdf
- Stratasys. (2020c). *TangoPlus*. Retrieved August 18, 2020, from <https://www.stratasys.com/materials/search/tango>
- Swanson, W. M., & Clark, R. E. (1974). Dimensions and Geometric Relationships of the Human Aortic Valve as a Function of Pressure. *Circulation Research*, *35*(6), 871–

882. <https://doi.org/10.1161/01.RES.35.6.871>

Swindle, M. M., Smith, A. C., & Hepburn, B. J. S. (1988). Swine as models in experimental surgery. *Journal of Investigative Surgery*, 1(1), 65–79.

<https://doi.org/10.3109/08941938809141077>

Thoracic Aortic Aneurysm. (2019). The Society of Thoracic Surgeons. Retrieved August 30, 2020, from <https://ctsurgerypatients.org/adult-heart-disease/thoracic-aortic-aneurysm>

Tian, D., Rahnavardi, M., & Yan, T. D. (2013). *Aortic valve sparing operations in aortic root aneurysms : remodeling or reimplantation ?* 2(1), 44–52.

<https://doi.org/10.3978/j.issn.2225-319X.2013.01.14>

Tsang, H. G., Rashdan, N. A., Whitelaw, C. B. A., Corcoran, B. M., Summers, K. M., & MacRae, V. E. (2016). Large animal models of cardiovascular disease. *Cell Biochemistry and Function*, 34(3), 113–132. <https://doi.org/10.1002/cbf.3173>

Biochemistry and Function, 34(3), 113–132. <https://doi.org/10.1002/cbf.3173>

Ulrich, T. (2012). *New valves for babies that can grow with them*. Boston Children’s Hospital. Retrieved February 01, 2020, from

<https://vector.childrenshospital.org/2012/10/new-valves-for-babies-that-can-grow-with-them/>

Wang, K., Zhao, Y., Chang, Y. H., Qian, Z., Zhang, C., Wang, B., Vannan, M. A., & Wang, M. J. (2016). Controlling the mechanical behavior of dual-material 3D

printed meta-materials for patient-specific tissue-mimicking phantoms. *Materials and Design*, 90, 704–712. <https://doi.org/10.1016/j.matdes.2015.11.022>

Yoo, S.-J., Thabit, O., Kim, E. K., Ide, H., Yim, D., Dragulescu, A., Seed, M., Grosse-

Wortmann, L., & van Arsdell, G. (2016). 3D printing in medicine of congenital heart diseases. *3D Printing in Medicine*, 2(1). <https://doi.org/10.1186/s41205-016-0004-x>

Yoo, S. J., Spray, T., Austin, E. H., Yun, T. J., & van Arsdell, G. S. (2017). Hands-on surgical training of congenital heart surgery using 3-dimensional print models. *Journal of Thoracic and Cardiovascular Surgery*, 153(6), 1530–1540. <https://doi.org/10.1016/j.jtcvs.2016.12.054>

Appendices

A. Additive Manufacturing Models

A.1. First Mould Design Iteration

A.1.1. Steps Required to Create the Aortic Valve Model Via AM:

1. Design the model using a CAD software package. I used SpaceClaim to create the CAD model. The model was based on the parameters that were discussed in Chapter 3.
2. Prepare the model for AM. This was done by saving the model as an STL file using the save as function in SpaceClaim. The model was saved as a fine mesh STL file.
3. Check the quality of the STL model. Before sending the model to be printed, it was essential to check if the mesh had any issues. This was done using the mesh check function in SpaceClaim. After that, the fixed mesh function was used to fix any issues in the mesh.
4. Send the STL file to a company that offers AM services. I sent the files to Proto3000 and Niagara College.

Sometimes it is necessary to make some changes to the model. This is relatively simple as this requires editing the CAD file directly, then sending it again to the manufacturing partner.

Modifying the CAD model to include a pathology requires the following:

1. Discuss the design expectations with cardiac surgeons. This was done by asking the surgeons about their pathology of interest, and they mentioned that an aneurysm was an interesting pathology for the model.
2. Create the aneurysm at the specified area in the CAD model. The surgeons' expectation of an aneurysm was that of a sphere. The model was modified to include an aneurysm in the non-coronary sinus.
3. Save the model as STL and check for any mesh errors.

A.1.2. Design Steps of The First Mould: (Figures A.1 and A.2)

1. The design process started by using the CAD model of the aortic valve part as a reference. This was done by placing the CAD model at the center of a large block. This block was carved to create a negative of the CAD model within the block structure using the intersect operation in SpaceClaim.
2. After that, extending the boundaries of the carved sections until they reach the upper and lower limits of the block created two sections: the outer section and the internal section.
3. To separate the outer and inner sections into four parts, it was necessary to identify the best possible location that would allow for an easy casting process. The most critical section of the mould was the location of the aortic leaflets.

- Therefore, the leaflet area was used as the separation plane area of reference. Then, intersection operation was used to separate the mould into the four sections mentioned earlier including two outer sections and two internal sections. (see Figure A.2)
4. To create the leaflet structures, a gap of 0.1 mm was created to allow for separation. This gap was achieved by creating a positive 0.1 mm thick wall between the leaflets. The 0.1 mm dimension was chosen based on the minimum possible wall thickness achieved by a 3D printer using a 0.1 mm nozzle. This wall was placed at the lower section of the upper internal mould.
 5. To create the upper sections of the leaflets, the lower section of the upper internal mould was modified to allow for adequate alignment with the lower internal section of the mould.
 6. During the casting process, the internal sections need to be supported by a handle or locking mechanism to keep them in place during the casting material pouring process. Therefore, a handle base and structure were designed at the upper section of the outer mould to hold the internal upper mould. Also, a locking mechanism was designed for the internal lower mould to keep it in place.

7. M6 holes were created at the corners of the outer moulds to allow for M6 bolts to secure moulds during the casting process.

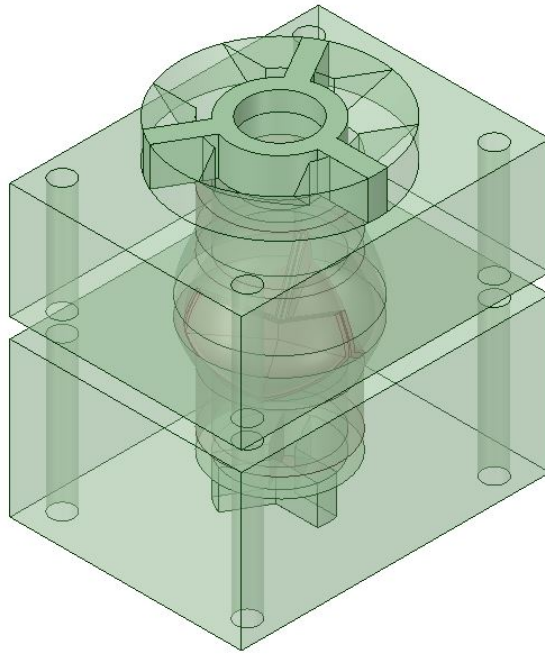


Figure A.1. Casting mould v1.

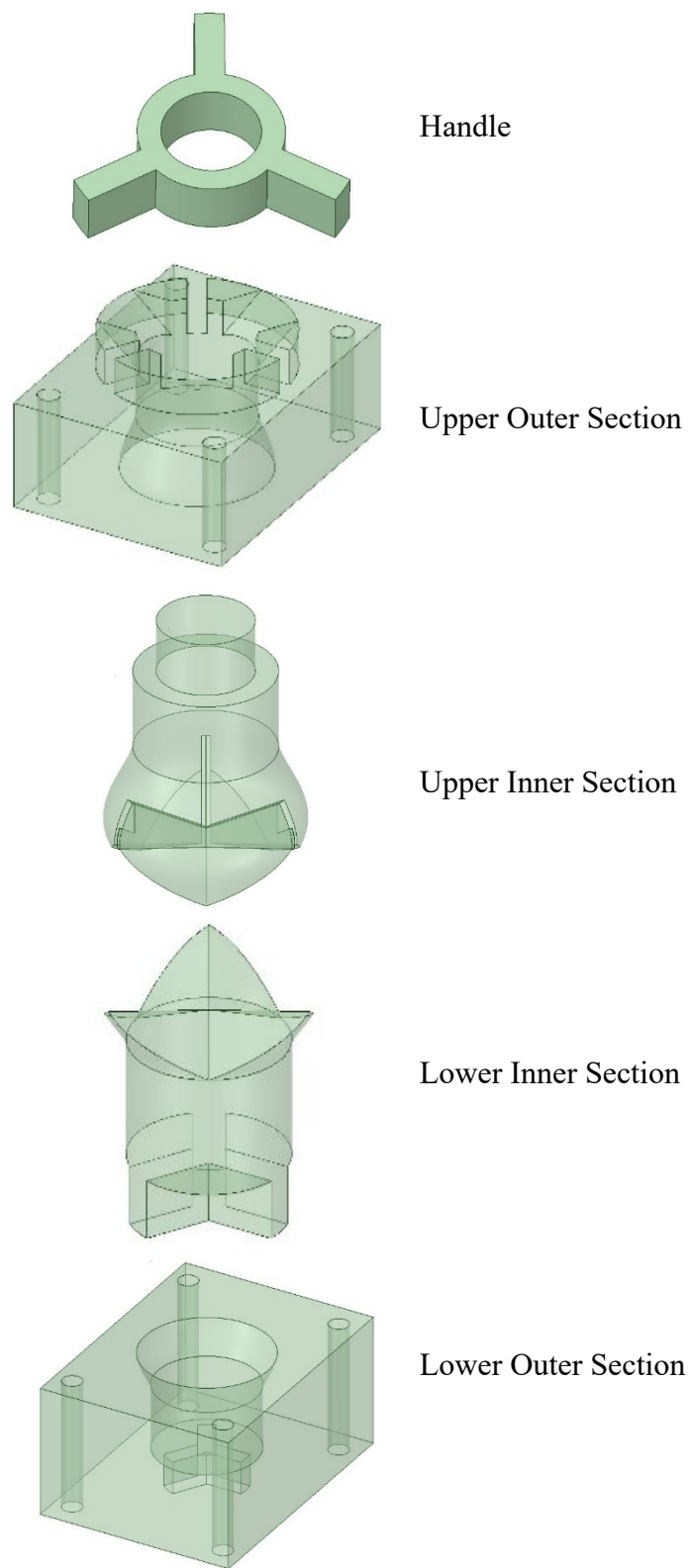


Figure A.2. Casting mould v1 Sections.

A.1.3. Casting Process Steps:

1. Design a suitable mould. This was done as shown previously in the design process of the casting mould v1.
2. Manufacture mould using additive manufacturing. The manufacturing process was done via 3D HUBS on-demand manufacturing platform (*Online 3D Printing Services*, 2020). The mould was 3D printed using PETG material as shown in Figure 3.8.
3. Prepare the casting materials according to the mixing instructions. In this research, the mixing ratio was 1:1 for all the casting materials. The mixing process was done in plastic containers using a stir stick to do the mixing.
4. Use mould release agent on all the sections of the mould. Universal mould release (UMR) agent (Alumilite Corporation, USA) was used on all the mould sections to ensure a smooth casting process. It was observed that not using a mould release agent led to a difficult casting process, especially for polyurethane.

5. Create a sealing layer using casting material if the mould material is porous. The moulds were 3D printed using PETG and PLA. Those materials were porous, and the casting materials seeped through them. However, after the first casting attempt, the porosity effect was less visible since some of the casting materials already solidified between the layers creating a seal.

6. Pour the casting materials according to the optimal acting time for each material. Generally, this was not critical for materials with relatively high viscosity. The only exception was seen while casting silicone A10 models. Silicone A10 had low viscosity and a relatively long-acting time (one hour). This meant that the silicone would stay as a liquid for up to one hour leading to challenges in covering all the required sections for casting. This issue was minimized by ensuring that the mould was tightly sealed using the bolts. Also, a mould release agent was used to act as a sealing medium between the mould and casting materials. Moreover, for silicone A10, a waiting time of one hour was used between the initial and final pouring processes to ensure that all the sections were covered.

7. Follow the instructions regarding the curing process including demoulding time and full curing schedule. The moulds were kept in a cardboard box in the lab for more than 24 hours (recommended demoulding time for silicone A10). After that, the moulds were cured in the lab for more than a week (full curing schedule for silicone A10).

A.2. Second Mould Design Iteration

The second iteration of the mould design was done after meeting with the cardiac surgeons to discuss the design modifications that were desired. The mould was based on the CAD design of the third iteration mentioned in Part 2 in Chapter 3.

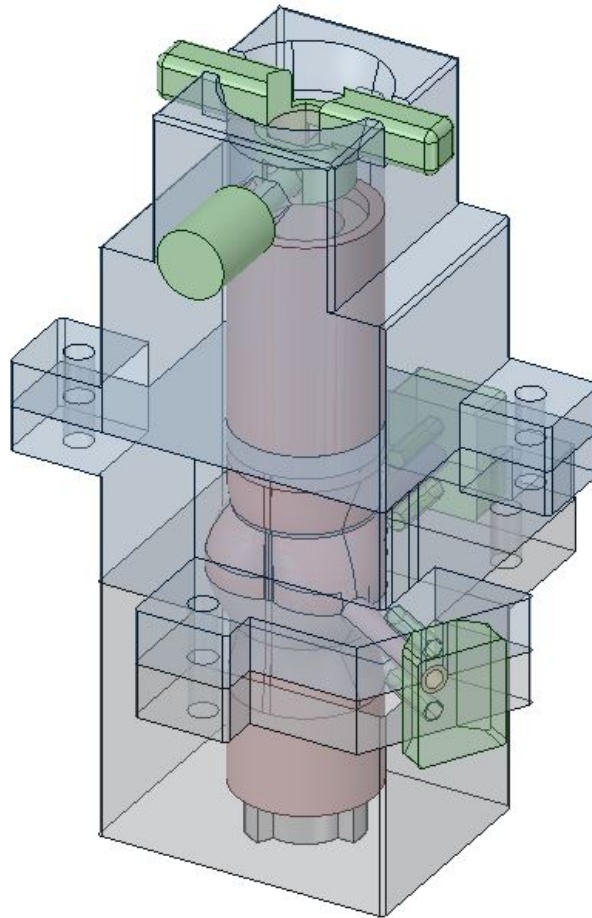


Figure A.3. Casting mould v2.

A.2.1. The Design Modifications of V2:

- Increase the length of the ascending aorta and make it a straight tube. This comment was received after showing the surgeons the 3D printed models that had curved ascending aorta. The surgeons were in favour of a simpler casting design that included a straight ascending aorta. From a casting design point of view, the straight tube design was easier to design and use during casting. The updated CAD model of the aorta was longer by 51 mm in the upper section and 22 mm in the lower section.
- One of the early suggestions by the surgeons was to include the coronary arteries. This was done by creating two tubes with an outer diameter of 6 mm and an inner diameter of 4 mm. The tube lengths were about 30 mm. The locations of the tubes were in the middle of the left and right coronary sinuses.
- Include realistic sinus of Valsalva. The surgeons supported this feature as it gave the model a more realistic representation of the aortic root. This was achieved by using blend operation to connect the main dimensions of the sinuses mentioned in Chapter 4. Regarding the mould design, the sinuses were created after the intersection operation between the updated cast and a solid block. This created the sinuses cavities in the mould.

- The separating wall thickness was increased from 0.1 mm to 0.5 mm. This is to allow for easier separation of the leaflets after the casting process.
- Including the coronary arteries increased the complexity of the mould. It was necessary to make sure that enough casting materials reached the coronary artery cavities. Also, the mould had to allow for the sinus holes to form after the casting. To achieve this, two coronary locks were designed to ensure complete coronary artery casting.

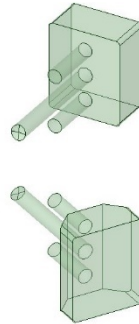
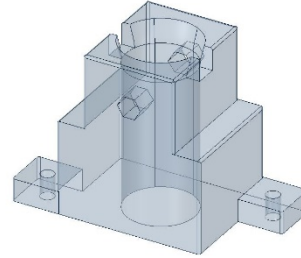


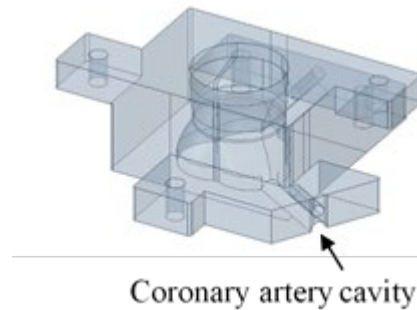
Figure A.4. Coronary arteries locks.

- Making a modular design was one of the design modifications of the second iteration. The design included three outer sections including a replaceable upper section, middle section, and lower section. The rationale to include a replaceable upper section was to cast ascending aorta pathologies, such as an aneurysm.

Outer upper section Modular upper section to maximize the design flexibility



Outer middle section The middle section included the upper carved geometries for the sinuses of Valsalva and the coronary arteries



Outer lower section The lower section included the lower carved geometries for the sinuses of Valsalva, the coronary arteries and the inner lower section lock

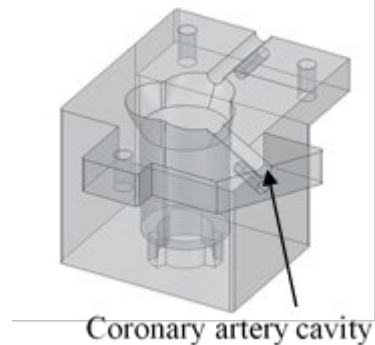
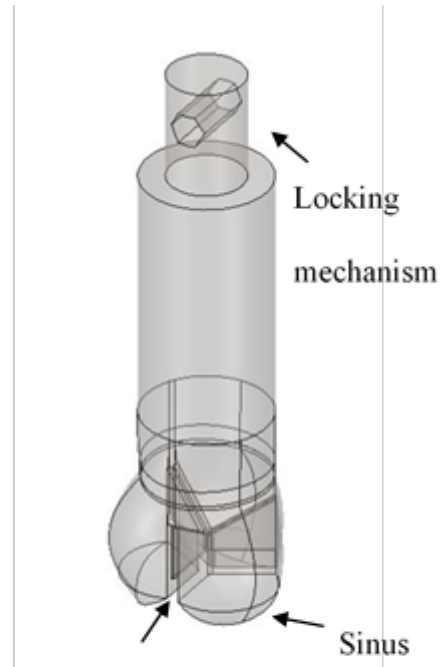


Figure A.5. Summary of mould v2 outer sections.

Inner upper section Includes a locking mechanism at the top to secure the mould. The lower section includes the inner upper geometries of the sinuses, leaflets, and the thin separating walls between them.



Leaflets cavity & separating wall

Inner lower section Includes a locking mechanism at the bottom. The upper section includes the lower geometries of the sinuses, leaflets and the thin separating wall between them

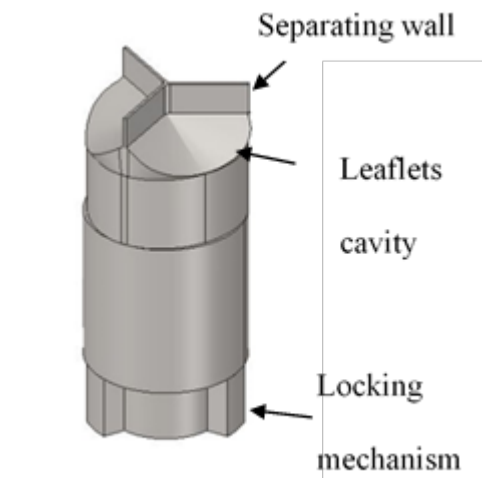


Figure A.6. Summary of mould v2 inner sections.

- Locking mechanisms were added to secure the upper inner section of the mould. This was done by creating slots and holes in the upper outer section. After that, a cylindrical lock was used to limit the Z-axis movement of the upper inner mould, and a fixture was used to limit the X and Y axes movements. One of the issues in the earlier prototypes of the mould was that a slight misalignment took place after pouring the silicone into the mould. The locking mechanisms solved this issue.

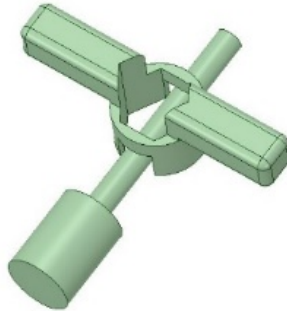


Figure A.7. Locking mechanism.

A.2.2. Steps to Modify the Second Mould:

1. Follow the steps suggested for modifying the CAD model of the aortic valve for AM. This is because the mould design depends on the cast design, which is the modified CAD design for AM in this case.
2. Redesign the relevant internal and external sections to reflect the design changes. Using the ascending aorta pathology as an example, the modifications included adding a sphere with a diameter of 50 mm in the

middle of the upper-middle section of the mould. This was done after asking the cardiac surgeons regarding their expectations of an aneurysm in the ascending aorta. The surgeons said that having the aneurysm as a sphere was acceptable.

3. An aneurysm is a dilation in the diameter of the aorta. Therefore, to complete the mould of the pathology, an outer mould had to be designed to ensure that the thickness of the ascending aorta would be the same in the affected area (Figure A.8). This can be done by intersecting the upper outer mould with a 56 mm diameter sphere. Also, the upper mould design must change to allow for a side to side assembly as opposed to the current assembly direction. This is to allow for the cast to be removed from the mould. Creating the outer mould was included as a future step.

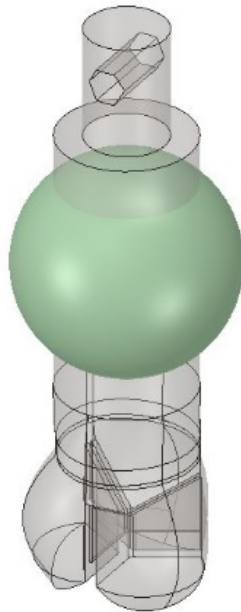


Figure A.8. Ascending aorta aneurysm.

A.3. Educational Model Design Steps:

1. Discuss the design expectations with the cardiac surgeons. The first iteration of the training setup was modified following the cardiac surgeons' feedback regarding what to expect during the training. The surgeons preferred a more realistic setup that resembles the aortic valve position during surgery. The first step was achieved by creating a box housing for the model to mimic the chest cavity.
2. Position the aortic valve 3D printed model as expected during the surgery. This was done by creating pins to hold the coronary arteries in place during the training. The position of the left coronary artery was downward-pointing toward the body, while the right coronary artery was positioned at a 120° angle of that position.

- Secure the training box to a table (optional). As a future step, several M6 holes could be added to the design for added stability. A permanent upper surface could also be designed to mimic the patient's chest with the aortic valve model and training box set below the level of the artificial chest surface.

B. Educational Model Evaluation

Examples of global rating systems based on OSATS:

Modified objective structured assessment of technical skill (OSATS)–global rating scale

Surgeon code:	Procedure:	Assessor:	Date:		
Please circle the candidate's performance on the following scale:					
	1	2	3	4	5
Respect of tissue	1 Frequently used unnecessary force on tissue of caused damage by inappropriate use of instruments	2	3 Careful handling of tissue but occasionally caused inadvertent damage	4	5 Consistently handled tissues appropriately with minimal damage
Time and motion	1 Make unnecessary moves	2	3 Efficient time/motion but some unnecessary moves	4	5 Clear economy of movement and maximum efficiency
Instrument handling	1 Frequently asked for the wrong instrument or used an inappropriate instrument	2	3 Competent use of instruments although occasionally appeared stiff or awkward	4	5 5 Fluid moves with instruments and no awkwardness
Suture handling	1 Awkward and unsure with repeated entanglement, poor knot tying and inability to maintain tension	2	3 Careful and slow with majority of knots placed correctly with appropriate tension	4	5 Excellent suture control with placement of knots and correct tension
Flow of operation	1 Frequently stopped operating or needed to discuss the next move	2	3 Demonstrated some forward planning and reasonable progression of procedure	4	5 Obviously planned course of operation with efficiency from one move to another
Knowledge of procedure	1 Insufficient knowledge. Looked unsure and hesitant	2	3 Knew all important steps of the operation	4	5 Demonstrated familiarity with all steps of the operation
Overall performance	1 Very poor	2	3 Competent	4	5 Clearly superior
Quality of final product	1 Very poor	2	3 Competent	4	5 Clearly superior
Total score:					

Figure B.1. Modified OSATS global rating scale (Hance et al., 2005).

Global rating scale of operative performance

Please circle the number corresponding to the candidate's performance regardless of the candidate's level of training

Respect for tissue	1	2	3	4	5
Frequently used unnecessary force on tissue or caused damage by inappropriate use of instruments			Careful handling of tissue but occasionally caused inadvertent damage		Consistently handled tissue appropriately with minimal damage to tissue
Time and motion	1	2	3	4	5
Many unnecessary moves			Efficient time/motion but some unnecessary moves		Clear economy of movement and maximum efficiency
Instrument handling	1	2	3	4	5
Repeatedly makes tentative or awkward moves with instruments through inappropriate use			Competent use of instruments but occasionally appeared stiff or awkward		Fluid movements with instruments and no stiffness or awkwardness
Knowledge of instruments	1	2	3	4	5
Frequently asked for wrong instrument or used inappropriate instrument			Knew names of most instruments and used appropriate instrument		Obviously familiar with instruments and their names
Flow of operation	1	2	3	4	5
Frequently stopped operating and seemed unsure of next move			Demonstrated some forward planning with reasonable progression of procedure		Obviously planned course of operation with effortless flow from one move to the next
Use of assistants (if applicable)	1	2	3	4	5
Consistently placed assistants poorly or failed to use assistants			Appropriate use of assistants most of the time		Strategically used assistants to the best advantage at all times
Knowledge of Specific Procedure	1	2	3	4	5
Deficient knowledge. Required specific instruction at most steps of operation			Knew all important steps of operation		Demonstrated familiarity with all steps of the operation
Overall performance	1	2	3	4	5
		Very poor	Competent		Clearly superior
QUALITY OF FINAL PRODUCT					
	1	2	3	4	5
Very poor			Competent		Clearly superior
Is donor vessel arteriotomy of appropriate size (1.5 diameter of graft)?					
					1/0
Is the anastomotic angle appropriate (10-20 degrees for the end to side anastomosis)?					
					1/0
Are sutures evenly spaced (about 1.5-2.2. mm apart)?					
					1/0
Are sutures at appropriate depth (2 mm) with no narrowing at the heel/toe of the anastomosis?					
					1/0
Is there no or minimal damage to normal vessels at the clamp sites?					
					1/0
Is there a technical defect leading to anastomotic leak (if yes score 0)?					
					1/0
Total Score ____					

Figure B.2. Modified OSATS including a checklist (Sidhu et al., 2007).

An example of a rating score adopted from OSATS can be seen in the figure below (Fann et al., 2010; Regehr & Macrae, 1997).

	Good	Average	Poor
Graft orientation (proper orientation for toe–heel, appropriate start and end points)	1	2	3
Bite appropriate (entry and exit points, number of punctures, even and consistent distance from edge)	1	2	3
Spacing appropriate (even spacing, consistent distance from previous bite, too close vs too far)	1	2	3
Use of Castroviejo needle holder (finger placement, instrument rotation, facility, needle placement, pronation and supination)	1	2	3
Use of forceps (facility, hand motion, assist needle placement, appropriate traction on tissue)	1	2	3
Needle angles (proper angle relative to tissue and needle holder, consider depth of field, anticipating subsequent angles)	1	2	3
Needle transfer (needle placement and preparation from stitch to stitch, use of instrument and hand to mount needle)	1	2	3
Suture management and tension (too loose vs tight, use tension to assist exposure, avoid entanglement)	1	2	3

Good, Able to accomplish goal without hesitation, showing excellent progress and flow; *Average*, able to accomplish goal with hesitation, discontinuous progress and flow; *Poor*, able to partially accomplish goal with hesitation. Adapted from Objective Structured Assessment of Technical Skill (OSATS).²

Figure B.3. Rating scale sample for assessment of coronary anastomosis.